Chapter

Cytological Diagnosis of Infectious Diseases: Identification of Pathogens and Recognition of Cellular Reactions

Yutaka Tsutsumi

Abstract

Cytological diagnosis of infectious diseases is as important as the cytodiagnosis of malignancies, because the detection of pathogens in cytological specimens is crucially valuable for prompt and appropriate patients' treatment. When compared with histological diagnosis, cytology is strong at detecting microbes under Papanicolaou and Giemsa stains. Host response against the infectious agent can be estimated by the type of background inflammatory cells. Patterns of the inflammatory cellular responses against extracellular and intracellular pathogens should be recognized. Immunocytochemical and molecular approaches can be applied, even when we have only one cytology specimen in hand. The cell transfer technique is useful to create plural material from one glass slide for immunocytochemistry and other techniques. In case of transmissible disorders including sexually transmitted diseases, the prompt and appropriate diagnosis will avoid avoidable transmission of infectious agents among people, and eventually contribute to the safety of the human society.

Keywords: cell transfer technique, cytodiagnosis, defense mechanism, host response, immunocytochemistry, infectious diseases, inflammatory cells, pathogens

1. Introduction

In the daily practice of cytological diagnosis, cytopathologists tend to focus on the diagnosis of premalignant and malignant diseases. Generally speaking, the cytology practice functions as screening for malignancy. However, the cytodiagnosis of infectious diseases and the identification of pathogens in cytological preparations must not be undervalued. The correct cytodiagnosis of infectious diseases leads patients to prompt and appropriate treatment. Histopathological diagnosis is strong at recognizing host responses against pathogens, while pathogens are more easily identified in the cytology specimen than the histology specimen. When infectious diseases are clinically suspected, it is better for us to perform Giemsa staining in addition to routine Papanicolaou staining.

In the present review article, the author presents varied aspects of cytomorphology of infectious diseases, in addition to general remarks for the defense mechanisms against infectious microorganisms. Immunocytochemistry

significantly contributes to the definite and final cytodiagnosis. Often times, only one cytology specimen is available in the daily practice, so that the special techniques "how we can detect pathogens in only one cytology preparation" are needed for evaluating with additional staining. Please refer to the previous articles, textbooks and web sites of the author, describing the cytological diagnosis of infectious diseases [1–7]. It is most regrettable that some of them were written in Japanese.

2. Defense mechanisms against infection

Defense mechanisms against infection are categorized into two types: nonspecific and specific. Both types cooperatively function as an effective anti-infection system. Varied inflammatory cells are involved in the processes [8–10].

2.1 Types of inflammatory cells

Types of inflammatory cells and their properties are briefly summarized in **Table 1**. Function of the cells and their proliferative and migratory activity are shown.

Representative light microscopic and electron microscopic features of the inflammatory cells are illustrated in **Figures 1** and **2**. Of note is that cytokines mediate intercellular communication with which the immune cells talk to each other [11]. Cytokines include interferons, interleukins, chemokines, lymphokines and tumor necrosis factors.

2.2 Nonspecific defense mechanisms against infection

2.2.1 Physical barriers

The epidermis of the skin and the surface mucosal layer on the mucosal membrane play an effective physical barrier against invasion of the pathogen. The cilia on the pseudostratified mucosa of the airway effectively excrete the pathogen.

Cell type	Function	Proliferative activity	Migratory potential
Granulocyte			
Neutrophil	Phagocytosis	None	Migratory
Eosinophil	Allergy, anti-helminth function	None	Migratory
Basophil	Histamine production	None	Migratory
Mast cell	Histamine production	Proliferative	Migratory
Monocyte	Phagocytosis	Proliferative	Migratory
Macrophage	Phagocytosis, granuloma reaction	Proliferative	Migratory
B-lymphocyte	Humoral immunity	Proliferative	Migratory
T-lymphocyte	Cellular immunity/helper activity	Proliferative	Migratory
NK cell	Innate immunity	Proliferative	Migratory
Plasma cell	Antibody production	None	None
Dendritic cell	Antigen presentation	Proliferative	None

Table 1.
Inflammatory cells and their properties.

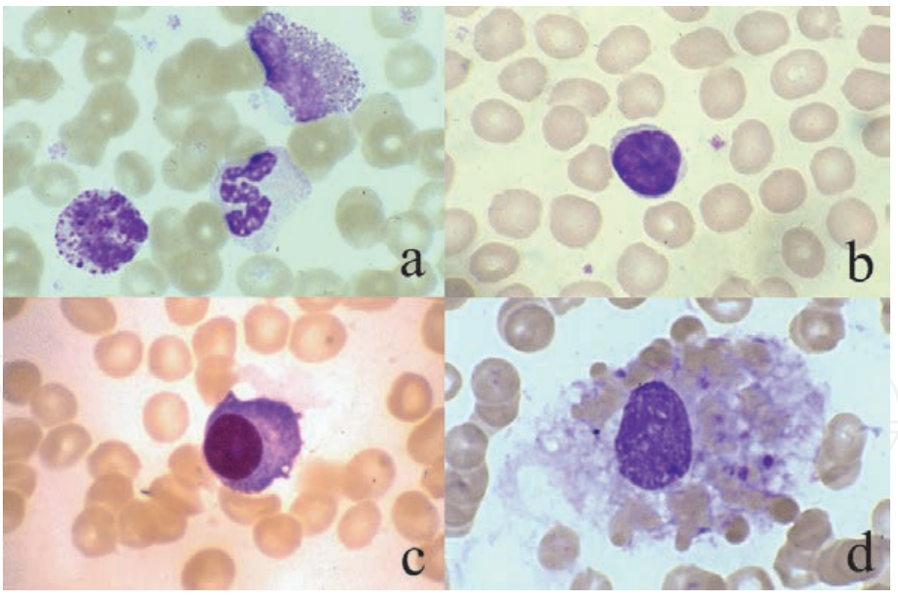

Figure 1.
Types of inflammatory cells (may-Giemsa). a: Three kinds of granulocytes (from left to right: Basophil, neutrophil and eosinophil) seen in the bone marrow smear. b: Small lymphocyte, c: Plasma cell, d: Hemophagocytic (activated) macrophage. Compare the cytoplasmic granules in the granulocytes. The cytoplasm of the small lymphocyte is scanty, and the plasma cell contains basophilic cytoplasm with a prominent Golgi area. The macrophage actively phagocytizes red cells and platelets.

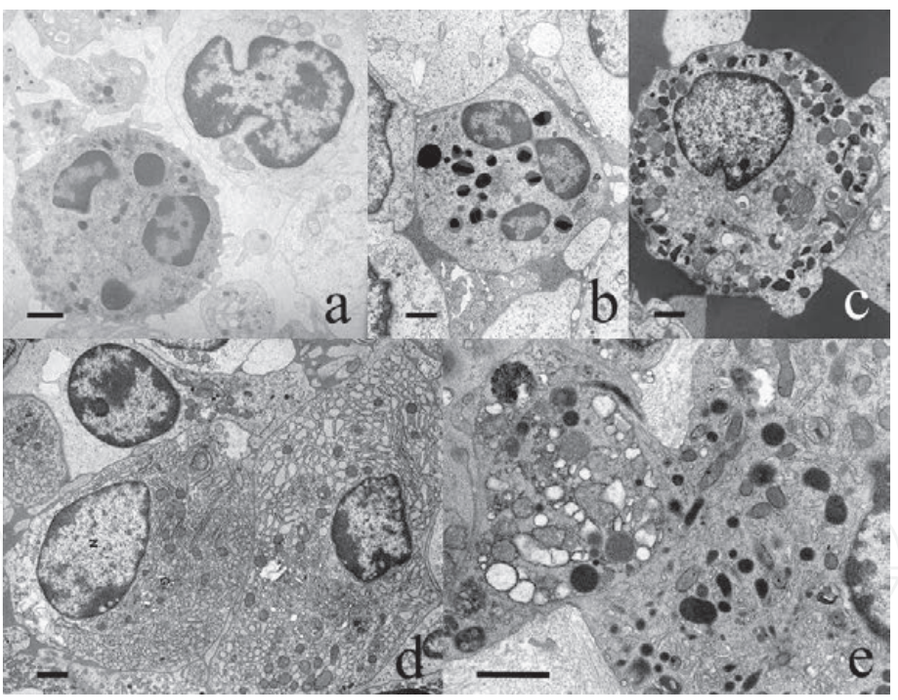

Figure 2.
Electron microscopic appearance of inflammatory cells. a: Neutrophil (left) and lymphocyte (right), b: Eosinophil, c: Basophil, d: Two plasma cells in the small bowel mucosa, e: Activated macrophage in soft tissue. The lymphocyte has an indented nucleus, while the granulocytes possess segmented nuclei. The cytoplasmic granules feature the respective granulocytes: Small-sized granules in the neutrophil, large crystalline granules in the eosinophil, and large rounded granules often with a fingerprint image in the basophil. The plasma cells contain a round nucleus with peripherally condensed heterochromatin and the cytoplasm rich in rough endoplasmic reticulum. The large-sized macrophage possesses an ameboid cytoplasmic process and numbers of electron-dense lysosomal granules. Bars indicate 1 μm.

2.2.2 Antibacterial secretory proteins

The secretory juice secreted from secretory glands contains varied antibacterial proteins such as lactoferrin, lysozyme (muramidase) and defensins [12].

Lactoferrin shows a bacteriostatic function by combining and competing trivalent ferric ions mandatory for the growth of bacteria and fungi. Lactoferrin is secreted from the lactating breast, serous salivary glands, lacrimal glands, eccrine sweat glands, gastric glands and prostatic glands. Of particular note is that protease digestion of lactoferrin yields lactoferricin and lactoferrampin, potent antimicrobial peptides derived from the lactoferrin molecule [13]. Lysozyme operates as a bactericidal or bacteriolytic molecule by cutting the joint sequence of *N*-acetylglucosamine and *N*-acetylmuramic acid in the peptide glycan network on the cell wall of Gram-positive bacteria [14]. Defensins belong to bactericidal proteins strongly binding to phospholipids [12]. Numbers of serous secretory glands secrete both lysozyme and defensins, together with lactoferrin. In the small bowel mucosa, lysozyme and defensins are actively secreted from Paneth cells (**Figure 3**). Representative microscopic features of production of lactoferrin and lysozyme in varied secretory epithelial cells are displayed in **Figure 4**.

2.2.3 Phagocytes and natural killer (NK) cells

Bacteria are nonspecifically phagocytized by phagocytes such as neutrophils and macrophages [15]. **Figure 5** exhibits bacteria phagocytized by neutrophils. Because of the lack of proliferative activity, neutrophils are predominantly seen in acute inflammation. Macrophages are proliferative, so that they mainly appear in chronic inflammation. Myeloperoxidase, lysozyme and defensins show bactericidal activities in the phagocytic vacuole (primary granule) of the neutrophil [16]. In the secondary (specific) granule of neutrophils, lactoferrin is contained. The main bactericidal enzyme functioning in the macrophage is lysozyme (see **Figure 3b**). NK cells correspond to CD56-positive large granular lymphocytes [17]. The cytoplasmic granules of the NK cell contain bactericidal, antiviral and apoptosis-inducing proteins common with the CD8-positive killer (cytotoxic) T-lymphocyte, such as perforin, granzymes (A and B) and T-cell intracellular antigen-1 (TIA-1).

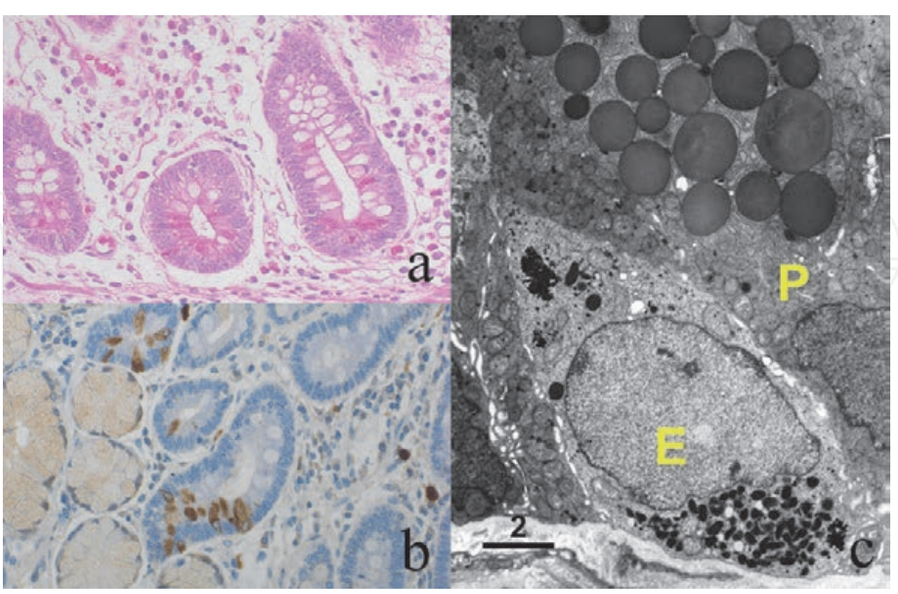

Figure 3.
Paneth cells in the duodenal mucosa. a: H&E, b: Lysozyme immunostaining, c: Electron microscopy. Paneth cells are distributed at the bottom of the intestinal crypt. Coarse eosinophilic granules are accumulated in the luminal side, and strongly immunoreactive for lysozyme. Macrophages scattered in the lamina propria mucosae express lysozyme immunoreactivity. Ultrastructurally, large-sized (around 2 μm in diameter) and round-shaped exocrine granules in the supranuclear cytoplasm of a Paneth cell (P) are homogeneously electron-dense. Compare them with infranuclear small-sized, electron-dense secretory granules of an endocrine cell (E). Bar = 2 μm.

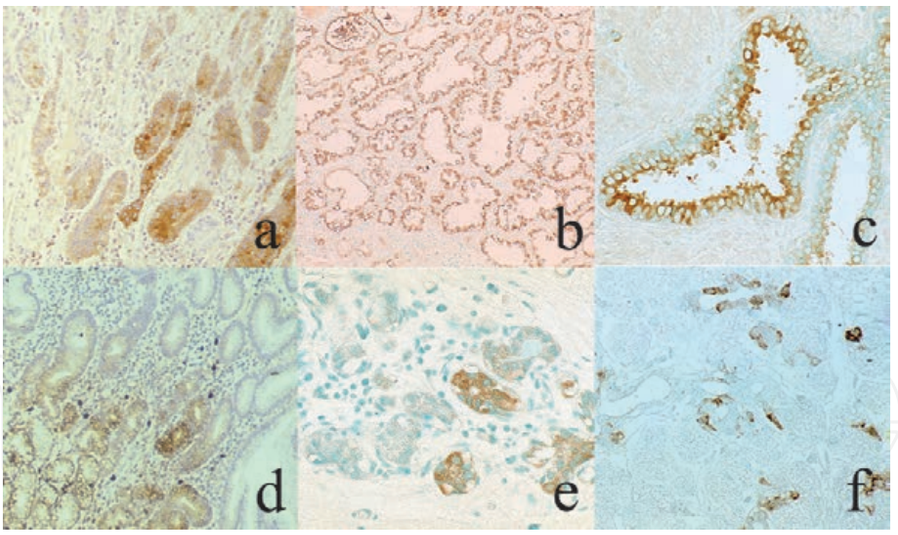

Figure 4.
Distribution of lactoferrin (upper panels: a–c) and lysozyme (lower panels: d–f) in secretory glands (immunostaining). a: Gastric fundic gland, b: Lactating breast, c: Prostatic gland, d: Gastric pyloric gland, e: Non-lactating breast, f: Parotid gland. Lactoferrin is actively expressed in the fundic gland, lactating breast and prostatic acini. The pyloric gland in the gastric antrum, normal mammary ductules and serous acinar cells of the salivary gland are immunoreactive for lysozyme.

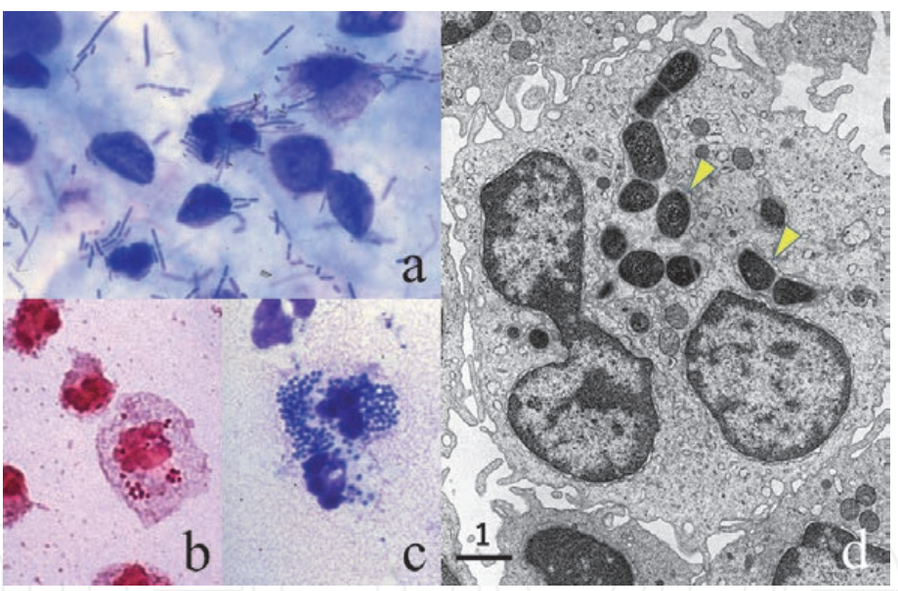

Figure 5.
Bacteria phagocytized by neutrophils. a: Escherichia coli *in the urine (acute cystitis; Giemsa),* Neisseria meningitidis *in the cerebrospinal fluid (gram), c:* Neisseria gonorrhoeae *in the urethral discharge (Giemsa), d: Electron microscopy of a neutrophil phagocytizing bacilli in the pleural effusion. Neutrophils actively phagocytize the bacilli (a and d) and cocci (b and c). Note that the bacilli are localized in lysosomal granules (d, arrowheads). Bar = 1 μm.*

These cells play significant roles in the host defense against pathogens for the initial two weeks after infection, until the establishment of the "specific" (humoral and/or cellular) immune reaction.

It should be noted that neutrophils form neutrophil extracellular traps (NETs), a filamentous spiderweb-like network entrapping bacteria, after cell death called NETtosis [18]. NETs are composed of DNA stretches and anti-bacterial proteins, including lactoferrin and myeloperoxidase [19]. NETs are richly formed in the abscess lesion, as shown in **Figure 6**.

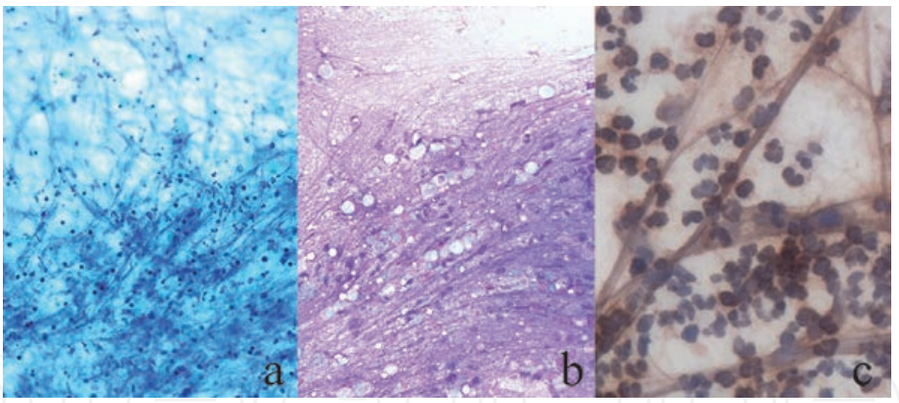

Figure 6.
Neutrophil extracellular traps (NETs) seen among aspirated neutrophilic exudates aspirated from a mammary abscess lesion. a: Papanicolaou, b: Giemsa, c: Lactoferrin immunostaining. Long and basophilic filamentous structures are formed among the neutrophils. NETs, composed of DNA and anti-bacterial proteins such as lactoferrin, entrap the causative bacteria with a spiderweb-like network to avoid them from spreading.

2.2.4 Innate immunity and Toll-like receptors

Acute viral infection usually calms down in one week. The strong anti-viral mediators are type I interferons (IFN-alpha and IFN-beta). The IFNs are produced by the keratinocyte of the epidermis and squamous mucosa, the columnar cells of the intestinal and airway mucosa and Langerhans (dendritic) cells distributed among the epithelial cells [20, 21]. Toll-like receptors (TLRs) expressed on these cells specifically recognize microbe-derived components such as lipoproteins, lipopolysaccharide, viral double-stranded RNA, non-methylated CpG islands of DNA and flagellin to induce IFN secretion. Toll means great and curious in German. In the human being, there are 10 kinds of TLRs. The TLR-mediated innate immunity, as well as phagocytosis by neutrophils and macrophages and the NK cell-mediated defense, comprise major functions of the vertebrate intrinsic system for the exclusion of the pathogen.

2.3 Specific defense mechanisms against infection

The specific acquired immunity consists of humoral immunity and cell-mediated (cellular) immunity [8, 9]. Production of specific antibodies by B-lymphocytes is the key mechanism of the humoral immunity. Serum complements secreted from the liver activate neutralizing activity of specific antibodies. The key players of the cell-mediated immunity are cytotoxic (killer) T-lymphocytes and activated macrophages. It takes a certain period (usually two weeks to one month) until establishing the specific acquired immunity.

The specific defense mechanisms against infection should be divided into two categories: the systemic immunity versus local (mucosal) immunity. The pathogen invading the inside of the body are specifically protected by IgG-mediated humoral immunity and also by CD8-positive cytotoxic T-lymphocyte-mediated cellular immunity.

The mucosal immunity provides a defense mechanism protecting invasion of the pathogen across the mucosa [22]. Dimeric secretory IgA (sIgA) functions as a mediator of the mucosal humoral immunity, but it hardly shows a neutralizing (killing) activity. The lamina propria mucosae contains numbers of IgA-producing plasma cells. sIgA is secreted onto the mucosal surface after coupling with "secretory component (SC)" produced by the columnar epithelial cells. **Figure 7** schematically displays the process of formation of sIgA. Microscopic features of IgA secretion in

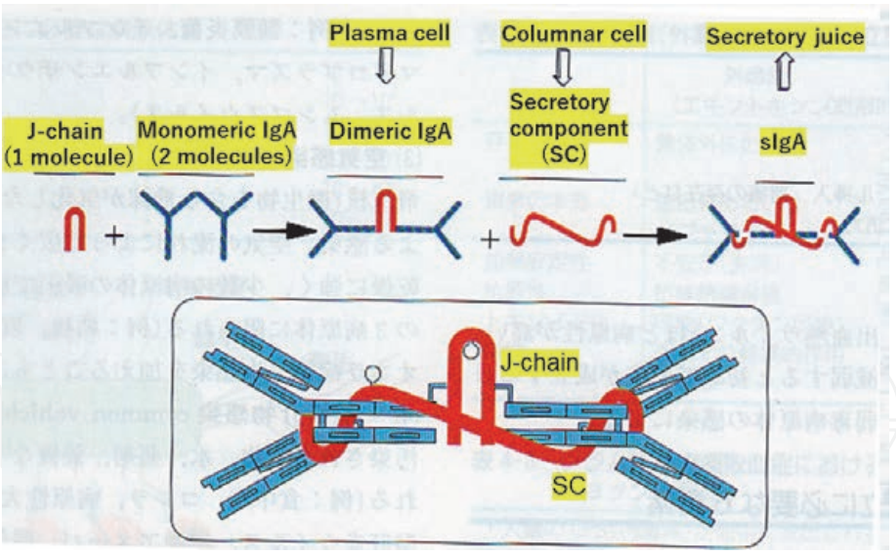

Figure 7.
Schematic presentation of the process of formation of secretory IgA (sIgA). IgA is secreted onto the mucosa after binding with secretory component (SC), a product of mucosa-lining columnar epithelial cells. Dimeric IgA consists of two molecules of monomeric IgA and J-chain. IgA-producing plasma cells are richly distributed in the normal bowel mucosa.

intestinal metaplasia of the stomach are demonstrated in **Figure 8**. sIgA is uniquely resistant to protease digestion. It is of note that IgG can also be secreted onto the mucosal surface after coupling with IgG Fc-binding protein, a unique IgG Fc receptor of secretory type, produced by mucin-secreting cells in the mucosa [23, 24].

Extrathymic T-lymphocytes are distributed among the mucosal columnar cells as "intraepithelial lymphocytes" predominantly expressing CD8 and T-cell receptor gamma/delta on the cell surface [25] (**Figure 9**). Intraepithelial lymphocytes significantly increase in certain mucosal infections such as *Giardia lamblia* infection (giardiasis). The extrathymic T-lymphocytes locally recruit in the "crypt patch" located in the lamina propria mucosae. Because of the lack of education in the thymus, the extrathymic T-lymphocytes, self-reactive to provoke apoptosis of the

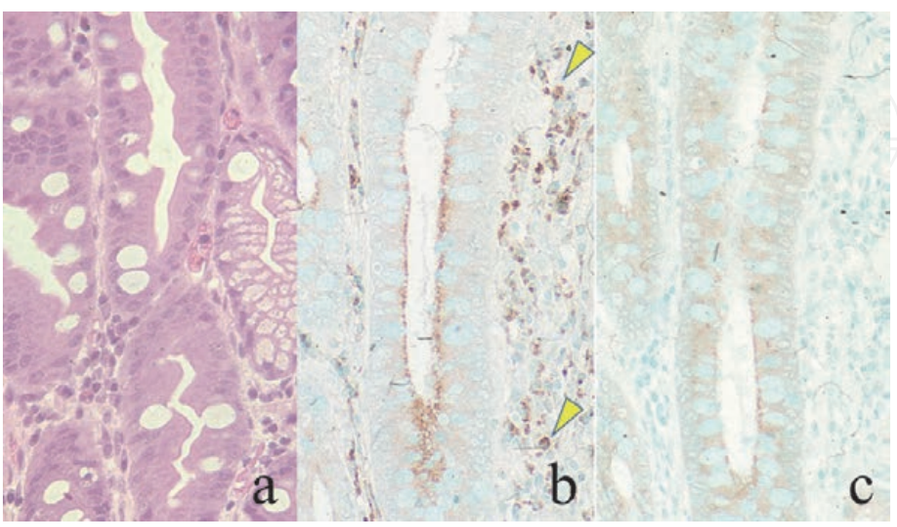

Figure 8.
Intestinal metaplasia of the gastric mucosa showing secretory IgA transportation. a: H&E, b: IgA, c: Secretory component (SC). Goblet cells and absorptive-type cells with brush borders are observed in the metaplastic gland. The columnar cells of the intestinal type produce SC, which traps dimeric IgA secreted from IgA plasma cells (arrowheads) in the lamina propria mucosae. The apical cytoplasm of the columnar cells is immunoreactive for IgA, representing the intracellular transportation of sIgA.

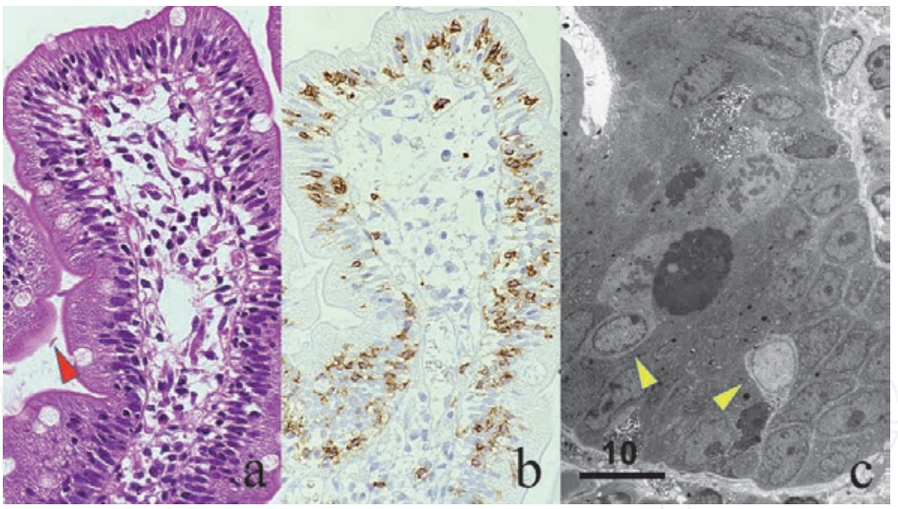

Figure 9.
Intraepithelial lymphocytes (IELs) in the duodenal mucosa, accentuated by Giardia lamblia *infection. a: H&E, b: CD8 immunostaining, c: Electron microscopy. Marked increase of IELs is noted in the intestinal villi. The red arrowhead indicates a giardian protozoa. CD8 immunostaining clearly demonstrates the dense distribution of the killer-type T-lymphocytes among the columnar epithelial cells. Ultrastructurally, small lymphocytes are seen in the intercellular space among the columnar cells (yellow arrowheads). Small cytoplasmic granules are scattered in the cytoplasm. Bar = 10 μm.*

columnar epithelial cells, may control the number and function of indigenous bacterial flora living in the lumen.

The mucosa-associated lymphoid tissue (MALT) is distributed in the intestinal and airway mucosa. The largest MALT is called as Peyer's patch in the ileal mucosa (**Figure 10**). The B-lymphocyte-rich lymphoid follicles with activated germinal centers are covered with dome-shaped columnar epithelial cells without villous structures. In contrast to the other part of the gut mucosa, B-lymphocytes and microfold (M) cells are distributed among the dome columnar cells. The M cells are special epithelial cells suited for efficient endocytosis and transcytosis, and function as gateways to the mucosal immune system [26]. The MALT is known to play a central role in the mucosal homing of B-lymphocytes destined to secrete IgA.

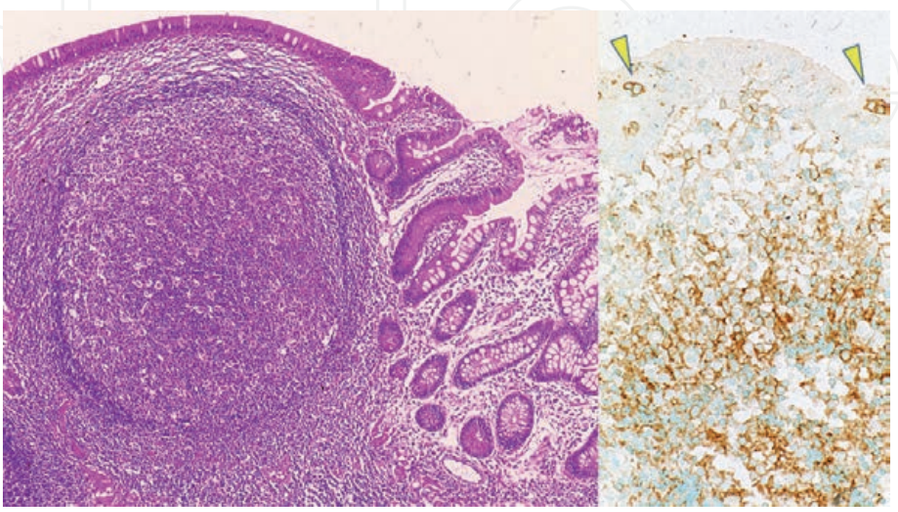

Figure 10.
Peyer patch in the ileal mucosa. Left: H&E, right: CD20 immunostaining. The lymphoid follicle with an activated germinal center is covered with dome-shaped columnar epithelial cells without villous structures. CD20-positive B-lymphocytes are distributed not only in the lymphoid follicle but also among the dome columnar cells (arrowheads).

2.4 Three major patterns of host responses against infection

From the pathological point of view, there are three major mechanisms of host responses against infection, depending on the type of pathogens and the mode of infection (either extracellular or intracellular infection).

1. Neutrophilic reaction against extracellular pathogens

2. Cellular immune reaction against intracellular pathogens

3. Humoral immunity via neutralizing antibody reaction

Table 2 summarizes the features of the defense mechanisms and host responses against pathogens. Patterns of the host response against pathogens are listed up in **Table 3**.

2.4.1 Neutrophilic reaction against extracellular pathogens

The extracellular pathogens growing outside the host cell, such as suppurative bacteria (*Staphylococcus*, *Streptococcus*, *Escherichia coli*, *Pseudomonas aeruginosa*, *Actinomyces*, etc.) and hypha-forming fungi (*Candida*, *Aspergillus* and *Mucorales*),

Defensing cell type	Pathogen	Host response	Compromised condition
Neutrophils	Extracellular pathogens	Abscess/phlegmone	Neutropenia
T-cells/Macrophages	Intracellular pathogens	Granuloma/lymphocytic infiltration	Cellular immunodeficiency*
B-cells/Neutralizing antibodies	Bacterial capsule/exotoxin viremic viruses	Not specified	Complement deficiency

**Steroid administration and acquired immunodeficiency (AIDS).*

Table 2.
Defense mechanism, pathogens and host responses.

I. **Neutrophilic accumulation** (abscess/phlegmone) against extracellular pathogens: Infection by suppurative bacteria, Enterobacteria, anaerobic bacteria, Actinomyces, Candida, Aspergillus and Mucorales provokes neutrophilic reactions.

II. **Cellular immunity** reactive against intracellular (cytozoic) pathogens:
   1. **Granuloma formation**: tuberculosis, Hansen's disease (tuberculoid leprosy), syphilis (stage III), typhoid fever, cryptococcosis, histoplasmosis, coccidioidomycosis, toxoplasmosis and leishmaniasis
   2. **Lymphocytic infiltration**: viral infection and rickettsiosis
   3. **Plasmacytic infiltration**: syphilis (stages I and II)
   4. **Macrophage infiltration**: xanthogranuloma/malakoplakia, *Legionella* pneumonia, lepromatous leprosy

III. **Host responses of other types**
   1. **Suppurative granuloma**: cat scratch disease (bartonellosis), lymphogranuloma venereum (chlamydiosis), listeriosis, yersiniosis, melioidosis, tularemia, brucellosis, sporotrichosis and chromomycosis
   2. **Eosinophilic infiltration**: infestation of nematodes and trematodes
   3. **Eosinophilic granuloma**: allergic bronchopulmonary aspergillosis
   4. **Foreign body granuloma**: parasitic ova (worm egg tubercle), primary *Anisakis* infestation

Table 3.
Host response against pathogens.

are principally phagocytized by neutrophils [27]. Infection of the extracellular pathogen thus results in abscess and phlegmonous inflammation, solely composed of neutrophils. In case of infection by non-invasive (extracellular) protozoa like *Trichomonas vaginalis*, neutrophilic exudation is activated to characteristically form so-called "cannon balls" (clusters of neutrophils). When the specific antibodies against the pathogen and complements are present in the body fluid, the phagocytic activity of neutrophils is significantly enhanced through an opsonin effect. Capsule-forming microbes frequently escape phagocytosis by neutrophils. In case of infection by anaerobic bacteria, massive ischemic necrosis is commonly associated.

Representative cytological features of neutrophil-mediated inflammation are illustrated in **Figure 11**. Accumulated neutrophils grossly correspond to pus (pyogenic exudates).

2.4.2 Cellular immune reaction against intracellular pathogens

Neutrophils and antibodies are ineffective against intracellular (cytozoic) pathogens. Instead, cell-mediated immunity functions as the major defense mechanism [28]: The infected host cells themselves are eliminated. The intracellular pathogen represents virus, chlamydia, rickettsia, protozoa, yeast-form fungi (*Cryptococcus*, *Histoplasma*, *Coccidioides*, etc.) and certain types of bacteria such as *Mycobacterium*, *Legionella* and *Salmonella*. Microscopically, lymphocytic infiltration (CD8-positive T-cell reaction) or granulomatous reaction is seen.

When macrophages are activated by the T-lymphocytes, epithelioid granulomas are formed. The epithelioid cells derive from activated macrophages. Multinucleated giant cells of Langhans type are often formed by plasma membrane fusion of the macrophages. Typical examples include tuberculosis, cryptococcosis and stage III syphilis. Necrosis is often associated with the granulomatous reaction, and in case of tuberculosis, caseous necrosis is characteristic. Typically, epithelioid granuloma with central necrosis is surrounded by small lymphocytes. Examples of cytology appearance of the granulomatous reaction in tuberculosis are shown in **Figure 12**.

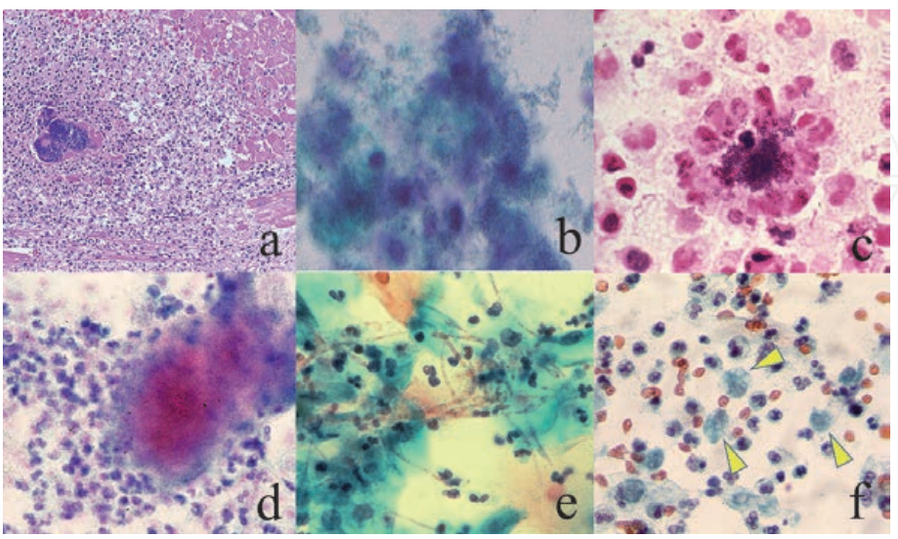

Figure 11.
Neutrophilic response against extracellular pathogens. a: MRSA-induced microabscess in the heart muscle in septicemia (H&E), b: Enterococcus faecium*-induced acute cystitis (urine sediment, Papanicolaou), c:* Streptococcus milleri*-induced pyothorax (Gram), d:* Actinomyces israelii*-induced endometritis (Papanicolaou), e: Hypha-forming* Candida albicans*-induced vaginitis (Papanicolaou), f:* Trichomonas vaginalis*-induced vaginitis (Papanicolaou). Extracellular pathogens, including* T. vaginalis *(arrowheads), are attacked by neutrophils. Neutrophils can fight against microbes larger than themselves (e and f).*

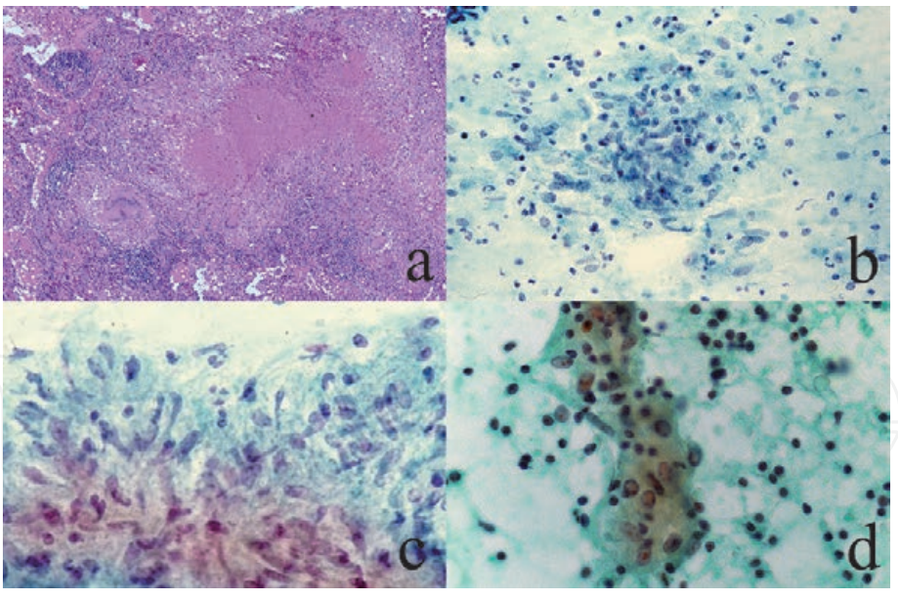

Figure 12.
Granulomatous inflammation against Mycobacterium tuberculosis*. a: Caseous granuloma in the lung (H&E), b and c: Epithelioid granuloma (Papanicolaou), d: A Langhans-type giant cell with lymphocytic infiltration. Three-layered structure is seen in caseous granuloma: Central caseous necrosis, epithelioid granuloma and lymphocytic cuffing (a). The epithelioid cells are rounded-spindle-shaped (c). Necrotic background is observed in b, and lymphocytes surround the multinucleated giant cell in d.*

In contrast, viral and rickettsial infection provokes infiltration of small T-lymphocytes without granulomatous reaction (**Figure 13**). In case of viral meningitis, lymphocytes are the major component in the cerebrospinal fluid. When lymphocytes are predominantly seen in the urine, the possibility of follicular cystitis caused by persistent infection of beta-hemolytic streptococci should be considered [29]. Similarly, the cervical smear preparation may contain lymphocytic reactions to be diagnosed as follicular cervicitis, and the possibility of *Chlamydia trachomatis* infection should be considered [30].

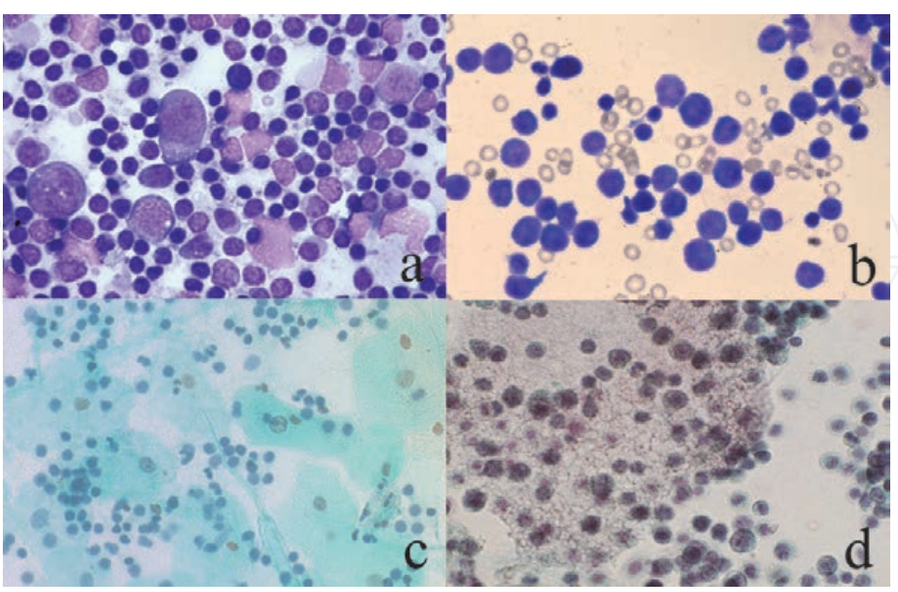

Figure 13.
Lymphocytic reaction in cytology specimens. a: Stamp smear of the reactive lymph node (Giemsa), b: Infiltration of activated lymphocytes in cerebrospinal fluid in a case of varicella-zoster virus-induced meningitis (Giemsa), c: Small lymphocytes seen in urine (Papanicolaou), d: Pneumocystis jirovecii *Pneumonia (Papanicolaou). In the lymph node, activated large-sized blastic cells are intermingled with small lymphocytes (a). Lymphocytes in viral meningitis reveal activated features with enlarged nuclei (b). Small lymphocytes are rich in the urine in a case of follicular cystitis (c). Small lymphocytes are seen around a cluster of* P. jirovecii*, resembling clustered hemolytic red cells (d).*

In case of *Legionella* pneumonia, macrophages comprise the main cellular reactant scarcely with lymphocytic infiltration. In cutaneous and visceral leishmaniasis, activated macrophages actively phagocytize the protozoan bodies. In visceral leishmaniasis (kala azar), the microbes are seen in activated Kupffer cells. In stages I and II syphilis, dense infiltration of plasma cells is characteristic. The gastrointestinal mucosa with chronic active gastritis and inflammatory bowel disease, as well as the nasal mucosa with chronic rhinitis and the gingival tissue with periodontitis or radicular dentigerous cyst, are also densely distributed by plasma cells. Plasma cells are often clustered in inflammatory foci of subacute inflammation or a subacute phase of inflammation [31]. Cytological features are represented in **Figure 14**. The cellular immunity-mediated removal of the infected parenchymal cells may cause functional insufficiency of the organs and tissues: Examples include hepatitis and encephalitis.

2.4.3 Humoral immunity via neutralizing antibody reaction

Neutralizing antibodies in the serum effectively eliminate pathogens that are distributed extracellularly. Typically, the neutralizing antibodies are produced against bacterial exotoxins, bacterial capsules and viral virions. Anti-viral antibodies are effective against the viral particles in the blood (during viremia) and body fluid. These features are applied to vaccination practice, and permanent immunity can be expected [32]. Vaccines injected subcutaneously induce IgG-type neutralizing antibodies in the serum. Oral vaccines such as Sabin vaccine against poliovirus and Rotavirus vaccine induce secretory IgA in the gut lumen. It is of note that IgG-type neutralizing antibodies in the serum can be transported with mucin by the IgG Fc-binding protein secreting from mucin-producing cells [23, 24]. Individuals with inherited complement deficiency, particularly the deficiency of C3 (the major opsonin), are vulnerable to recurrent pyogenic infections especially with

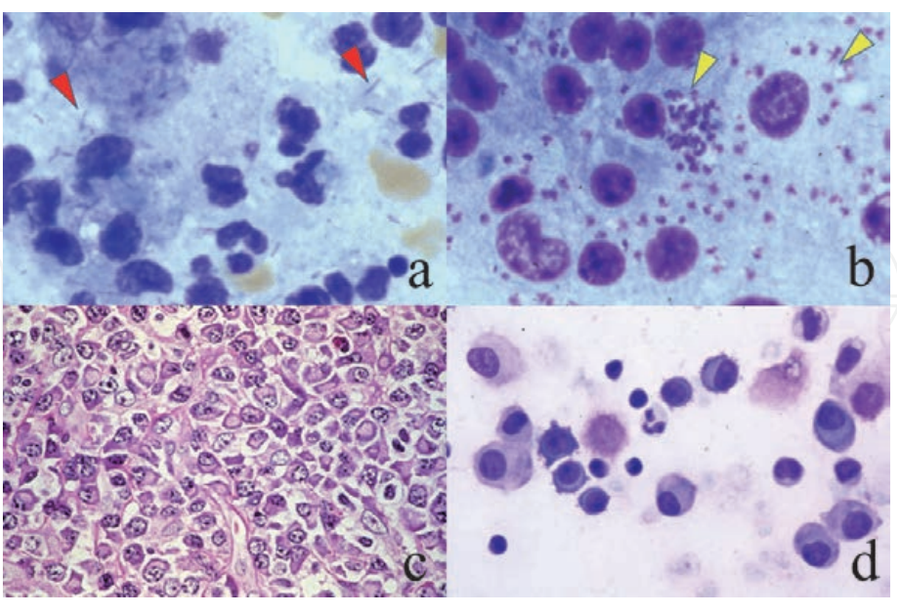

Figure 14.
Macrophage activation and plasma cell infiltration. a: Stamp preparation of Legionella pneumophila *pneumonia (Giemsa), b: Stamp preparation of the spleen with visceral leishmaniasis, c: Stage II syphilis (skin biopsy, H&E), d: Plasma cell infiltration in pleural effusion (Giemsa). Macrophages are activated but with minimal lymphocytic response in legionnaire's pneumonia and in leishmaniasis. The pathogens, rods (red arrowheads) in a and protozoan bodies (yellow arrowheads) in b, are phagocytized by the macrophages. Dense infiltration of plasma cells is a microscopic hallmark of stages I and II syphilis (c). The appearance of plasma cells in pleural effusion is infrequently encountered, since the plasma cells are poorly migratory. A subacute phase of infective pleuritis is suggested.*

encapsulated bacteria, including *Streptococcus pneumoniae* and *Neisseria meningitidis*. It is of note that sporadic meningococcal meningitis in adults may accompany inherited complement deficiency [33].

The activated humoral immunity is microscopically represented by follicular hyperplasia with enlarged germinal center formation in the lymph node and a variety of organs and tissues [34]. In fact, follicular hyperplasia is a microscopic feature of autoimmune disorders [35]. It has been clarified that a variety of cytokines are secreted from immunocytes to communicate each other and to secrete immunoglobulins. In particular, tumor necrosis factor (TNF) receptor-1 signaling is required for the differentiation of follicular dendritic cells, germinal center formation and antibody responses [36]. The germinal center also contains stimulated lymphocytes secreting interleukin-2 (IL-2) and interferon-gamma (IFN-γ) [37]. Representative examples of activated humoral immunity are demonstrated in **Figure 15**.

2.5 Host reactions against pathogens of other types

Host reactions against pathogens of other types are commented below.

1. Suppurative granuloma: An intermediate form of abscess and granuloma, that is called "suppurative granuloma" (abscess surrounded by granuloma), is seen in cat scratch disease (Bartonella infection), tularemia, listeriosis, yersiniosis, melioidosis and cutaneous mycosis (sporotrichosis and chromomycosis) [38]. Microscopic features of cat scratch disease involving the spleen are demonstrated in **Figure 16**.

2. Xanthogranuloma and malakoplakia: In certain situations, low-virulent extracellular pathogens, particularly *E. coli*, may grow intracellularly in the cytoplasm of macrophages, resulting in formation of xanthogranuloma (yellow-colored granuloma) [39]. Malakoplakia, a special form of the

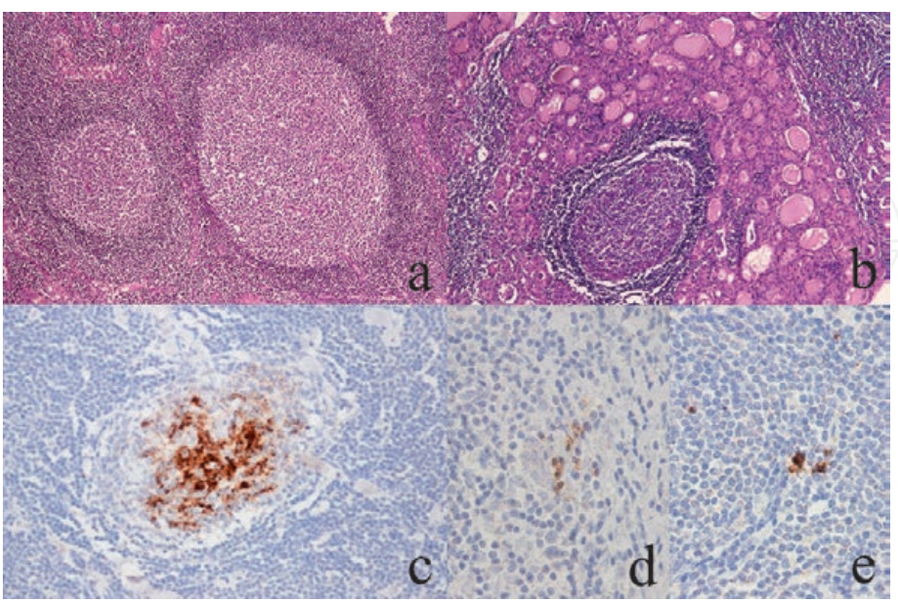

Figure 15.
Follicular (germinal center) hyperplasia, representing enhanced humoral immunity. a: Enlarged cervical lymph node (H&E), b: Hashimoto thyroiditis (H&E), c: TNF-alpha, d: IFN-gamma, e: IL-2. Lymphoid follicle formation with enlarged germinal centers microscopically indicates enhanced B-lymphocyte activation. Autoimmune disorders like Hashimoto thyroiditis often show follicular (germinal center) hyperplasia. TNF-alpha is densely deposited on the follicular dendritic cells (c). Lymphocytes immunoreactive for IFN-gamma and IL-2 are observed in the activated germinal center.

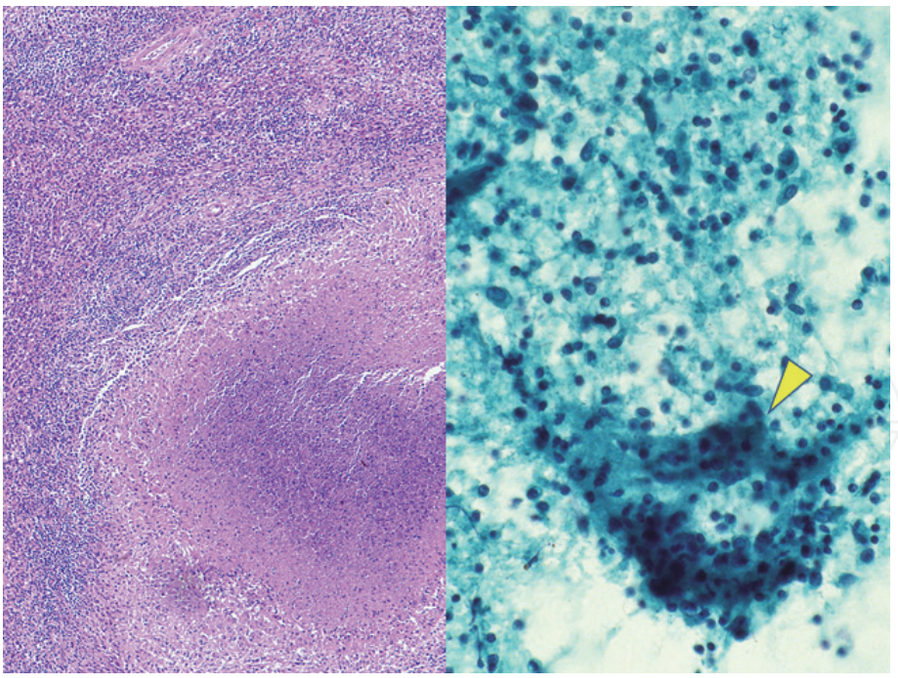

Figure 16.
*Suppurative granuloma seen in cat scratch disease (*Bartonella henselae *infection). Left: H&E (spleen), right: Stamp preparation (Papanicolaou). The surgically resected spleen grossly contains plural splenic abscesses. Histologically, suppurative granulomas, consisting of central abscess and surrounding epithelioid granuloma, are noted. Stamp cytological preparation demonstrates a cluster of epithelioid cells (arrowhead) in mildly necrotic background admixed with neutrophils and lymphocytes.*

xanthogranuloma, is microscopically featured by Michaelis-Gutmann bodies (round-shaped calcified and basophilic cytoplasmic inclusions). These lesions may be seen in the kidney, urinary bladder, epididymis, colon and gallbladder. Examples of malakoplakia and xanthogranulomatous inflammation are illustrated in **Figure 17**.

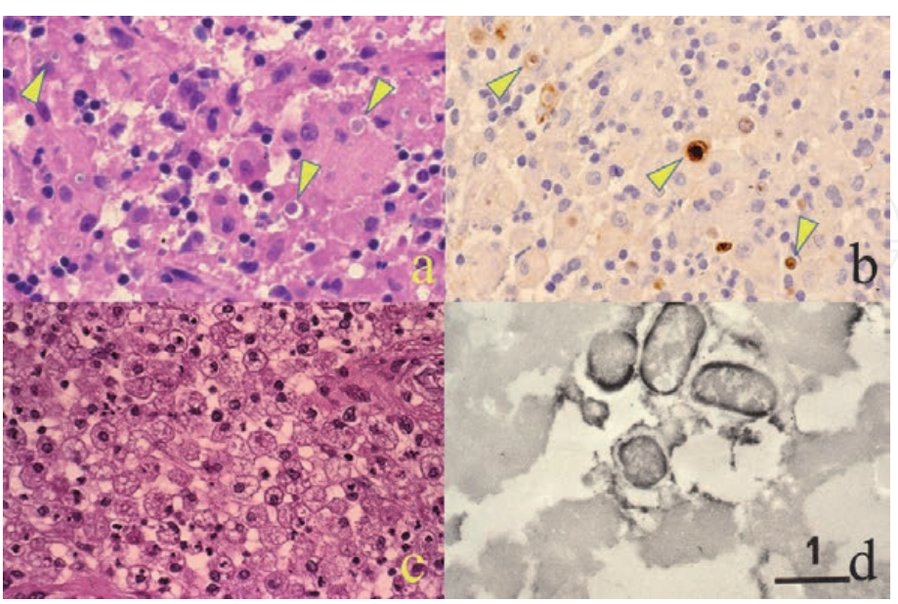

Figure 17.
Malakoplakia of the rectal mucosa (a, b) and xanthogranulomatous epididymitis (c, d). a and c: H&E, b and d: Immunostaining for E. coli *antigen (pre-embedding immunoelectron microscopy using a paraffin section in d). Malakoplakia is microscopically featured by Michaelis-Gutmann bodies, rounded basophilic cytoplasmic inclusions immunoreactive for* E. coli *antigens (arrowheads). Xanthogranuloma consists of accumulated foamy macrophages. Both lesions are caused by* E. coli *infection under an immunocompromised condition. Rod-shaped bacteria with cell wall labeling are proven in the cytoplasm of the foamy macrophage (d). Bar = 1 μm.*

3. Eosinophilic infiltration: Infestation of parasites, particularly round worm (nematode) and fluke (trematode), provokes infiltration of eosinophils and IgE-type immune response, common with the type 1 allergic reaction [40] (**Figure 18**). Cestode (tapeworm) infestation usually lacks the eosinophilic reaction. In case of allergic lung reaction against *Aspergillus* (allergic bronchopulmonary aspergillosis), eosinophilic granuloma (granuloma with eosinophilic infiltration) is observed [41]. Occasionally, foreign body reactions against worm bodies and ova are observed. Formation of multinucleated foreign body giant cells is characteristic (**Figure 19**). Parasitic ova induce foreign body granulomas to form so-called "worm egg tubercles". When eosinophilic infiltration is associated, immune-mediated eosinophilic granulomas are formed [42]. In case of anisakiasis, foreign body reactions without eosinophilic infiltration are seen against the Anisakis larva if the infestation occurs for the first time in a non-immunized patient after eating raw sea fish [43]. The mechanisms may be similar to the nonspecific phagocytic action of macrophages against genuine foreign bodies such as asbestos bodies and injected paraffin by augmentation mammoplasty.

4. Acellular hemorrhagic necrosis: In opportunistic infection associated with neutropenia and cellular immunodeficiency, the inflammatory cellular reactions are poorly provoked, resulting in hemorrhagic necrosis of the tissue [44].

3. Use of immunocytochemistry for cytology specimens

You must not give up additional staining even when you have one and only cytology specimen in hand. The resources for applying immunocytochemistry to the one and only cytology specimen are presented below. In case of liquid-based cytology (LBC), additional plural specimens are easily available. In Japan, however, the LBC procedure is still underdeveloped because of the low cost-performance. Therefore, these techniques are practically valid and helpful [45].

3.1 Cell block preparation

The sediments of liquid specimens such as pleural and pericardial effusions, ascites, the content of cystic lesions and urine can be kept for a long period of time as cell blocks after formalin fixation and paraffin embedding [46]. Immunostaining and *in situ* hybridization (ISH) method can be performed by preparing multiple paraffin sections from the cell block. So far, several technical inventions have been reported how to prepare cell blocks [47].

In **Figure 20**, chronic active Epstein–Barr virus (EBV) infection seen in a male case aged at his 20's is presented [48]. The patient manifested collagen disease-like signs and symptoms, such as fever, skin rash, muscle weakness, liver dysfunction and eosinophilia. In the ascites cytology specimen, a number of large granular lymphocytes (a form of atypical lymphocytes) were detected in the background with red cells, eosinophils and hemophagocytic macrophages. A cell block was prepared to know the nature of the lymphoid cells. The large-sized lymphocytes expressed natural killer cell markers such as CD45 and CD56, and EBV-encoded small nuclear RNA (EBER) was demonstrated in the nuclei by the ISH technique. The final diagnosis was chronic active EBV infection with virus-associated hemophagocytic syndrome. The prognosis of this disease is poor. In fact, the patient died of duodenal ulcer perforation seven months later. Of note is that EBV does not

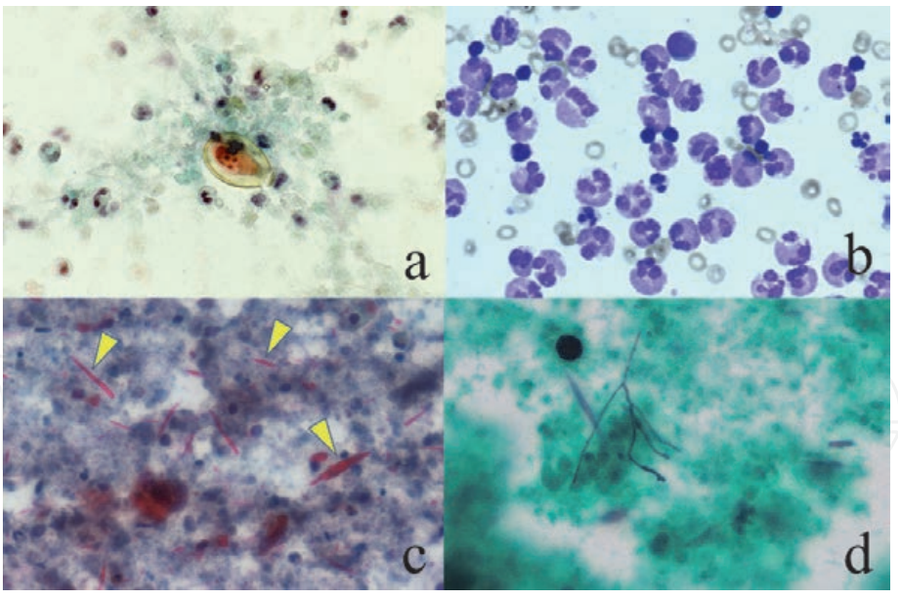

Figure 18.
Eosinophilic infiltration. a: Bile cytology in clonorchiasis (Papanicolaou), b: Eosinophilia in pleural effusion in tuberculosis (Giemsa), c and d: Allergic bronchopulmonary aspergillosis (sputum cytology, c: Papanicolaou and d: Grocott). A small-sized ovum of Clonorchis sinensis *with miracidium formation is seen in the bile and surrounded by eosinophils with bilobed nuclei (a). Eosinophils densely seen in the hemorrhagic pleural effusion in a case of tuberculosis may represent an allergic reaction against acid-fast bacilli (b). In allergic bronchopulmonary aspergillosis, rhomboid-shaped and red-colored Charcot-Leiden's crystals (arrowheads) deriving from eosinophilic granules are seen. Degraded eosinophils are observed in the background (c). Grocott stain identifies a few distorted* Aspergillus *hyphae phagocytized by a multinucleated giant cell (d).*

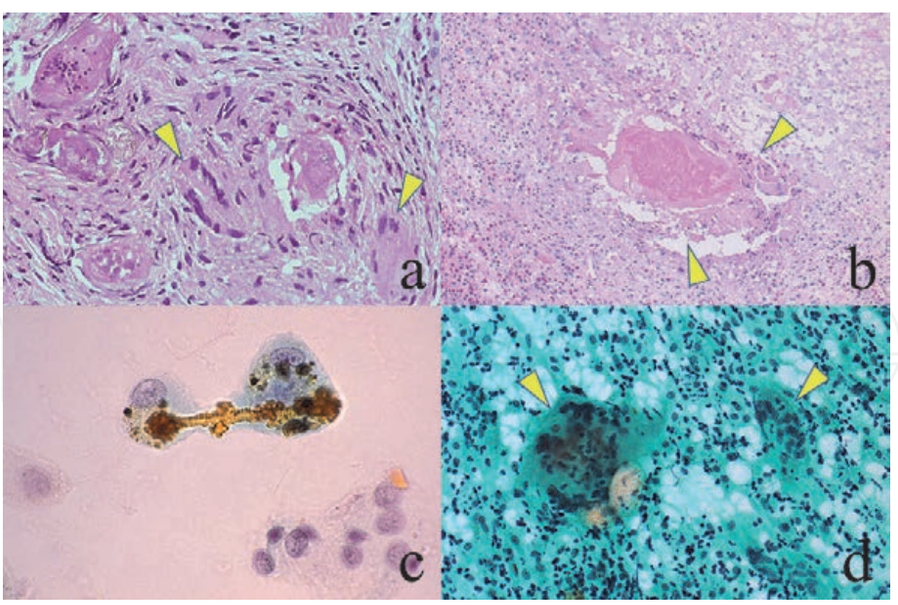

Figure 19.
Foreign body granulomatous reactions. a: A worm egg tubercle formed in the colonic submucosa in Schistosoma haematobium *infestation (H&E), b: An omental nodule by* Anisakis *larva migration (H&E), c: Asbestos body in the sputum (Papanicolaou), d: Fine needle aspiration from a nodular lesion post augmentation mammoplasty (Papanicolaou). Foreign body reactions with multinucleated giant cells are noted around schistosoma eggs with miracidium formation (a) and a dead nematode larva (b). Eosinophilic reactions are scarcely seen. For the comparison, two examples of genuine foreign bodies are shown. Asbestos bodies (c) and paraffin oil droplets (d) injected by augmentation mammoplasty are phagocytized by macrophages. A long, brown-colored asbestos fibril is engulfed by two macrophages in c. vacuolated cytoplasm filled with lipid-soluble substances is characteristic, and multinucleated giant cells are dispersed in d. Arrowheads indicate multinucleated giant cells.*

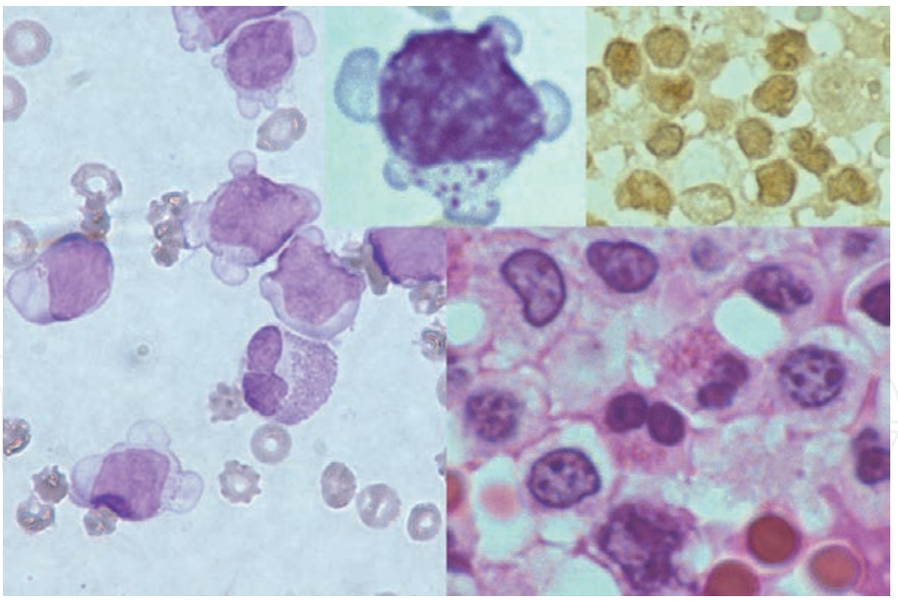

Figure 20.
Chronic active EBV infection (ascites cytology, left, Giemsa, left inset: High-powered view, right: Cell block H&E, right inset: EBER). Hemorrhagic ascites contains large granular lymphocytes and eosinophils. Azurophilic granules are noted in the cytoplasm of the large granular (atypical) lymphocytes. In cell clock preparation, the nuclei of atypical lymphocytes are positive with EBER-ISH method. No intranuclear inclusions are visible.

produce viral particles in the infected cell, so that no intranuclear inclusions are formed and thus the EBER technique is needed.

3.2 Re-staining method

A re-staining method is applicable to the single (one and only) cytology specimen [49, 50]. At first, the cells or areas of target should be marked on the back side of the glass slide with a diamond-tip pen and then photomicrographed. After removal of the coverslip in xylene, stained dyes can be removed by dipping in acid alcohol solution (50% ethanol containing 0.5% hydrochloric acid) for hours or simply dipping specimens in tap water overnight. The immunostained cells or areas of target are re-photomicrographed for comparison.

In case of Giemsa-stained glass slides or immunostained preparations on trimethoxy[3-(phenylamino)propyl]silane-coated glass slides, the re-staining method is especially valuable, since the cell transfer technique described below is not applicable due to tight attachment of the cells.

In **Figure 21** showing scraping cytology of herpes simplex virus (HSV) infection on the vulva, the re-staining method visualizes intranuclear and intracytoplasmic viral antigens. A commercially available polyclonal antibody was used for immunostaining. Vulvar HSV infection belongs to sexually transmitted disease (STD).

Figure 22 demonstrates chlamydial cytoplasmic inclusions, so-called "nebular inclusion bodies", in the scraping cytology from the uterine cervix. Chlamydiosis also represents STD. The inclusions are clearly re-stained with a monoclonal antibody B104.1 against *Chlamydia trachomatis*. Tiny cytoplasmic inclusions, visualized with immunostaining, are scarcely recognizable in the Papanicolaou-stained preparation.

3.3 Cell transfer technique

If you have one and only glass slide of Papanicolaou-stained cytology specimen or hematoxylin and eosin (H&E)-stained histology specimen and you want to

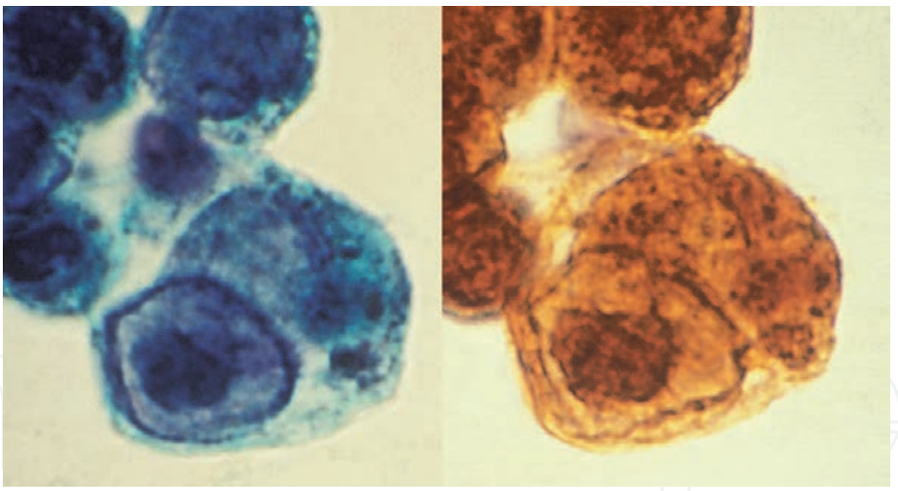

Figure 21.
Herpes simplex virus infection (scraped from vulva, left: Papanicolaou, right: HSV immunostaining). With re-staining method, viral antigen immunostained with a polyclonal antibody are localized both in the haloed nuclei and in the cytoplasm.

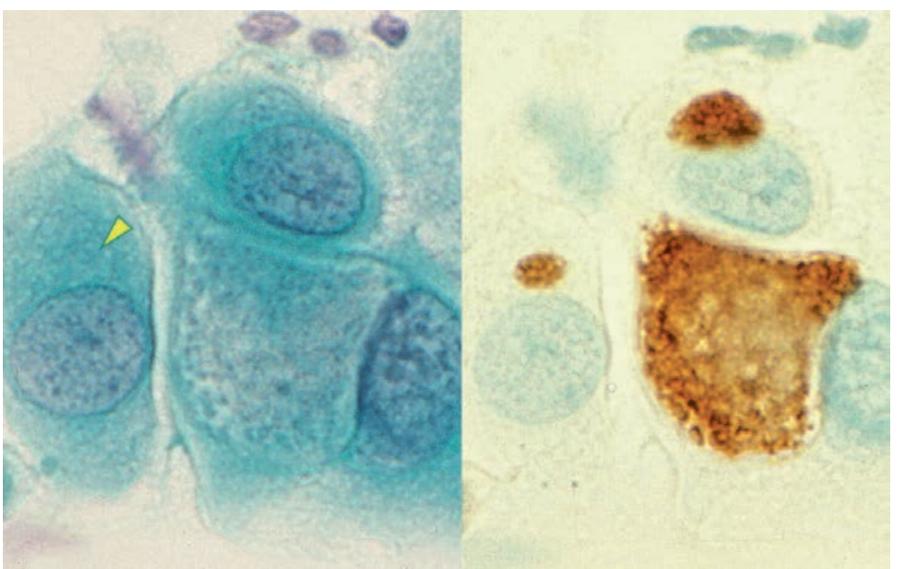

Figure 22.
Chlamydial infection (cervical smear, left: Papanicolaou, right: Immunostaining with monoclonal antibody). With re-staining method, the nevular inclusion bodies in the cytoplasm are clearly labeled for the chlamydial antigen. A tiny inclusion in the left-sided cell (arrowhead) is scarcely recognizable in the pap smear.

evaluate the expression of immunocyto/histochemical markers, the cell transfer technique [51] is quite useful and valuable (**Figure 23**). Firstly, cover slips must be removed by dipping in warmed xylene. Secondly, the specimen is covered with a mounting medium/resin at 2–3 mm thickness, in order to form a coating film of the solidified mounting medium in a warm incubator overnight. Then, the film of the solidified resin should be peeled off the glass slide by dipping in warm water for one hour to get the cells or tissues transferred onto the film side. The solidified resin film is placed in water on the silane-coated glass slide to be dried in a warm incubator. Finally, the resin component can be removed by dipping in xylene to get the cells and tissues transferred to a new glass slide. You can obtain plural glass slides if the solidified resin is cut by scissors into several pieces.

Cells smeared outside the cover slip can be transferred to another glass slide without removing the cover slip (**Figure 23**). This is particularly useful in case of gynecological cytology specimens.

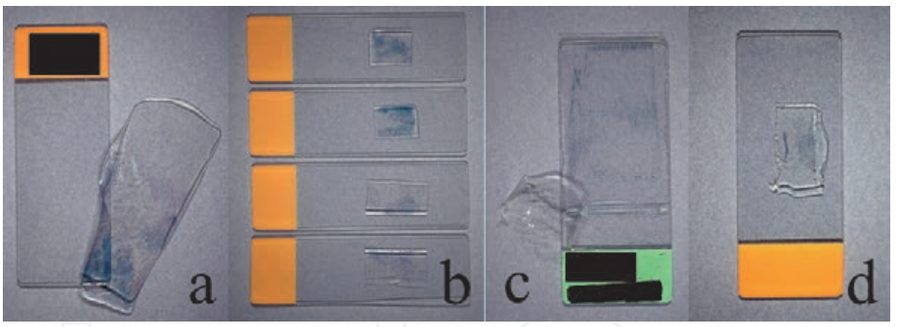

Figure 23.
Cell transfer technique. a&b: Papanicolaou-stained cells in the cervical smear are transferred to solidified resin film, and the film was cut into pieces to get plural specimens placed on silane-coated glass slides. c&d: Cells smeared outside the cover slip can be transferred to another glass slide without removing the cover slip.

By a conventional technique of cell transfer, it takes time to have the cells transferred. Itoh et al. [52] invented a time-saving method to get the cells transferred in one hour (**Table 4**). In brief, the mounting medium should be diluted two-fold by xylene, and the rein film should be solidified on a hot plate at 70–80C.

When the target cells in the specimen are few in number, it is recommended to have the cells marked with a diamond-tip pen on the back side of the glass slide before removal of the cover slip. When an archival long-kept and fully dried specimen is used, the cover slip removal is not easily achieved. In order to accelerate the removal, xylene solution should be warmed up to 70–80C and/or the cover slip should be cracked with a diamond-tip pen.

Harada et al. [53] reported that detachment of the cover slip is accelerated by using a packaging duct tape, as summarized in **Table 5**. **Figure 24** illustrates the step of Harada's method for rapid removal of the cover slip. The method is applicable to archival glass slides long kept at room temperature for 20 years. It takes only one hour to remove the cover slip. By combining Harada's method with the above-mentioned Itoh's quick method for the cell transfer, old cytology glass slides become ready for immunocytochemical analysis within a few hours.

1. *Removal of cover slip*
   The cover slip can be removed by dipping in warm xylene
2. *Application of mounting medium*
   The mounting medium (e.g. Malinol®, Muto Chemicals, Tokyo) should be two-fold diluted by xylene and one mL of the diluted resin is placed onto the smeared cells on the glass slide.
3. *Solidification*
   The resin should be solidified for 30 minutes on a hot plate at 70–80C.
4. *Softening*
   The glass slide with an adherent resin film should be soaked for 15 minutes in warm water at 50–60C.
5. *Detachment*
   The softened resin film can be peeled off the glass slide with forceps. The detached film can be divided into several pieces with scissors.
6. *Pasting*
   The resin film is soaked in water and pasted onto a new silane-coated glass slide. Caution is needed for the recognition of the right side of the film. After removal of excessive water, the cell-transferred glass slide should be dried on a hot plate at 70–80C. You can prepare plural glass slides when the resin film is cut into several pieces by scissors.
7. *Removal of solidified resin*
   The solidified resin can be removed by dipping in xylene. Hydration is then achieved through placing the glass slide in ethanol. The specimen is ready for immunostaining.

Table 4.
Itoh's time-saving cell transfer technique.

1. *Preparing warm xylene*
   A glass container is kept warm at 62–64C in an incubator.
2. *Preparing a packaging duct tape cut to the cover slip size*
   The packaging duct tape should be cut to fit the cover slip, a little bit larger than the size of the cover slip.
3. *Soaking of the glass slide in warm xylene*
   The glass slide is soaked in warm xylene for 40 minutes.
4. *Wiping out xylene*
   Warm xylene is wiped completely from the cover slip with KimWipes® (Kimberly Clark Corp, Irving, Texas, USA).
5. *Sticking the packaging duct tape*
   A piece of the packaging duct tape is evenly stuck onto the cover slip. Confirm uniform sticking of the packaging duct tape (without bubbling) by observing from the back side.
6. *Peeling off the cover slip*
   The packaging duct tape should be removed together with the cover slip at a breath without hesitation.
7. *Soaking the glass slide in xylene*
   The glass slide is then soaked in xylene at room temperature, being ready for the next step.

Notice: The steps 4–7 should be performed as quick as possible.

Table 5.
Harada's method for rapid removal of cover slip.

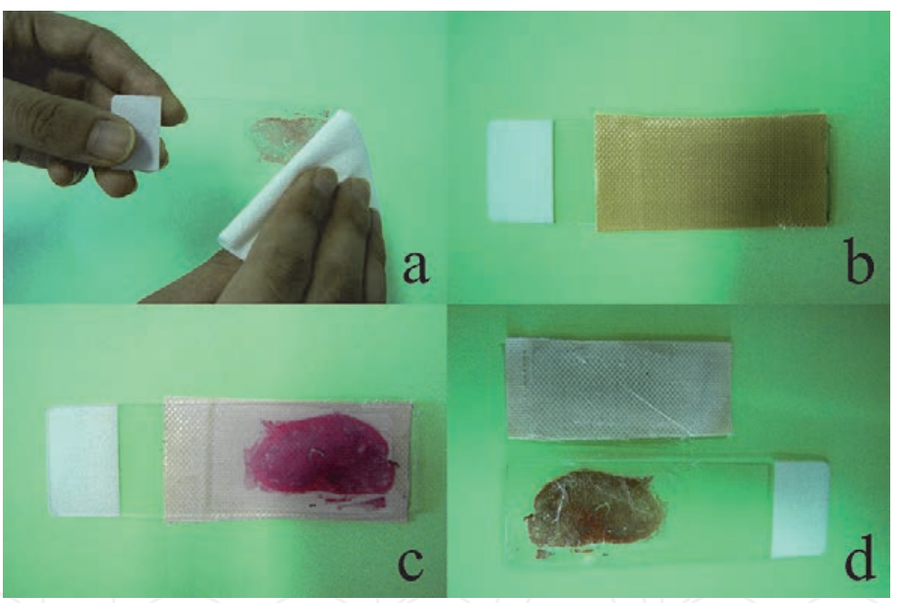

Figure 24.
Harada's rapid removal of cover slip using packaging duct tape (H&E-stained prostate section kept at room temperature for 20 years). a: Wipe off warm xylene with KimWipes®, b: Stick a piece of the packaging duct tape cut a little bit larger than the cover slip evenly onto cover slip, c: Confirm from the back side that the tape was uniformly stuck without bubbles, d: Peel off the packaging duct tape together with the cover slip at a breath.

Figure 25 displays identification of human papillomavirus (HPV) type 16 genome in the nuclei of severely dysplastic cervical squamous cells. The cells in the routine cervical smear were transferred onto the silane-coated glass slide, and the ISH technique was applied to localizing the viral genome in the nuclei of the dysplastic cells. The cell transfer step is essentially requested to avoid detaching the cells during the staining step, because heating pretreatment of the specimen is inevitable for the ISH technique. In this way, the Papanicolaou-stained cytomorphology and the state of HPV infection can directly be compared in the same cervical cells.

The cervical smear was prepared from a postmenopausal lady, and we had one and only glass slide in hand. The cells on the glass slide were transferred to another silane-coated glass slide. The clustered atypical parabasal keratinocytes in the background of senile colpitis were positively stained for p16-INK4a, indicating the

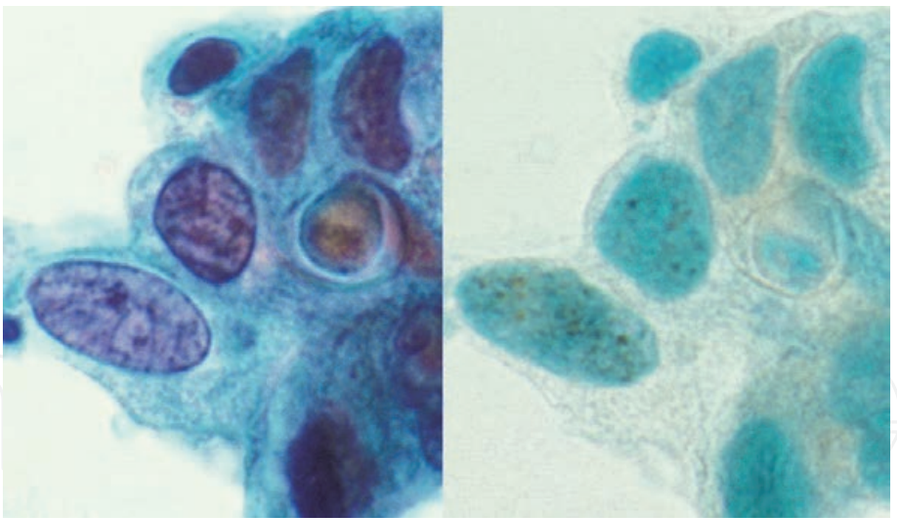

Figure 25.
Severe dysplasia of uterine cervix (left: Papanicolaou, right: ISH for HPV, type 16 genome). The cells were transferred onto a silane-coated glass slide to localize HPV, type 16 genome by ISH technique, requiring heating pretreatment. Dotted signals are seen in the dysplastic nuclei. The microscopic features of HPV infected cells can directly be compared with those of pap staining.

carcinogenic HPV infection (HPV-infected genuine dysplasia or high-squamous intraepithelial lesion) [45], as illustrated in **Figure 26**. In this way, genuine HPV-related dysplasia was distinguished from reactive (benign) atypia of the parabasal keratinocytes secondary to senile atrophy. Heating pretreatment is an essential step for immunolocalizing p16-INK4a that is a tumor suppressor gene product for modulating the cell cycle. Carcinogenic HPV infection inactivates retinoblastoma (RB) gene leading to the overexpression of p16-INK4a. In other words, the p16-INK4a is a marker of HPV-infected cells in the uterine cervix [54].

It should be noted that the cell transfer technique is applicable to paraffin sections, as well as Papanicolaou-stained cytology specimens in the gynecologic and respiratory fields, but Giemsa-stained cytology preparations employing dry fixation

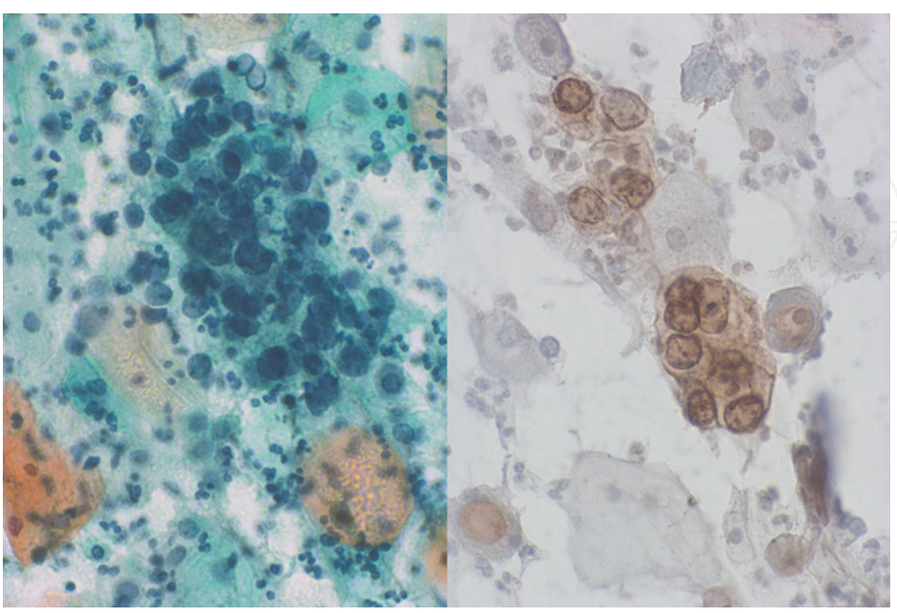

Figure 26.
Moderate dysplasia of uterine cervix after menopause (left: Papanicolaou, right: Immunostaining for p16-INK4a). Dysplastic change and reactive atypia secondary to senile colpitis should be distinguished. The expression of p16-INK4a confirmed the precancerous state of the cervix in this postmenopausal female patient. After the cell transfer onto the silane-coated glass slide, p16-INK4a was immunostained by employing heat-induced antigen retrieval.

and cytology specimens of liquid form smeared on silane-coated glass slides are not suitable for the cell transfer technique.

The cell transfer technique can be applied to the transfer of the cohesive cells cultured on the plastic slide (Nunc Lab-Tek® chamber) to the silane-coated glass slide. Xylene is not applicable to the plastic slide and the cover slip cannot be placed on the plastic slide. The broken glass slides can be repaired by employing the cell transfer technique (**Figure 27**) [55].

3.4 Application of cytology specimens to ultrastructural study and polymerase chain reaction analysis

The ethanol-fixed cytology specimens can be applied to electron microscopic and immunoelectron microscopic study. Fine structures of viral particles and chlamydial bodies are preserved even after ethanol fixation. **Figure 28** demonstrates immunoelectron microscopic observation of chlamydial antigen in a uterine cervical columnar cell. In the nebular inclusion body in the ethanol-fixed cell, both elementary bodies and reticulate bodies of the chlamydial microbe are clearly observed. The plasma membrane of the particles is positively labeled with the monoclonal antibody [56]. **Figure 29** schematically illustrates the cell cycle of *C. trachomatis* in the infected cell. Smaller-sized elementary bodies represent the infectious particles, while larger-sized reticulate bodies belong to the proliferative form. ISH technique can also be applied to cytology preparations [57].

Pathogens are often localized in a limited part in the specimen. It is practical and convenient for us to focus target on the infected cell for (immuno)electron microscopic study. At first, immunostaining with diaminobenzidine color reaction should be performed at the light microscopic level. After taking photomicrographs, the cover slip is removed, the specimen is re-fixed in 1% osmium tetroxide solution, and the cells are targeted for epoxy resin (Epon) block preparation by employing the inverted beam capsule method. Ethanol fixation accelerates penetration of antibody molecules into the cell, so that routine method for the light microscopy gives us an excellent result also at the ultrastructural level. Fine morphology of particulated microbes is well preserved even after ethanol fixation.

The cytology specimen can be analyzed with polymerase chain reaction (PCR) analysis by employing the cell transfer technique. The solidified resin film prepared

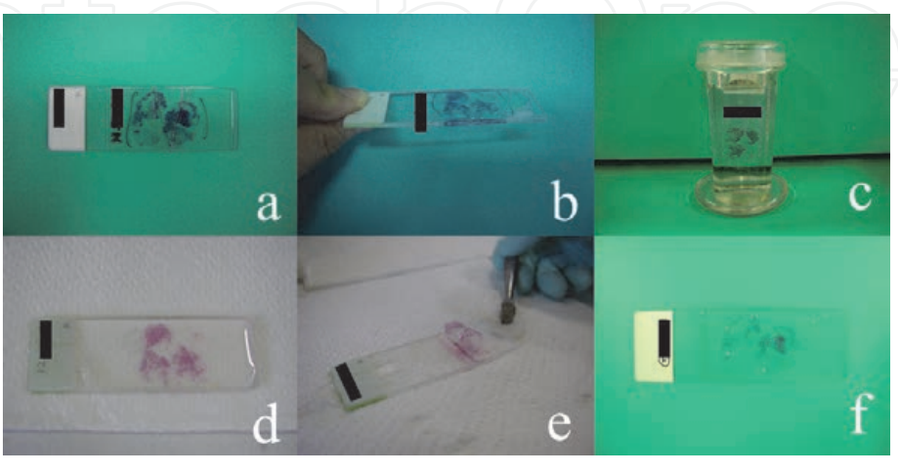

Figure 27.
Repair of a broken glass slide employing the cell transfer technique. a: The glass slide was broken, b: The broken slide is supported by another glass slide underneath adhered with epoxy glue, c: Cover slip is removed in warm xylene, d: Mounting medium (resin) is covered on the glass slide, e: Solidified resin film is peeled off after dipping in warm water, f: The resin film is pasted onto a new glass slide. After enough drying, the resin is removed in xylene and then a cover slip is set.

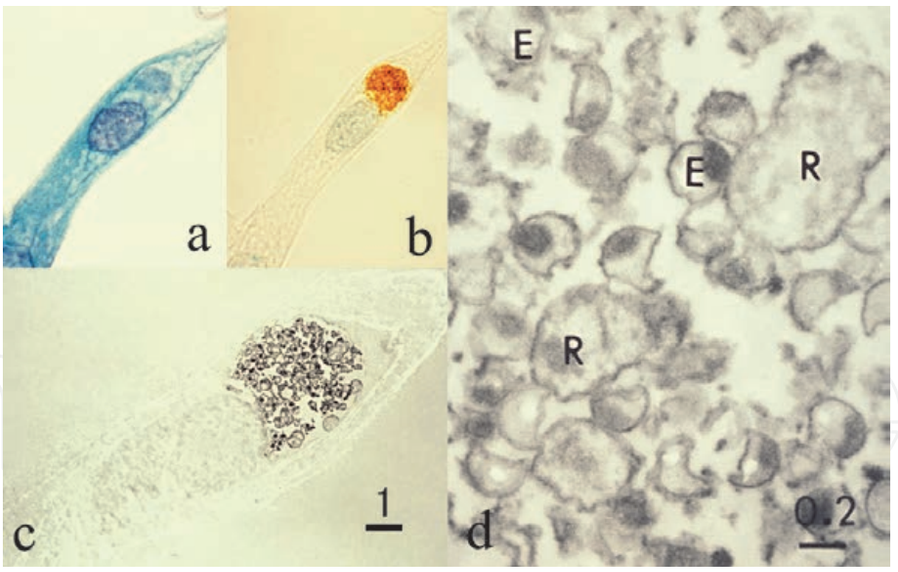

Figure 28.
Immunoelectron microscopic study for chlamydial antigen using an ethanol-fixed cervical smear. a: Papanicolaou, b: Immunostaining for Chlamydia trachomatis *antigen, c&d: Immunoelectron microscopy using the pre-embedding method, c: Low power, d: High power, E: Elementary body, R: Reticulate body, bars = 1 μm (c) and 0.2 μm (d). The chlamydial antigen is localized on the particle membrane. Reticulate bodies are larger than elementary bodies. Fine morphology is fairly well preserved even after ethanol fixation.*

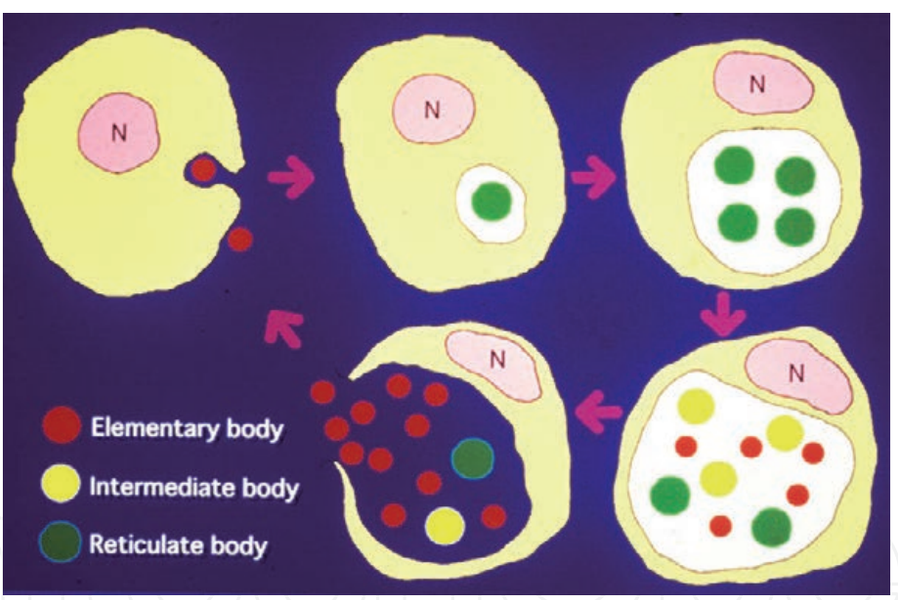

Figure 29.
Schematic presentation of the growth cycle of Chlamydia trachomatis*. Smaller-sized elementary bodies (red) infect the cell, and larger-sized reticulate bodies (green) proliferate to form intracytoplasmic nevular inclusions. Intermediate bodies (yellow) indicate a transitional form between the reticulate ad elementary bodies. N = nucleus.*

from a Papanicolaou-stained smear should be cut by scissors. Parts of the specimen are kept as Papanicolaou-stained slides, while DNA or RNA can be extracted from the other parts after xylene treatment [45].

Figure 30 illustrates *Entamoeba gingivalis* colonization in inflamed exudate seen around an intrauterine contraceptive device (IUD). Microscopically, amebic trophozoites are scattered around actinomycotic grains [58]. The patient aged in her 50's complained of white-colored fluor genitalis. After removal of the IUD, cytological specimens were sampled from the surface of the device. The postmenopausal lady totally forgot the artificial material inserted in her uterus. In order to confirm the diagnosis, PCR analysis was performed by utilizing the cell transfer technique.

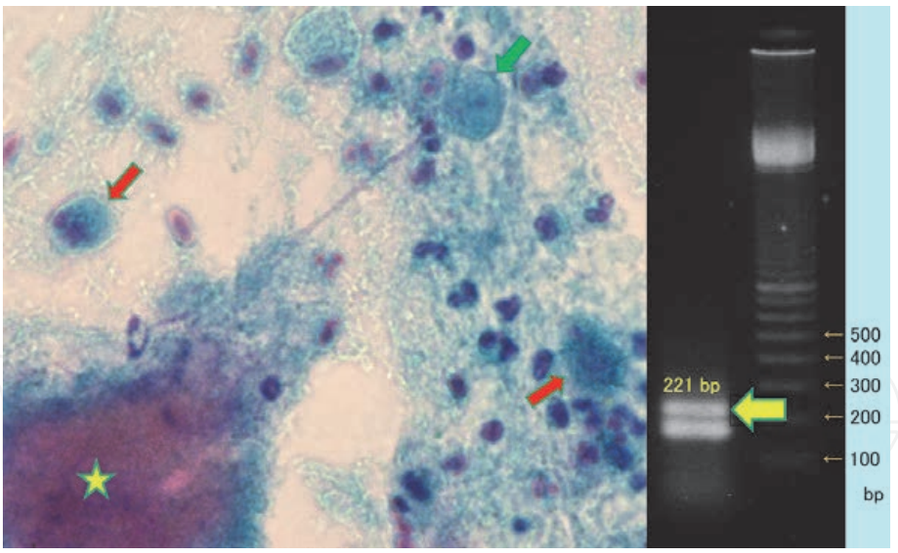

Figure 30.
Entamoeba gingivalis *colonized around an intrauterine contraceptive device, analyzed by PCR employing the cell transfer technique. Left: Papanicolaou, right: Electrophoresis banding of the amplified product. Amoeba-like cells phagocytizing neutrophils (red arrows) are seen around the actinomycotic grain (asterisk). The centrally located nucleus with a prominent karyosome is seen (green arrow). DNA was extracted from cell-transferred pieces. PCR was run for 35 cycles. DNA sequence of* E. gingivalis *was proven from the 221 base-paired band (yellow arrow). Sense primer: 5′-tcagataccgtcgtagtcct-3′, antisense primer: 5′-cctggtgtgcccttccgt-3′.*

The DNA sequence of *E. gingivalis* was identified from the 221 based band on the gel. It was evident that oral sex had caused the infection of anaerobic residents of the oral cavity (both *Actinomyces* and *E. gingivalis*) [59] around the artificial material. The growth of *Actinomyces*, an obligate anaerobic microbe, allowed the survival of *E. gingivalis*, an obligate anaerobic protozoan, in the uterine cavity.

4. Cytodiagnosis of bacterial infection

The cytology service has a significant role in the detection and presumptive identification of microorganisms [60]. Generally speaking, the cytodiagnosis of bacterial infection can be reached more easily for extracellular pathogens than for intracellular pathogens. It should also be noted that bacteria are more steadily observed in Giemsa-stained preparations than in Papanicolaou-stained preparations. For immunocytochemical confirmation, the techniques mentioned above (the usage of cell block and re-staining or cell transfer technique) are valuable. Representative examples of the cytodiagnosis of bacterial infection are described below.

4.1 Bacterial vaginosis

Large-sized Gram-positive rods, *Lactobacillus* or so-called Döderlein bacilli, are the normal flora (indigenous microbiota) of the vagina and maintain the local acidity at pH 3.8–4.5 by producing lactic acid. Their length ranges from 2 to 9 μm, with the width of 0.5 to 0.8 μm. The lactic flora produces hydrogen peroxide and antimicrobial peptides (bacteriocins) to inhibit growth of other microbes [61]. The number of the non-mobile bacilli is increased around the period of ovulation through the secretory phase of the menstrual cycle. Döderlein bacilli are seen in healthy mature (premenopausal) women, but after menopause without hormonal activity, they are no longer observed in the cytology preparation. In Papanicolaou-stained preparations, they look like homogeneously basophilic large rods without

spore formation. The background generally shows paucity of inflammation, but they are occasionally phagocytized by neutrophils [62].

In case of bacterial vaginosis (vaginitis), abnormal bacteria grow and Döderlein bacilli are markedly decreased or totally disappear [63, 64]. Representative example is Gardnerella vaginitis caused by infection of *Gardnerella vaginalis*, a small (1 to 1.5 μm-sized) Gram-negative non-mobile coccobacillus. The small bacteria, *G. vaginalis*, often cluster on the squamous cells of the superficial type to form so-called "clue cells". *Gardnerella* infection is often evident in a proliferative phase of the menstrual cycle. The infection is commonly associated with neutrophilic reaction, but poor neutrophilic response may be seen in some cases, hence the term "bacterial vaginosis", instead of bacterial vaginitis.

Another microbe causing bacterial vaginosis is *Mobiluncus*, spp., a V-shaped or crescentic, mobile, obligate anaerobic bacillus with unstable Gram reactivity. The size is intermediate between Döderlein bacillus and *G. vaginalis*. *Atopobium (Fannyhessea) vaginae*, a small-sized (less than 1 μm), obligate anaerobic Gram-positive elliptical coccobacillus often forming a short chain (somewhat resembling streptococcus), is a recently reported member causing bacterial vaginosis [65]. The growth of filamentous long-shaped bacillus, *Leptothrix*, may be associated with bacterial vaginosis. After menopause, these bacteria may often be replaced by enterobacteriae such as *Escherichia coli* and *Klebsiella pneumoniae*. *Pseudomonas aeruginosa* may colonize the vaginal mucosa, accompanying biofilm formation (refer to **Figure 37**). All these microbes provoke neutrophilic exudation.

Figure 31 displays representative cytomorphology of vaginal bacteria in Papanicolaou-stained preparations.

4.2 Chlamydial infection

Chlamydiosis is a representative and common STD. Symptomatic non-gonococcal urethritis is seen in male patients, while symptoms are mild in females. Columnar epithelial cells infected with *Chlamydia trachomatis* contain round-shaped cytoplasmic inclusion bodies named as nevular inclusion bodies [66]. The

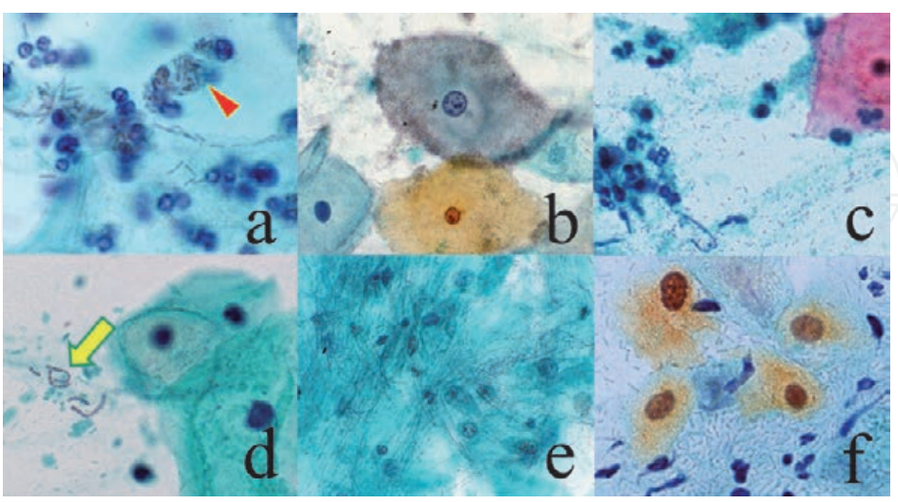

Figure 31.
*Döderlein bacillus (*Lactobacillus*) and microbes causing bacterial vaginosis (cervical smears, Papanicolaou). a: Döderlein bacillus, b:* Gardnerella vaginalis*, c:* Mobiluncus*, d:* Atopobium vaginae*, e:* Leptothrix*, f:* Klebsiella pneumoniae*. Döderlein bacilli, a normal vaginal resident, is large-sized and occasionally phagocytized by neutrophils (arrowhead).* G. vaginalis *is small-sized and often clustered on the superficial keratinocytes to form "clue cells".* Mobiluncus *is intermediate-sized and V- or crescent-shaped.* A. vaginae *appears as chained coccoid microbes, resembling* Streptococcus *(arrow).* Leptothrix *is non-pathogenic filamentous bacteria.* K. pneumoniae *Is a capsule-forming, large-sized bacillus mainly seen on the postmenopausal vaginal mucosa.*

life cycle of Chlamydia is shown in **Figure 29**. Immunocytochemistry using the re-staining method or cell transfer technique is quite effective for making a diagnosis of chlamydiosis (refer to **Figures 22** and **28**). In most cases of chlamydiosis, bacterial vaginosis is associated, so that a variable number of neutrophils are seen in the background. Chlamydial infection commonly causes lymphoid follicle formation in the mucosa: Lymphocytic background may be seen in the cervical smear preparation, as *C. trachomatis*-associated follicular cervicitis [67].

Chlamydial inclusions are also seen in cytology specimens scraped from male urethra. *C. trachomatis* causes epididymitis and salpingitis. Extragenital chlamydiosis should be of notice [68]. Chlamydial pharyngitis and proctitis are mediated by oral sex and anal sex, respectively. Acute chlamydial conjunctivitis occurs in sexually active young men, and the cytoplasmic inclusions are demonstrated by quick Giemsa (Diff-Quik) staining. Representative features are shown in **Figure 32**.

4.3 Gonococcal infection

Gonorrhea is a classic example of STD. *Neisseria gonorrhoeae*, a Gram-negative paired coccus (diplococcus), causes acute urethritis in male, and it shows high affinity to urethral epithelial cells [69]. **Figure 33** demonstrates urine cytology from a 28 year-old single Japanese male patient. It should be of note that paired cocci are specifically attached onto the large-sized squamous cells of urethral origin. Typically, diplococci are phagocytized by neutrophils. Cytological diagnosis of gonorrhea can be made immediately.

4.4 Bacteria growing in liquid specimens and effusions

Acute cystitis is common in women, most often caused by *Escherichia coli* infection. Pyruria is an important sign of bacterial cystitis. In case of acute cystitis in

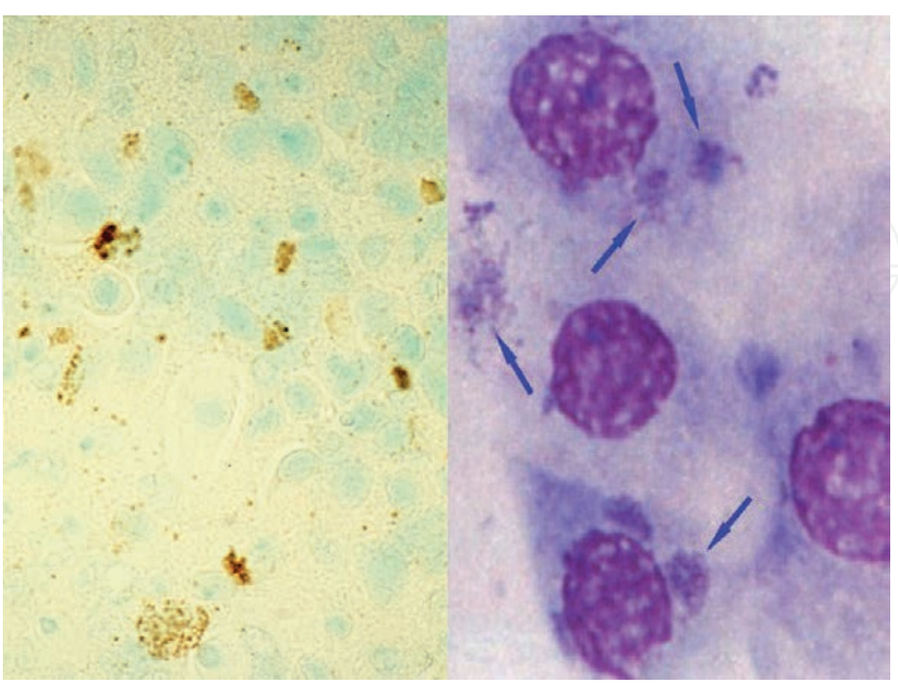

Figure 32.
Chlamydial infection (left: Immunostaining for chlamydial antigen in scraped male urethra with methylgreen counterstain, right: Giemsa-stained scraping cytology of conjunctiva). Numbers of urethral and conjunctival epithelial cells possess chlamydial cytoplasmic inclusion bodies. Note extragenital infection of C. trachomatis *on the eye (arrows).*

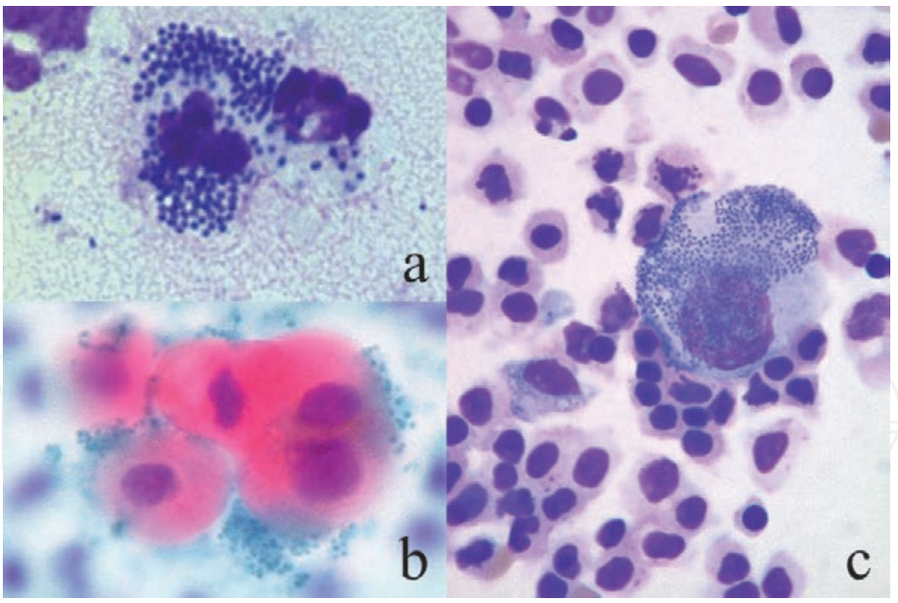

Figure 33.
Gonococcal infection (a: Urethral discharge, Giemsa, b&c: Urine cytology, Papanicolaou [b] and Giemsa [c]). Paired cocci are phagocytized by a neutrophil in pyogenic urethral discharge (a). Neisseria gonorrhoeae *reveals specific affinity to urethral squamous epithelial cells (b&c). The background urothelial cells of urinary bladder origin are devoid of colonization. By courtesy of Mr. Tomohiro Watanabe, Chuken Kumamoto, Japan.*

aged men, the association of prostatic gland hyperplasia causing urethral stenosis should be considered. Urinary bladder cancer may often associate bacterial growth in the urine. Rods mostly represent *E. coli*, while chained cocci usually belong to *Enterococci* (**Figure 34**). Refer also to **Figure 11b**, where cocci (*Enterococcus faecalis*) are actively phagocytized by neutrophils in urine. Particularly when neutrophilic reaction is evident, the diagnosis of bacterial cystitis should be added to that of urothelial carcinoma.

Similarly, bile cytology specimens may reveal bacillary growth around adenocarcinoma cells. The possibility of ascending purulent cholangitis due to malignant

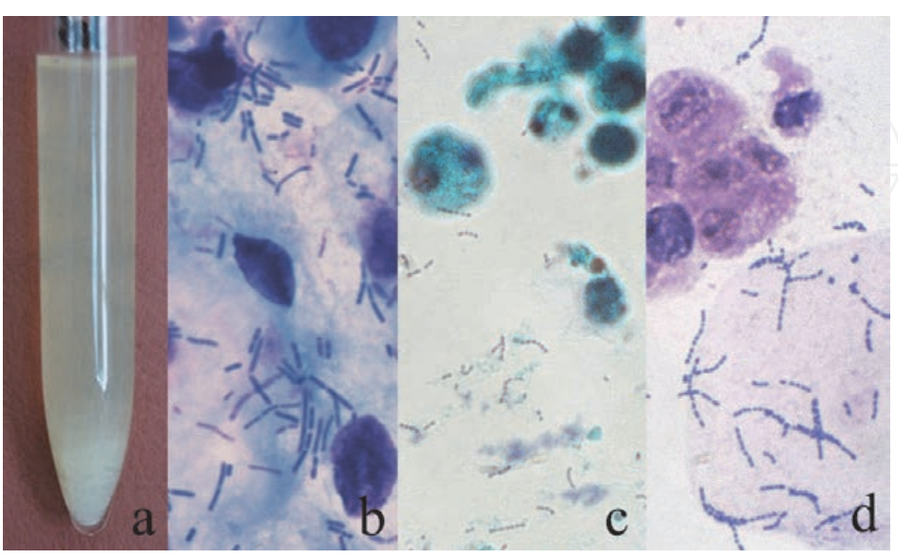

Figure 34.
Bacterial acute cystitis (a: Gross appearance of pyuria, b: Rods, Giemsa, c&d: Chained cocci with urothelial cancer cells, Papanicolaou [c] and Giemsa [d]). White-colored urine sediment (consisting of neutrophils) is formed at the bottom of the test tube. Rods causing cystitis commonly belong to Escherichia coli *(a&b).* Enterococcus faecalis *or* E. faecium *also causes acute cystitis (c&d). It is of note that urinary bladder cancer often accompanies secondary bacterial cystitis.*

bile duct obstruction should be excluded. It may indicate an emergency state requiring prompt antibiotics therapy. Therefore, the cytodiagnosis must be adenocarcinoma plus bacillary colonization. Giemsa staining is superior to Papanicolaou staining for identifying infection of the extracellular bacteria.

When you find bacilli in specimens of ascites or pleural effusion, you should check how the specimen was kept until the centrifugation procedure to get the sediment [70]. If the specimen was kept overnight at room temperature, bacterial grew after the specimen sampling. Neutrophilic response is absent. In the urine sample left for a prolonged time, urease activity of the bacteria, yielding ammonium irons, provokes urine alkalization that leads to deposition of ammonium-magnesium phosphate crystals and non-crystalline phosphate. Representative cytological features are shown in **Figure 35**. Compare them with the specimen of genuine bacterial pleuritis caused by *Streptococcus milleri* as shown in **Figure 11c**.

4.5 Morphological change of Gram-negative rods

Administration of wide-spectrum penicillin and cefem antibiotics may provoke considerable morphological changes of the Gram-negative *Enterobacteriae* in the bile and urine. These include filamentous deformation and spheroplastic change. The beta-lactam antibiotics bound to the penicillin-binding proteins on the bacterial cell membrane hamper the bacterial growth, leading to the shape changes [71, 72]. In the bile shown in **Figure 36**, *Klebsiella pneumoniae* accompanied marked elongation and spheroid change. Microbial culture of the bile was positive for *K. pneumoniae*. The morphologically altered bacteria somewhat resemble fungi. The filaments and spheroplasts are negative with Gram and Grocott stains. *Pseudomonas aeruginosa* in the urine may also show marked filamentous change. Because of the effect of antibiotics treatment, neutrophilic response may be suppressed.

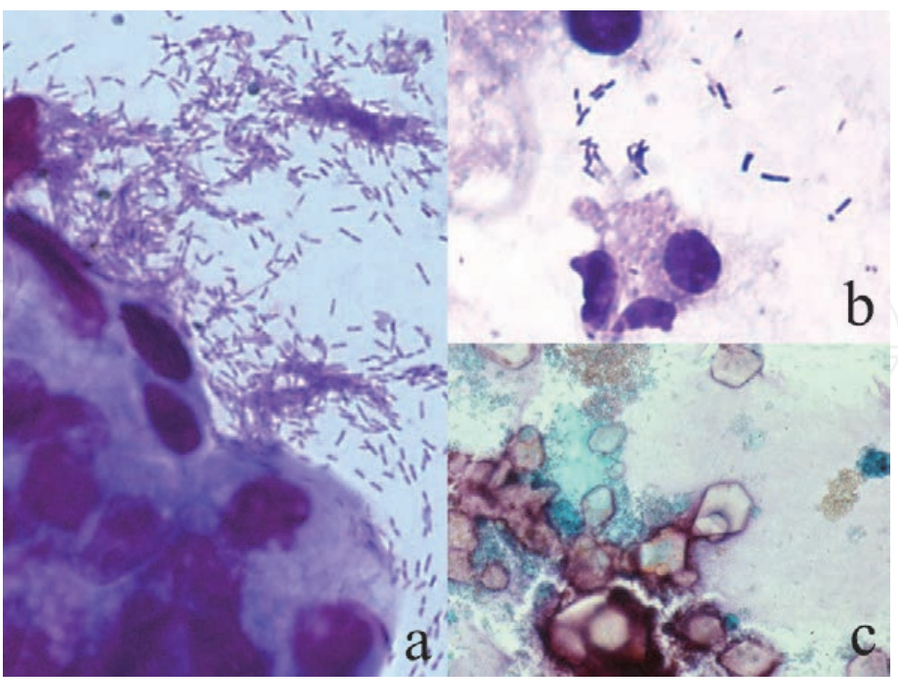

Figure 35.
Bacterial growth in liquid cytology material (a: Rods growing with adenocarcinoma of the bile duct, bile cytology, Giemsa, b: Rods growing in ascitic fluid, Giemsa, c: Ammonium-magnesium phosphate crystals in alkaline urine induced by bacillary growth). In the bile, marked growth of rods is seen around adenocarcinoma cells (a). The possibility of secondary ascending infection of Enterobacteriae *should be excluded. The growth of rods in the ascitic fluid may have occurred after specimen sampling (b). The specimen was kept overnight at room temperature, and neutrophils appear to be autolytic. Deposition of crystals occurs when the urine sample was left for a prolonged time (c). Bacterial urease activity accelerates alkalization of the urine.*

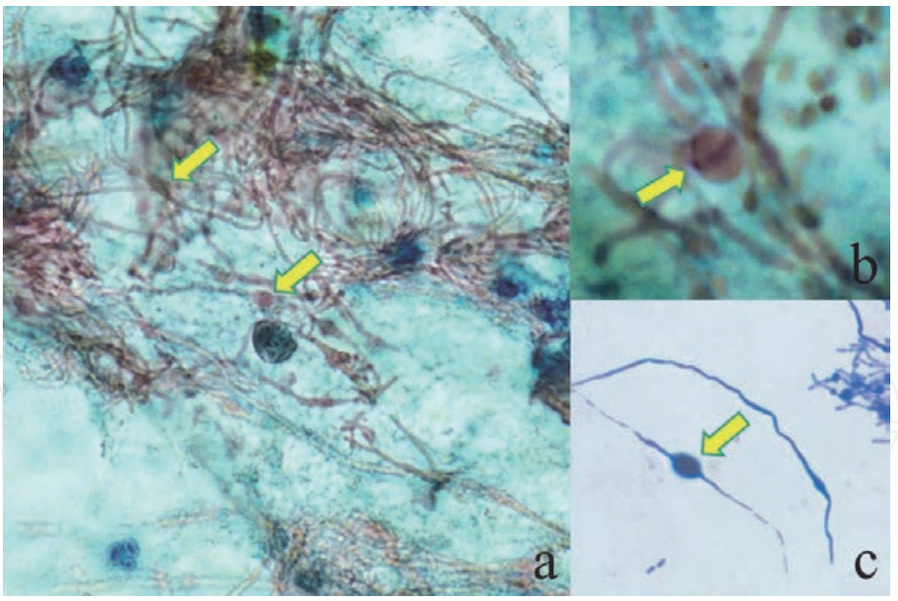

Figure 36.
Antibiotics-induced shape changes of Klebsiella pneumoniae *in the bile: Formation of filaments and spheroplasts (a&b: Papanicolaou, c: Giemsa). The rounded form is called as spheroplast (arrows). Beta-lactam antibiotics bound to penicillin-binding protein on the bacterial cell membrane provokes shape changes of the gram-negative rods. Microbial culture confirmed infection of* K. pneumoniae *in this case. Distinction from fungal colonization is requested.*

Under an immunocompromised condition, *Enterobacteria* such as *E. coli* and *K. pneumoniae* may proliferate within the cytoplasm of macrophages in the digestive and urinary organs to manifest xanthogranulomatous inflammation and malakoplakia, as mentioned above (**Figure 17**).

4.6 Biofilm infection

Pseudomonas aeruginosa of mucoid form commonly accompanies biofilm infection. Biofilm-forming bacteria stick to each other and also to the surface of material or injured mucosa. The adherent bacteria become embedded in a slimy (mucoid) extracellular matrix or secretory capsule. The biofilm protects the microbe from the attack by neutrophils, antibodies, complements and antibiotics: biofilm infection represents a state of resistance of the bacteria to antibiotics therapy [73, 74]. The biofilm-forming *P. aeruginosa* may thus cause persistent and intractable infection particularly in the airway. The neutrophilic host response is thus often minor in degree. Representative examples of biofilm infection are displayed in **Figure 37**. Refer also to **Figure 44f**. Gallbladder adenocarcinoma was cytologically associated with biofilm infection of rods, *P. aeruginosa*, embedded in mucoid matrix. In the vagina of the aged after hysterectomy, infection of *P. aeruginosa* of mucoid-type is proven cytologically.

Biofilm may also be formed by capsule-forming bacteria such as streptococci, staphylococci and enterococci.

4.7 Scraping/touch smear cytology of autopsied lung

We pathologists commonly encounter pneumonia in autopsy cases. Nosocomial (hospital-acquired) pneumonia is often caused by Methicillin-resistant *Staphylococcus aureus* (MRSA) or *Enterobacteriae*, while community-acquired pneumonia may result from infection of *Streptococcus pneumoniae*, *Haemophilus influenzae*,

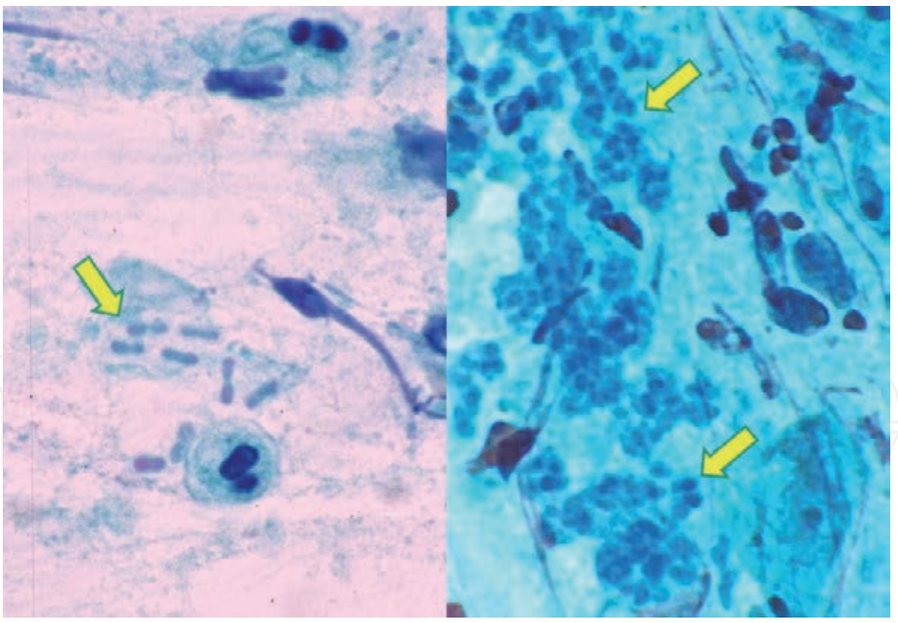

Figure 37.
Biofilm infection of Pseudomonas aeruginosa *(Papanicolaou, left: Bile, right: Vaginal smear in the aged). Mucoid-type colonies (arrows) are formed in both the bile and vagina. Adenocarcinoma was found in the left case, while a history of hysterectomy was recorded in the right case aged in her 70's. The rods are embedded in thick capsule. Microbial culture identified* P. aeruginosa *in both cases. The biofilm infection is resistant to chemotherapy.*

Moraxella (Branhamella) catarrhalis, etc. In case of lethal lobar pneumonia, candidate causative microbes include *S. pneumoniae* and *Legionella pneumophila* [75].

Giemsa-stained scraping or touch smear cytology sampled from the pneumonia lesion is practical in determining the causative microorganism during autopsy services. It is important for pathologists to avoid biohazard. *S. pneumoniae* is transmissible by droplet transmission, while *L. pneumophila* does not show human-to-human transmission. Giménez staining is also useful for demonstrating the microbe. **Figure 38** illustrates scraping cytology sampled from lethal lobar pneumonia in the aged patient. See also **Figure 14a**. Rods were phagocytized by macrophages, so that the causative microbe was identified as *L. pneumophila*, an intracellular microorganism. It is of note that the main cellular reactants against *L. pneumophila* are macrophages. Because of the paucity of lymphocytic response, granulomas are not formed. The importance of *L. pneumophila* as a cause of community-acquired lobar pneumonia of the aged should be emphasized [76].

4.8 Nocardiosis

Nocardiosis is usually encountered in immunocompromised patients [77, 78]. *Nocardia asteroides*, a Gram-positive filamentous and aerobic bacterium, can be demonstrated in bronchial brushing cytology specimens. A young male suffering from ulcerative colitis under steroid treatment complained of fever, coughing and phlegm. Cavitation was radiologically identified in his left upper lobe of the lung, and mycotic infection was clinically suspected. A quick-witted cytotechnologist performed Grocott staining in the cytology preparation. Grocott-stained filamentous bacteria were identified in the background of neutrophilic response, and the diagnosis of nocardiosis was made. The filamentous bacteria were not easily recognized in Papanicolaou-stained preparation, because they do not form aggregated grains. They were additionally positive with Gram and Ziehl-Neelsen's stains. Gram positivity and weak acid-fastness characterize *Nocardia*. **Figure 39** illustrates

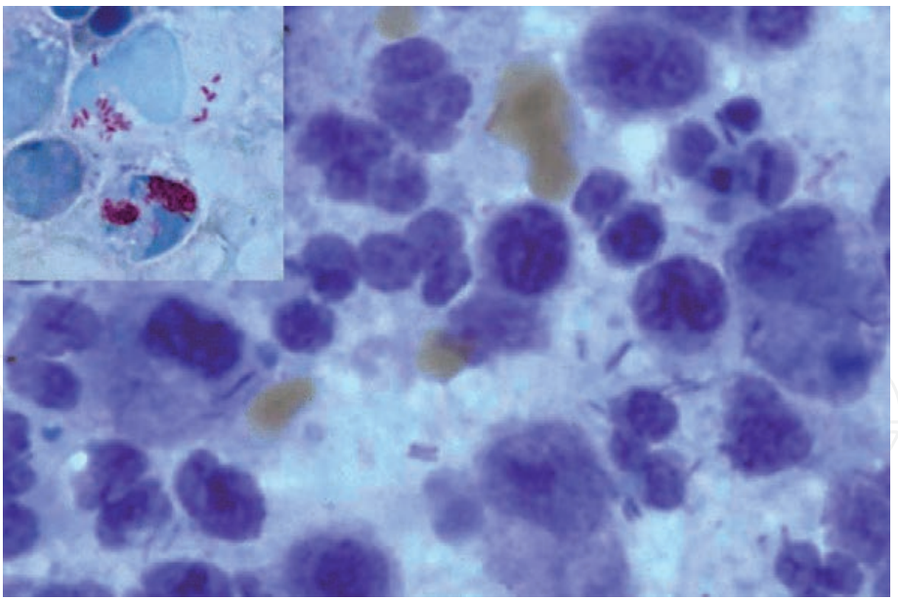

Figure 38.
Lobar pneumonia caused by Legionella pneumophila *(touch smear preparation of the autopsied lung, Giemsa, inset: Giménez). Rods are phagocytized by macrophages and neutrophils, indicating* L. pneumophila*-induced lobar pneumonia. Giménez stain is a simple method for visualizing the pathogen in red. Confirmation of the causative pathogen during autopsy assists at avoiding biohazard.* L. pneumophila *does not show human-to-human transmission, while* Streptococcus pneumoniae*, another causative candidate of lobar pneumonia, may infect the human by droplet transmission.*

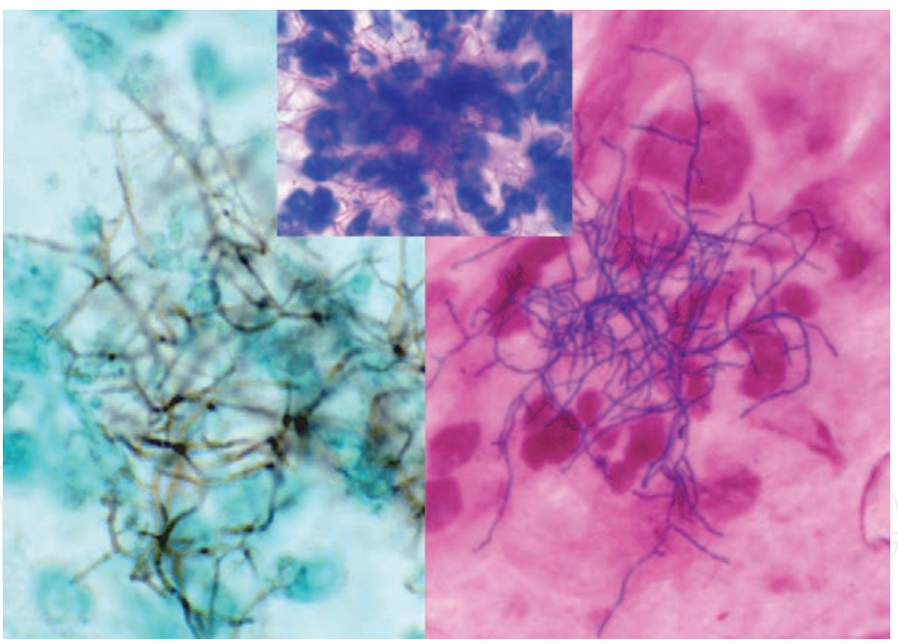

Figure 39.
Nocardiosis of lung (bronchial brushing cytology, left: Grocott, right: Gram, inset: Ziehl-Neelsen). In a young male patient with steroid treatment against ulcerative colitis, lung abscess was noticed. In the bronchial brushing cytology, clusters of filamentous bacteria are observed with Grocott and gram stains. Neutrophilic reaction against the pathogen is evident. The filaments are weakly acid-fast. It is often difficult to identify the filaments under Papanicolaou staining. Nocardia asteroids *was identified by microbial culture.*

cytopathologic appearance of lung nocardiosis. Microbial culture identified *N. asteroides*, and administration of sulfonamides was clinically quite effective.

4.9 Actinomycosis

Actinomycosis, infection of *Actinomyces israelii*, happens in immunocompetent individuals [79, 80], in sharp contrast to nocardiosis. Formation of sulfur granules,

reaching 1–2 mm in size, is characteristic of actinomycosis (**Figure 40**). Refer also to **Figure 11d**. The sulfur granule is a dense cluster of obligately anaerobic filamentous bacteria embedded in the homogeneous, periodic acid-Schiff (PAS)-reactive matrix called Splendore-Hoeppli material. The filaments are visualized with Gram, PAS and Grocott stains. Active neutrophilic response against the grains can be observed. In the lung, the sulfur granules are commonly seen within the destroyed airway, and inflammatory pseudotumor may be formed as a result of severe inflammatory fibrosis. Actinomycosis is also encountered in the oral cavity, liver and pelvic organs, including the endometrium (see also **Figure 30**). Actinomycotic grains are often seen in the pit of the enlarged pharyngeal tonsil as a non-pathogenic resident microbe.

4.10 Tuberculosis and non-tuberculous mycobacteriosis

When epithelioid cell granuloma is seen in bronchial scraping cytology, the possibility of lung tuberculosis should be considered (**Figure 41**). See also **Figure 12**. Often times, necrotic background is associated [81, 82]. Infrequently, tuberculous pleuritis may induce eosinophilic exudation (**Figure 18b**).

It is an important mission of the cytopathologist to have the hospital staff noticed for the biohazard [83]. Under an immunosuppressed condition, numerous acid-fast bacilli are phagocytized by macrophages, and Giemsa staining discloses negatively stained long rods in their cytoplasm [84] (**Figure 42**). The outer membrane of the cell wall of mycobacteria contains large amounts of glycolipids, especially mycolic acids [85]. This unique cell wall structure not only gives acid-fastness but also inhibits the penetration of dyes in the Giemsa solution. *Mycobacterium tuberculosis*, a representative acid-fast bacillus, shows airborne transmission. Bronchial sampling is performed in the isolated room equipped for bronchofiberscopy, so that check-ups for the close contact persons are requested. Cytology laboratory may be contaminated with the transmissible dryness-resistant pathogen inside the droplet nucleus. The bacterial morphology is indistinguishable between tuberculosis

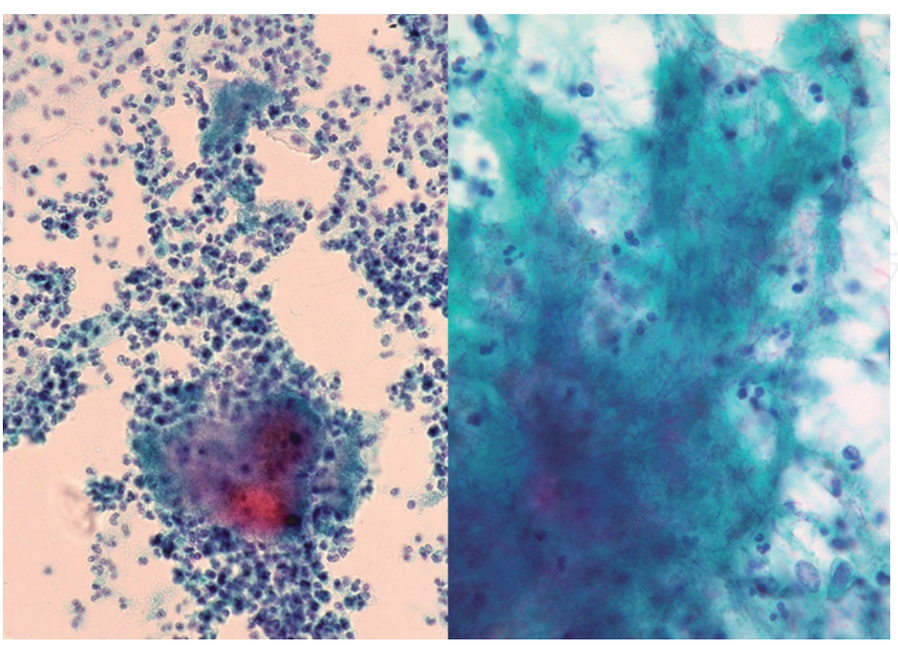

Figure 40.
Actinomycosis of the endometrium (scraping cytology, Papanicolaou, left: Low-power, right: High-power). Formation of sulfur granules is characteristic of Actinomyces israelii *infection. The granule is surrounded by neutrophils, and it consists of filamentous bacteria embedded in the hyaline matrix called Splendore-Hoeppli material. In contrast to nocardiosis, the diagnosis of actinomycosis can be reached with Papanicolaou staining. Endometrial actinomycosis may be provoked by the insertion of intrauterine contraceptive device.*

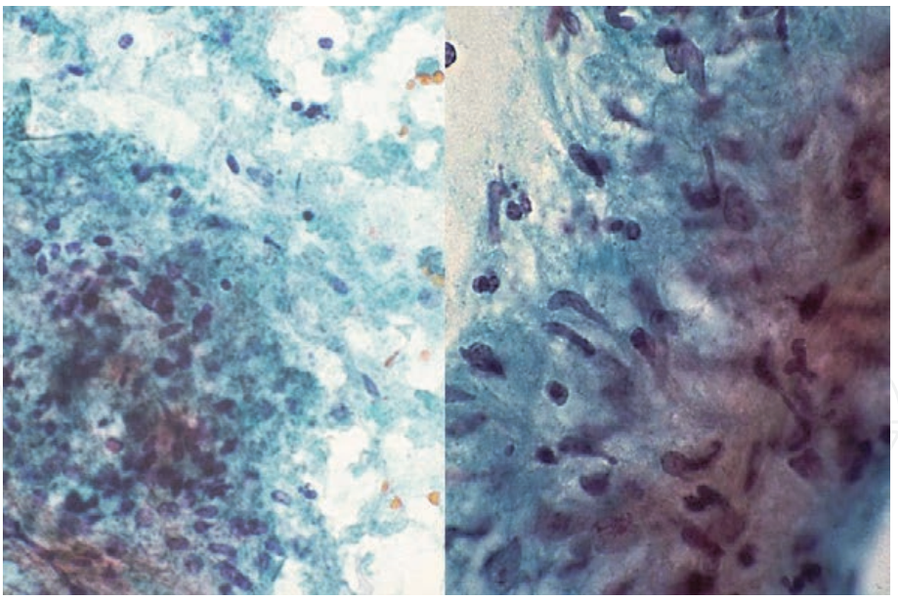

Figure 41.
*Pulmonary tuberculosis (bronchial brushing cytology, Papanicolaou, left: Low-power, right: High-power). Clusters of epithelioid cells represent a granulomatous reaction. The association of necrotic background (left) strongly suggests mycobacterial infection. It is difficult to distinguish tuberculosis (*Mycobacterium tuberculosis *infection) from non-tuberculous mycobacteriosis. Not only correct cytological diagnosis but also prompt warning against intrahospital biohazard are requested. Note also that non-tuberculous mycobacteria accompany no biohazard.*

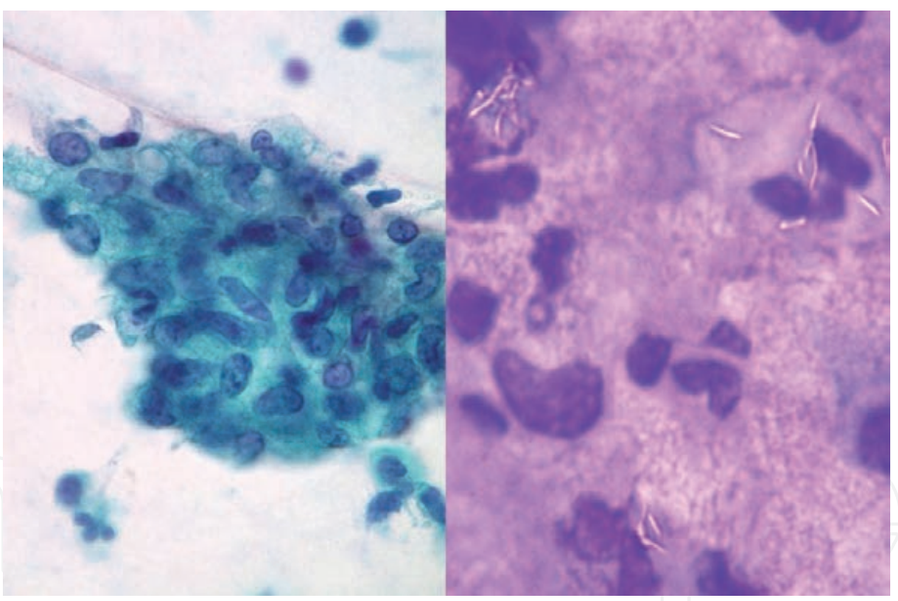

Figure 42.
Negative staining of mycobacteria phagocytized by macrophages (bronchial brushing cytology, left: Papanicolaou, right: Giemsa). Epithelioid granuloma is seen in Papanicolaou-stained preparation. Giemsa stain is useful to identify acid-fast bacilli, since the mycobacteria are resistant to be stained. Therefore, unstained bacillary images are clearly discernible in the cytoplasm of macrophages. No bacilli are visible in the pap smear. In this case, Mycobacterium avium *(a representative non-tuberculous mycobacterium) was cultured. By courtesy of Mr. Tomohiro Watanabe, Chuken Kumamoto, Japan.*

and non-tuberculous mycobacteriosis [82]. The distinction of the two is important since non-tuberculous mycobacteria do not show human-to-human transmission. Identification of *M. tuberculosis* by polymerase chain reaction, as well as the interferon gamma-releasing assay (QuantiFeron or T-Spot) [86] using the blood of the patient and close contact persons, are essentially important to avoid occupation-related infection. In case of tuberculosis, not only correct cytodiagnosis but also prompt warning against intrahospital biohazard are thus strongly requested.

When epithelioid granuloma and neutrophilic reaction are seen in the same specimen, the possibility of suppurative granuloma should be suspected. The typical example is cat scratch disease (bartonellosis) (**Figure 16**) caused by *Bartonella henselae* infection [87]. This tick-associated infection is commonly seen in the cervical or axillary lymph node and infrequently involving the spleen.

4.11 Bacteria seen in the blood

Some bacteria may be observed in the peripheral blood (**Figure 43**). Spiral microbes of *Borrelia recurrentis* are seen in the peripheral blood in an early stage of relapsing fever. The febrile disease is endemic in the African continent [88]. In case of bacterial septicemia, bacteria phagocytized by phagocytes (neutrophils and monocytes) are occasionally identified in peripheral blood preparations. In *Capnocytophaga canimorsus* septicemia caused by dog bite, a few bacilli are phagocytized by neutrophils [89]. *Streptococcus suis*, an important pathogen of pigs, may cause meningitis and lethal septicemia in the human who farms pigs or handles pork. The disease is endemic in southeastern Asia [90]. *In situ* hybridization (ISH) study of the buffy coat of the peripheral blood in septicemia infected with *Escherichia coli/Klebsiella pneumoniae*, *Staphylococcus aureus* or *Pseudomonas aeruginosa* exhibits bacterial DNA signals in the cytoplasm of neutrophils, even after chemotherapy [91].

4.12 Bacteria seen in sputum preparations: importance of Gram staining

Gram staining is cheap and quick technique to identify pathogens on smear preparations of the sputum, exudates, liquid materials and effusions. The importance of Gram staining in the diagnosis of pneumonia should be emphasized [92, 93]. It takes minutes to get results.

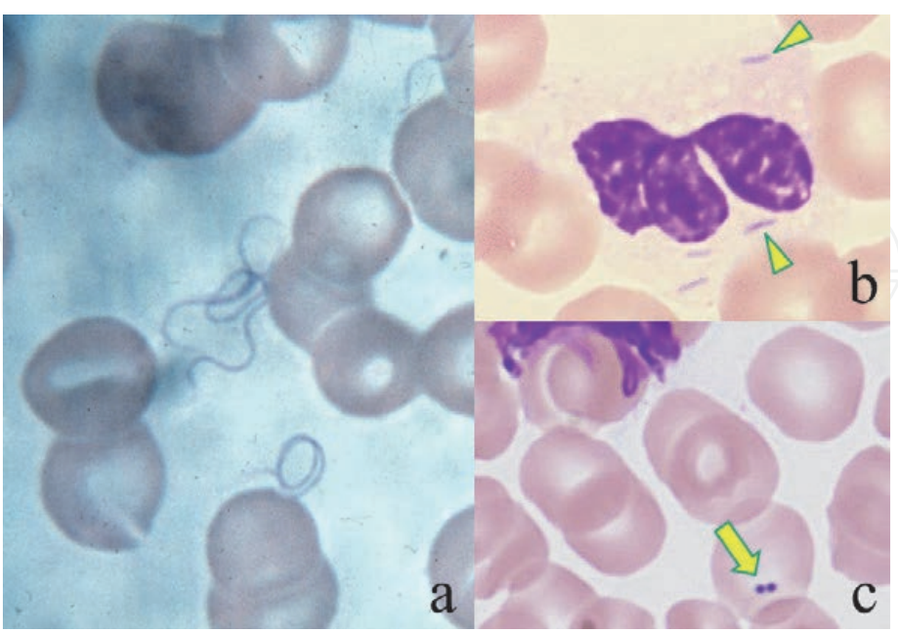

Figure 43.
Bacteria seen in the blood (Giemsa, a: Relapsing fever, b: Capnocytophaga canimorsus *septicemia, c:* Streptococcus suis *septicemia). Close observation of Giemsa-stained peripheral blood preparations occasionally identifies pathogens. In an early stage of relapsing fever, spiral pathogens,* Borrelia recurrentis*, appear in the blood. Fulminant and lethal septicemia of zoonotic origin is rare. Arrowheads indicate rods phagocytized by neutrophils in a case of dog bite-induced* C. canimorsus *infection. Diplococci are seen on a red cell (arrow) in case of* S. suis *septicemia seen in a pig breeder.*

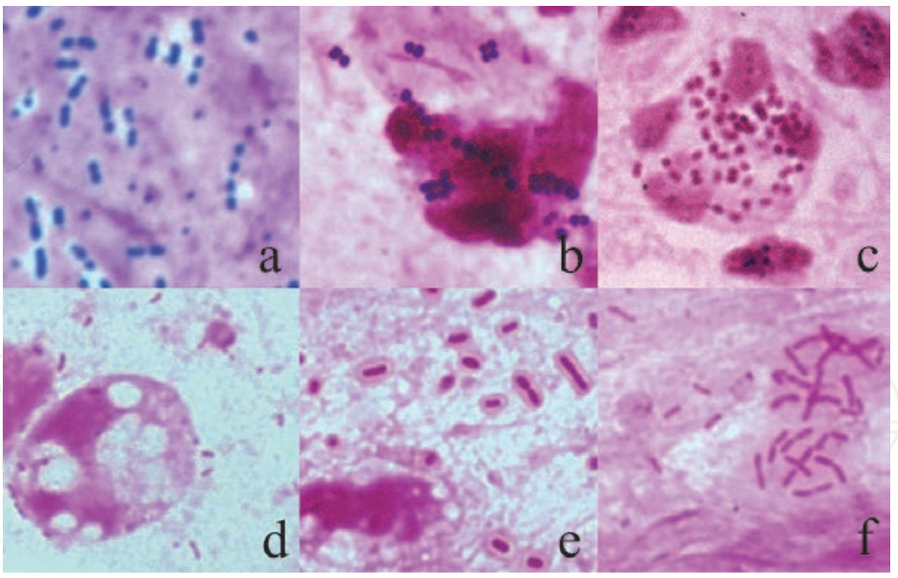

Figure 44.
Pathogens causing pneumonia in the sputum (Gram, a: Streptococcus pneumoniae*, b: Methicillin-resistant* Staphylococcus aureus *(MRSA), c:* Moraxella (Branhamella) catarrhalis*, d:* Haemophilus influenzae*, e:* Klebsiella pneumoniae*, f:* Pseudomonas aeruginosa*). Gram-stained preparations give us prompt identification of pathogens causing pneumonia. Cocci are seen in a-c, and rods in d-f. Gram stain is positive in a&b, but negative in c-f. the bacteria are phagocytized by neutrophils in b&c, while the capsule-forming pathogens are escaped from phagocytosis in a, d-f. mucoid form is observed in f. the rods in e&f are much larger than those in d.*

Typical microscopic appearance of Gram-stained sputum preparations is illustrated in **Figure 44**. These include *Streptococcus pneumoniae*, Methicillin-resistant *Staphylococcus aureus* (MRSA), *Moraxella (Branhamella) catarrhalis*, *Haemophilus influenzae*, *Klebsiella pneumoniae* and *Pseudomonas aeruginosa*. Gram positivity and the shape (cocci or bacilli), as well as the size, capsule formation and the pattern of appearance (paired, clustered or chained), provide us with valuable information for the microbes. The presentation of bacteria phagocytized by phagocytic cells (mainly neutrophils and occasionally macrophages) or those surrounded by neutrophils strongly suggests the etiologic (pathogenic) agent of pneumonia. Whether pneumonia is community-acquired or hospital-acquired is also quite important for determining the causative bacteria. The bacteria on and around squamous epithelia are regarded as the normal flora residing in the oral cavity. It is needed for us to evaluate the number of squamous epithelia and neutrophils in the specimens.

5. Cytodiagnosis of fungal infection

Invasive fungal infection is treatment-resistant and often lethal [94]. Fungi are commonly visualized with PAS reaction and Grocott (methenamine silver) staining. Gram staining may be positive. Fungi infectious to the human being are divided into two forms: yeast and hypha-forming types. Hypha-forming fungi belong to extracellular pathogens, and provoke neutrophilic reaction. Yeasts, round in shape and not forming hyphae, infect intracellularly and protected by cellular immunity provoking granulomatous cellular reaction. Candida accompanying both yeast and hypha-forming (myceliform) morphology is placed in an intermediate form [95].

5.1 Candidosis

Superficial candidosis (moniliasis) represents the most common mycosis. *Candida albicans*, the major species of Candida, is characterized by dimorphic

appearance: ovoid yeast cells (germ spores) and filamentous pseudohyphae. *C. albicans* is a normal indigenous flora of the oral cavity, intestinal lumen and skin, residing as a form of yeasts.

Candida vaginitis is the most frequently encountered candidosis in cytology specimens [96]. Hypha-forming colonies are surrounded by neutrophils, and Döderlein bacilli, the normal flora, are no longer observed. Yeast form fungi are also intermingled (**Figure 45**). Refer also to **Figure 11e**. Vaginal candidosis is often associated with pregnancy, diabetes mellitus and acquired immunodeficiency syndrome (AIDS), and it is also experienced as a form of STD.

Candida (Torulopsis) glabrata can be identified in the Papanicolaou-stained cervical smear preparation as a form of paired and orange-colored yeasts. No hyphae are formed, Döderlein bacilli are preserved, and neutrophilic reaction is mild [97]. *C. glabrata* thus represents a normal vaginal flora and must not be misinterpreted as candida vaginitis. The simple and thoughtless comments such as "Candida-positive" may mislead the clinician to inappropriate and unnecessary treatment against candida vaginitis.

Candida is often seen in sputum and urine cytology (**Figure 46**). The appearance of yeast-form Candida without hypha formation in the sputum may represents the increased non-pathogenic flora. In fact, the neutrophilic response is minor in degree. In the pathogenic state, Candida consistently forms pseudohyphae. It should be recognized that mucosal candidosis is common in the oral cavity and upper airway, but candida scarcely provokes pneumonia. In case of candida cystitis, the urine cytology reveals both yeasts and pseudohyphae in the inflammatory (neutrophil-rich) background [95]. *Trichosporon cutaneum (beigelii)*, showing a microscopic resemblance with *Candida albicans*, may also cause mycotic cystitis [98]. Uneven PAS reactivity of *T. cutaneum* gives a hint for differentiation from *C. albicans*, but microbial culture is essential for confirming the causative fungus.

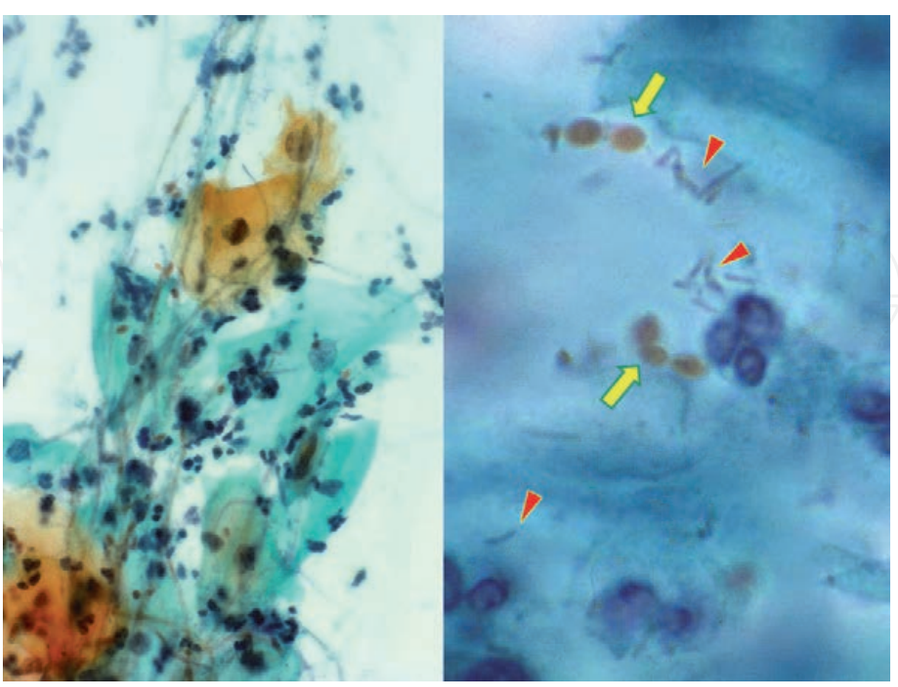

Figure 45.
Pathogenic and non-pathogenic Candida in cervical smear preparations (Papanicolaou, left: Candida vaginitis, right: Candida (Torulopsis) glabrata *as normal vaginal flora). Pathogenic* Candida albicans *forms pseudohyphae in the vagina and provokes neutrophilic reaction, causing candida vaginitis.* C. glabrata *forms paired and orange-colored yeasts without forming hyphae (arrows). The preservation of Döderlein bacilli (arrowheads) in the background is the proof for the lack of pathogenicity.*

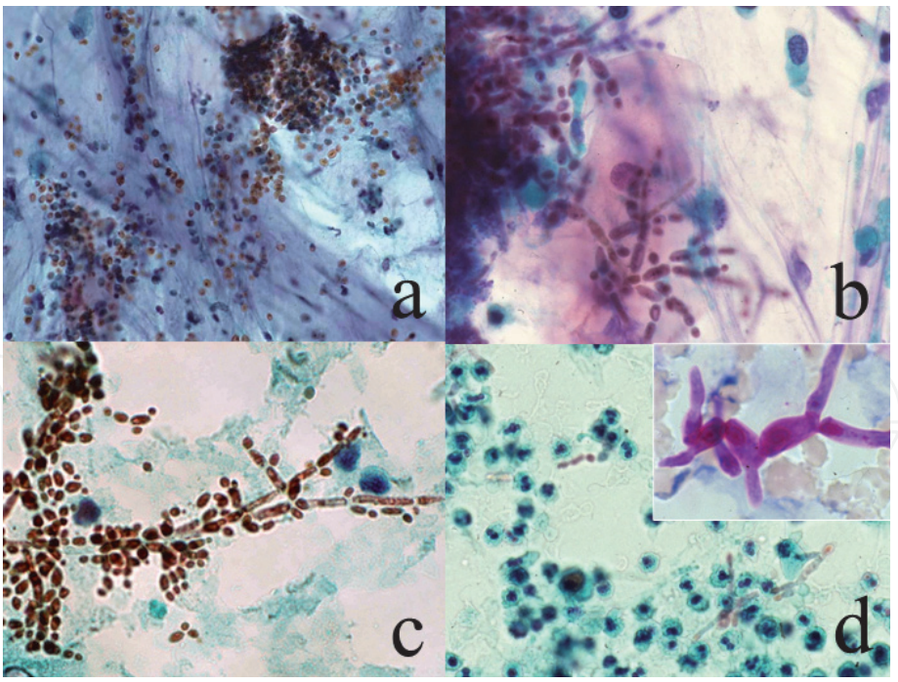

Figure 46.
Candidosis and trichosporonosis (Papanicolaou, a: Yeast form Candida in sputum, b: Candidosis in sputum, c: Candida cystitis, d: Trichosporon cystitis, inset; PAS). Candida yeasts often stain yellowish with Papanicolaou staining. When only yeast form is observed in the sputum, we can judge the microbe as non-pathogenic (a). Since Candida pneumonia is rare, hypha-forming Candida growth may occur in the oral cavity or pharynx (b). In the urine, typical orange-colored microscopic features of Candida infection, accompanying both yeasts and pseudohyphae, are noted (c). Trichosporon cutaneum*, microscopically resembling Candida, occasionally causes fungal cystitis (d). Uneven PAS reactivity is a feature of the Trichosporon species (inset).*

5.2 Cryptococcosis

Figure 47 demonstrates bronchial brushing cytology of pulmonary cryptococcal granuloma. Multinucleated giant cells of macrophage origin phagocytize small

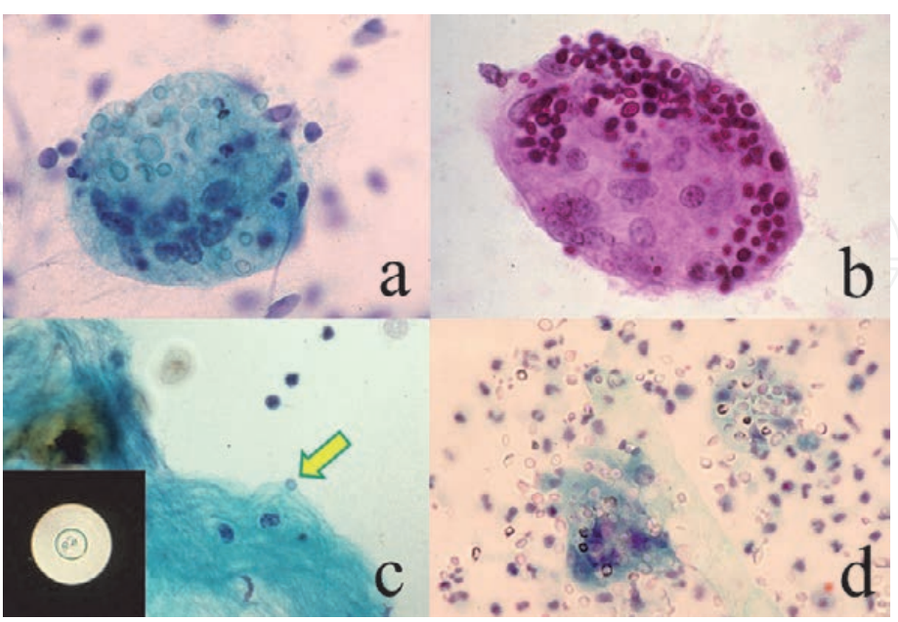

Figure 47.
Cryptococcosis (Papanicolaou [a,c&d], PAS [b], indian ink [inset], a&b: Sputum, c: Cerebrospinal fluid, d: Urine). In the sputum, multinucleated giant cells phagocytize numbers of translucent and PAS-positive small yeasts, representing cryptococcal granuloma of the lung. In the cerebrospinal fluid, only a few yeasts are seen (arrow). Indian ink method demonstrates an unstained yeast in the black background. In case of disseminated cryptococcosis, numerous yeasts are seen in the urine. Some are phagocytized by giant cells, but others are seen in a non-phagocytized free form.

transparent rounded yeasts in the cytoplasm. *Cryptococcus neoformans* grows in the cytoplasm of macrophages to provoke a granulomatous cellular reaction. It should be noted that cryptococcal infection is accelerated by impaired cellular immunity, e.g. after steroid therapy and in AIDS [99].

C. neoformans may infect the meningeal space [100]. Indian ink method clearly demonstrates capsule-forming yeasts in the cerebrospinal fluid (CSF). Usually, yeasts in the CSF are few in number (**Figure 47c**). In case of disseminated cryptococcosis seen in patients with suppressed cellular immunity, a large number of yeasts are observed, and they are often not phagocytized by macrophages. Urine cytology in disseminated cryptococcosis is displayed in **Figure 47d**.

5.3 Pneumocystosis

Pneumocystis jirovecii-induced acute interstitial pneumonia is seen in patients with severe suppression of cellular immunity after administration of steroid or in AIDS [101, 102]. *P. jirovecii* (previously called as *P. carinii*) is now categorized in the fungus, but unculturable *in vitro*. Grocott staining is essential for making the diagnosis of pneumocystosis in bronchial/alveolar lavage specimens (**Figure 48**). Pneumocystis pneumonia often manifests dry cough without formation of phlegm. Grocott-positive small cysts are clearly observed. PAS reactivity is negative. Lymphocytic reaction may be seen in the cytology specimen. In heavily infected specimens in AIDS patients, pathogens (cysts) look like clustered hemolytic red cells in Papanicolaou-stained preparations. With Giemsa staining, the nuclei of smaller-sized ameboid trophozoites are stained purple. Response of small lymphocytes may be provoked, as illustrated in **Figure 13d**.

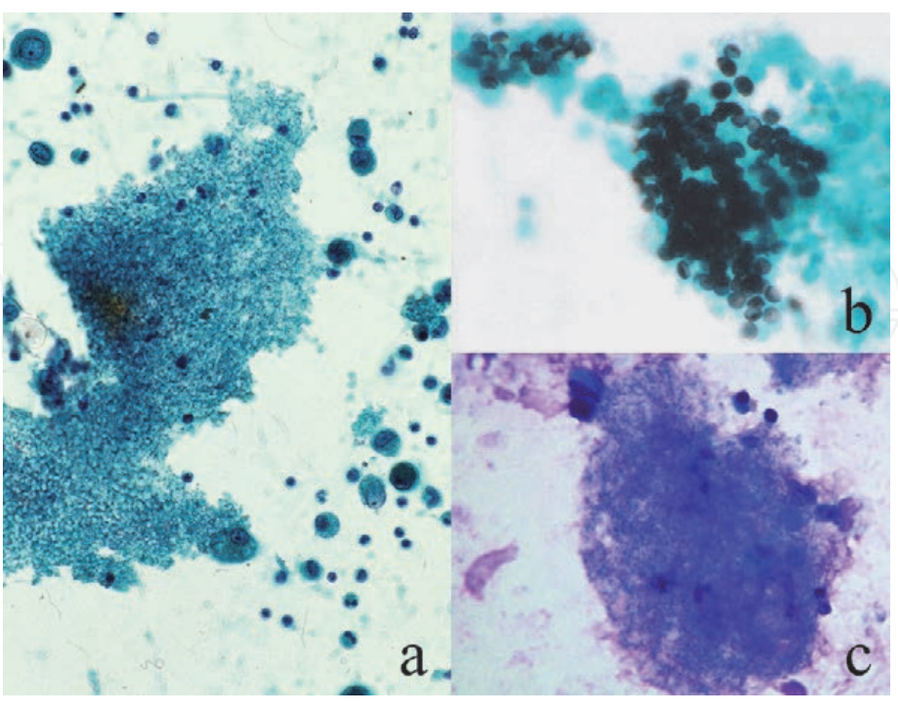

Figure 48.
Pneumocystis pneumonia (bronchial lavage, a: Papanicolaou, b: Grocott, c: Giemsa). Under suppressed cellular immunity, Pneumocystis jirovecii *appears in the airway as clustered translucent cysts in the pap smear, somewhat resembling hemolytic red cells (a). Lymphocytes and macrophages surround the pathogens. The cysts are clearly detected with Grocott stain (b). The cyst wall and dot-like structure within the cyst are stained black. Giemsa stains nuclei of small-sized trophozoites in purple (c).*

5.4 Aspergillosis

Aspergillus is a representative example of hypha-forming (myceliform) filamentous fungi, growing extracellularly [103]. Basophilic hyphae, typically accompanying Y-shaped bifurcation and septum formation, are arranged in the same direction (**Figure 49**). Non-viable hyphae show less basophilia. Neutrophils accumulate around the hyphae. The most common species is *Aspergillus fumigatus*. *A. flavus* occasionally secretes orange/red-colored pigment [104]. Melanin pigment is seen in *A. niger* that also produces calcium oxalate crystals [105].

In aspergilloma containing a fungus ball within the cavitated bronchus, conidial heads, globoid, radiate or broom-shaped, are formed in the aerobic (air-filled) cavity, and Grocott-positive conidia (conidiospores) may be seen in the bronchial lavage specimens. It should be noted that the round-shaped conidia closely resemble *Cryptococcus neoformans*. An important point of distinction is that the conidia floating in the air are not phagocytized by macrophages.

Aspergillus infrequently provokes an allergic reaction with eosinophilic granuloma formation. The status is called as allergic bronchopulmonary aspergillosis. A number of eosinophils and eosinophilic Charcot-Leiden crystals appear in the sputum, in association with a few injured fungal hyphae (see **Figure 18c** and **d**).

5.5 Mucormycosis

Mucormycosis (zygomycosis) is the infection by *Zygomycetes*, including *Mucor ramosissimus*, *Rhizomucor pusillus*, *Rhizopus oryzae*, etc. *Zygomycetes* is an opportunistic microbe mainly affecting premature babies and patients with neutropenia or severe diabetes mellitus. When compared with Aspergillus, the hyphae are less basophilic and thick and lack septum formation. The lamified angle of the hypha tends to be wide. The infection provokes neutrophilic responses. The main sites of

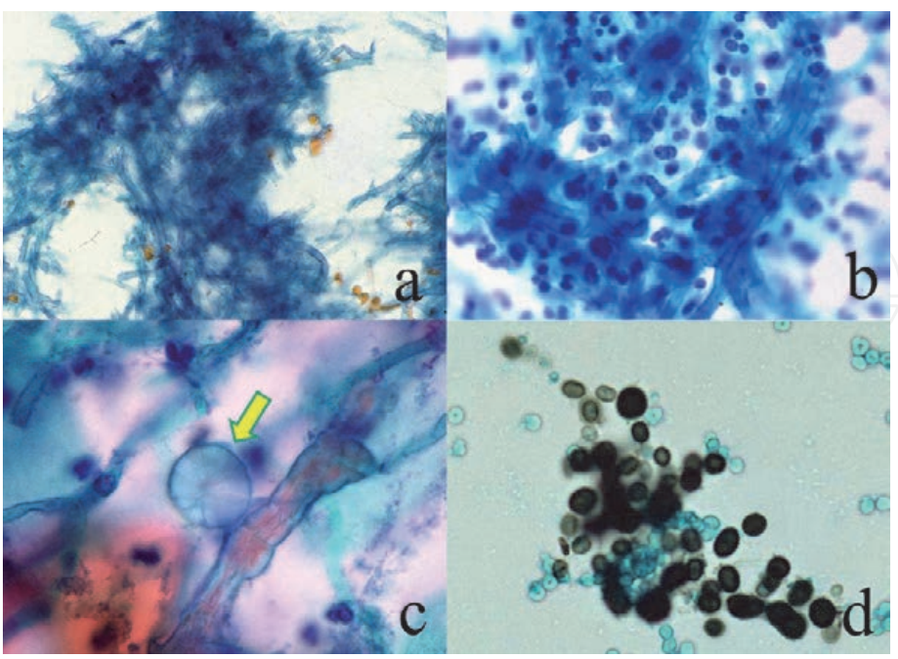

Figure 49.
Aspergillosis (a-c: Papanicolaou, sputum, d: Grocott, bronchial lavage). Basophilic branching hyphae are clustered in the sputum (a&b). Neutrophilic reaction is evident in b. calcium oxalate crystals (arrow) are closely associated with hyphae of Aspergillus niger *(by courtesy of Mr. Tomohiro Watanabe, Chuken Kumamoto, Japan). In the bronchial lavage specimen, Grocott-positive conidia (conidiospores) released from the conidial head formed in the cavity are seen. They resemble cryptococcal yeasts, but they are not phagocytized by macrophages.*

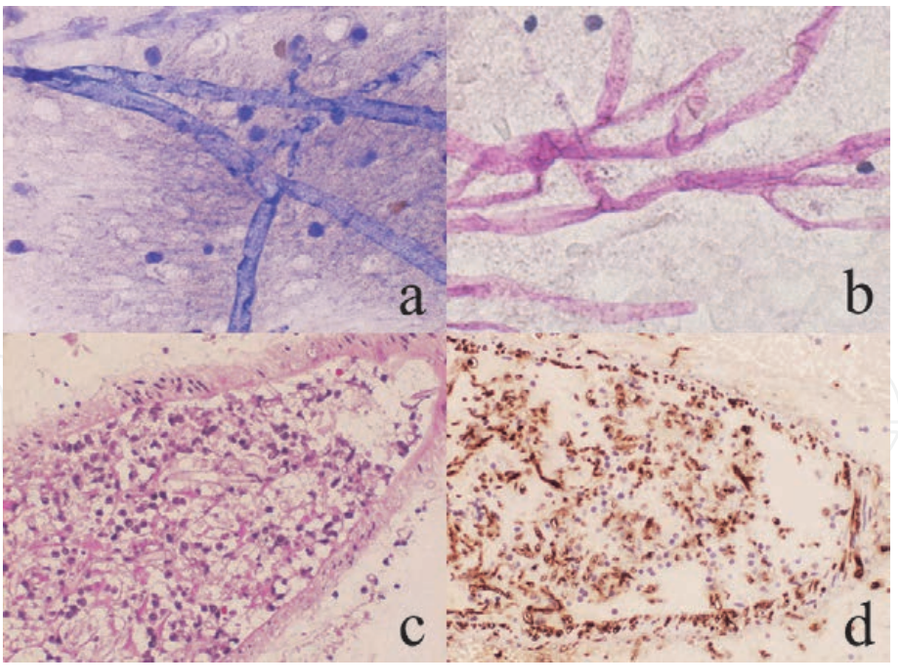

Figure 50.
Mucormycosis (invasive brain lesion, touch smear [a: Giemsa, b: PAS], angioinvasive histology [c: H&E, d: Immunostaining with a monoclonal antibody WSSA-RA-1]). The brain lesion of invasive mucormycosis is seen in a young boy. Thick branching hyphae without septum formation are noted. The brain biopsy specimen reveals vascular invasion of faintly basophilic hyphae that are clearly immunoreactive for Zygomycetes antigen.

involvement include the paranasal cavity and lung. Calcium oxalate crystal deposition and yellow pigment secretion may be associated with mucormycosis [106]. Lethal systemic dissemination may occur in neutropenic patients and in premature neonates [107]. **Figure 50** illustrates scraping cytology of the invasive brain lesion seen in a young boy. Thick branching hyphae without septum formation are noted.

6. Cytodiagnosis of viral infection

Intranuclear clusters of viral particles are recognized as intranuclear inclusion bodies. Intranuclear inclusion bodies characterize DNA virus infection, while most of the RNA viruses do not form inclusion bodies. Exceptionally, measles virus, an RNA virus, forms intranuclear inclusions. Some DNA viruses may cause cytoplasmic viral inclusions: hepatitis B virus to form ground-glassed hepatocytes and molluscum contagiosum virus (a family of pox viruses) to form molluscum bodies in keratinocytes. There are two types of intranuclear inclusion bodies, smudge (homogeneous or full) type and Cowdry A (haloed) type [108]. The viral infection principally provokes lymphocytic host response, when the patient is immunocompetent (see **Figure 13b**).

6.1 Viral inclusions

Representative examples of intranuclear viral inclusion bodies seen in cytology specimens are shown in **Figure 51**.

Human papillomavirus (HPV), a wart-forming DNA virus, provokes skin and mucosal lesions. Intranuclear inclusions are seen in the skin lesion (wart), but not observed in the mucosal lesions (refer to **Figures 25** and **26**). Both types associate koilocytosis, namely perinuclear haloe formation in the superficial keratinocytes. In gynecologic cytology specimens, koilocytosis is seen in condyloma acuminatum

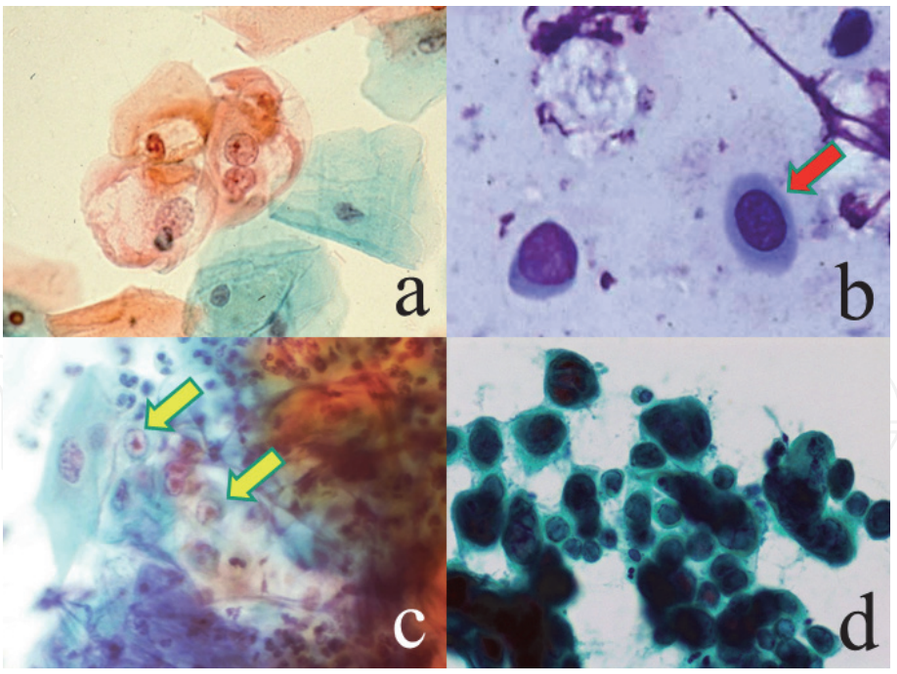

Figure 51.
Viral infections (Papanicolaou [a,c&d], Giemsa [b], a: Cervical smear, b: Conjunctival scraping, c: Corneal scraping, d: Touch smear from the nipple). Koilocytosis (perinuclear haloe formation) in the cervical superficial keratinocytes characterizes human papillomavirus infection (a). In condyloma acuminatum (a benign mucosal wart) caused by HPV 6/11, nuclear atypia is mild in degree. Intranuclear inclusions are seen in adenovirus infection in highly contagious epidemic keratoconjunctivitis (b) and in herpes simplex virus infection (c&d). Smudge (full)-type inclusion bodies (red arrow) are seen in b&d, while Cowdry type A inclusion bodies are noted in c (yellow arrows). Multinucleation of the infected keratinocytes is seen in d.

(a benign mucosal wart of STD type) and dysplastic (precancerous) cervical lesions. Cervical squamous cancer cells lack both intranuclear inclusions and koilocytosis [109].

Epidemic keratoconjunctivitis is a highly contagious eye disease caused by infection of adenovirus, types 8, 19 or 37. Quick Giemsa-stained epithelial cells scraped from the conjunctiva reveal intranuclear inclusion bodies of smudge type [110].

Infection of herpes simplex virus (HSV; human herpesvirus-1 or -2) typically accompanies intranuclear inclusion bodies of both smudge and Cowdry A types [111]. Scraping cytological features of herpetic keratitis and HSV infection of the nipple are illustrated. See also **Figure 21**, where vulvar keratinocytes are infected by HSV as a form of STD. Epstein-Barr virus (EBV, human herpesvirus 4) may cause neoplastic growth of lymphocytes and gastric epithelial cells, but intranuclear inclusions are not formed [112]. In case of chronic active EBV infection, the induction of large granular lymphocytes of NK cell lineage is characteristic, as demonstrated in **Figure 20**.

6.2 Opportunistic viral infections

Cytomegalovirus (CMV; human herpesvirus-5) is a representative example of the opportunistic virus activated in case of impaired cellular immunity. CMV provokes enlargement of the infected cells with formation of large basophilic (owl-eyed) intranuclear inclusion bodies. Granular intracytoplasmic inclusion bodies are also noted [113]. Hemorrhagic varicella (lethal infection of varicella-zoster virus [VZV; human herpesvirus-3) occurred in a child case of acute lymphoblastic leukemia after bone marrow transplantation. The cytology specimen aspirated from a hemorrhagic vesicle shows intranuclear inclusion bodies [114].

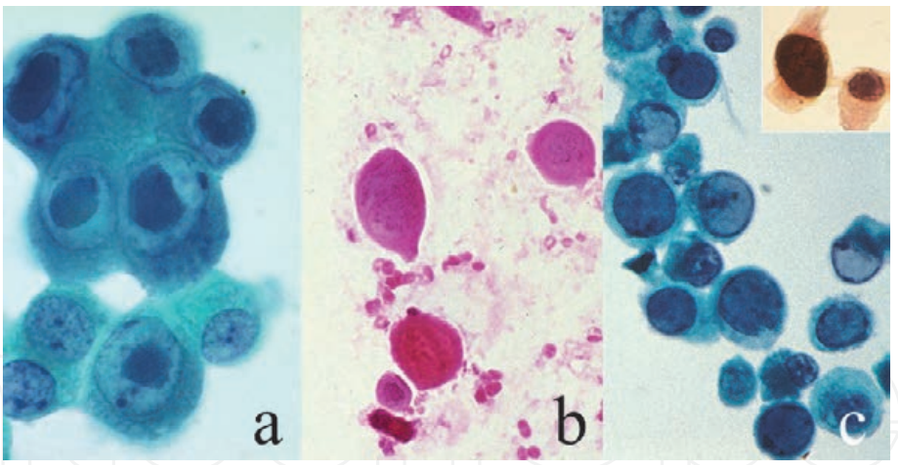

Figure 52.
Opportunistic viral infections (Papanicolaou [a&c], H&E [b], immunostaining for SV40 antigen [inset], a: Bronchial lavage, b: Aspiration from hemorrhagic vesicle, c: Urine cytology). In cytomegalovirus infection in AIDS, large basophilic intranuclear inclusion of Cowdry type a are diagnostic. Cytoplasmic granular inclusion bodies are also noted (a). In hemorrhagic varicella seen in a leukemic boy after bone marrow transplantation, intranuclear inclusion bodies of smudge type are seen in acantholytic keratinocytes in the aspirated vesicle fluid (b). BK virus infection provokes intranuclear inclusions of smudge type in urothelial cells, forming so-called "decoy cells" (c). Polyomavirus-specific SV40 antigen is proven in the nuclei (inset). The decoy cells showing nuclear enlargement should be distinguished from urothelial carcinoma.

BK virus-infected cells in the urine sediment are called "decoy cells", somewhat resembling urothelial cancer cells. Intranuclear inclusion bodies of smudge type are observed in the infected urothelial cells under suppressed cellular immunity. BK virus antigen or SV40 antigen can be demonstrated in the nuclei. Electron microscopy identified numerous round and small-sized viral particles in the nuclei [115].

Representative cytological features of opportunistic viral infection are displayed in **Figure 52**. The cellular (lymphocytic) response is scarcely seen in these immunocompromised cases.

7. Cytodiagnosis of protozoan infection

Protozoa, unicellular microbes usually measuring 5–20 μm, may accompany pseudopodia, flagellae or cilia. Most protozoa infect not only human but also animals, categorized in zoonotic infection [116]. Some protozoa such as *Entamoeba histolytica*, *Giardia lamblia* and *Trichomonas vaginalis* lack mitochondria [117].

7.1 Protozoa in cytology specimens

Representative features are demonstrated in **Figure 53**.

The most common protozoan experienced in routine cytology services is *Trichomonas vaginalis* in cervical smear preparations. This STD pathogen is seen adjacent to glycogen-rich superficial keratinocytes. Döderlein bacilli are no longer observed in the background. Neutrophils are often clustered to form so-called cannon (pus) balls [118]. *T. vaginalis* is a non-invasive protozoan and grows extracellularly, so that neutrophilic response is induced (**Figure 11f**). Cannon ball formation (clustering of neutrophils as cannon balls) is a microscopic hallmark of trichomoniasis.

Giardia lamblia commonly colonizes the duodenal and gallbladder mucosae. Bile cytology preparations may contain flagellated, symmetrical pear-shaped protozoan cells, characteristically having paired nuclei [119]. *G. lamblia*, non-invasive protozoan, commonly induces lymphoid follicle formation with marked increase intraepithelial lymphocytes in the duodenal mucosa [120], as displayed in **Figure 9**.

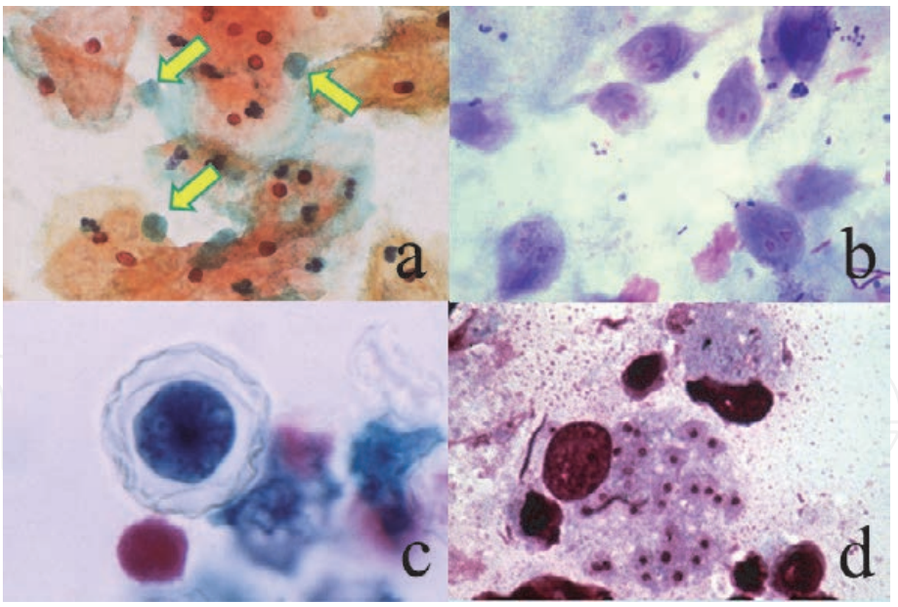

Figure 53.
Protozoan infections (Papanicolaou [a&c], Giemsa [b&d], a: Cervical smear, b: Bile, c: Corneal scraping, d: Touch smear of skin biopsy). Green-colored Trichomonas vaginalis *(arrows) commonly attaches to the superficial (orange-colored) keratinocytes (a). Bacterial vaginosis is associated. Flagellated binucleated trophozoites of* Giardia lamblia *are seen in the bile (b). Bacteria are co-infected. An acanthamebic cyst with thick wrinkled wall formation is seen in the painful cornea (c). Acanthamebic keratitis is caused by inappropriate usage of contact lens. Round-shaped protozoa phagocytized by macrophages represent amastigotes of* Leishmania tropica *(d). Small kinetoplasts are seen just adjacent to the centrally located nuclei.*

Cellular reaction in the bile is usually poor, but lymphocytic background may be associated. Regarding the enteric co-infection of *G. lamblia* and *Entamoeba histolytica* in a AIDS case, refer to **Figure 55**. *Acanthamoeba* is a free-living protozoan widely seen in environmental water. When one wears contaminated contact lenses, painful keratitis may happen. Scraping cytology from the turbid and eroded cornea identified cysts and trophozoites of *Acanthamoeba*, spp. [121]. Touch smear preparation or fine needle aspiration sampled from a biopsied skin tissue of cutaneous leishmaniasis demonstrates amastigotes of *Leishmania tropica* growing in the cytoplasm of macrophages [122]. Both round basophilic nuclei and small-sized kinetoplasts are observed in the non-flagellated protozoan cells. Indistinguishable cytological features are seen in visceral (systemic) leishmaniasis (kala azar), as shown in **Figure 14b**.

7.2 Protozoa in blood preparations

Blood smear preparations may contain protozoa. Malaria, Babesia and Trypanosoma should be of notice (**Figure 54**). Regarding the methods for detecting blood parasites (protozoa and nematode larvae), refer to review articles [123, 124].

Falciparum malaria and tertian malaria, mosquito-mediated febrile diseases, are caused by infection of *Plasmodium falciparum* and *P. vivax*, respectively. In falciparum malaria, ring forms are seen in normal-sized red cells, and often times two or more ring forms infect one red cell. Black-colored malaria pigment is associated. Neither ameboid forms nor schizonts appear in the peripheral blood. The red cells infected by the ameboid form of *P. falciparum* strongly express cell adhesion molecules on the surface, so that they adhere to the capillary endothelial cells expressing CD36 and intercellular cell adhesion molecule-1 (ICAM-1). This process of capillary obstruction is the direct cause of cerebral (malignant) malaria [125]. In tertian malaria, ring forms are fewer in number, and the ring forms are associated

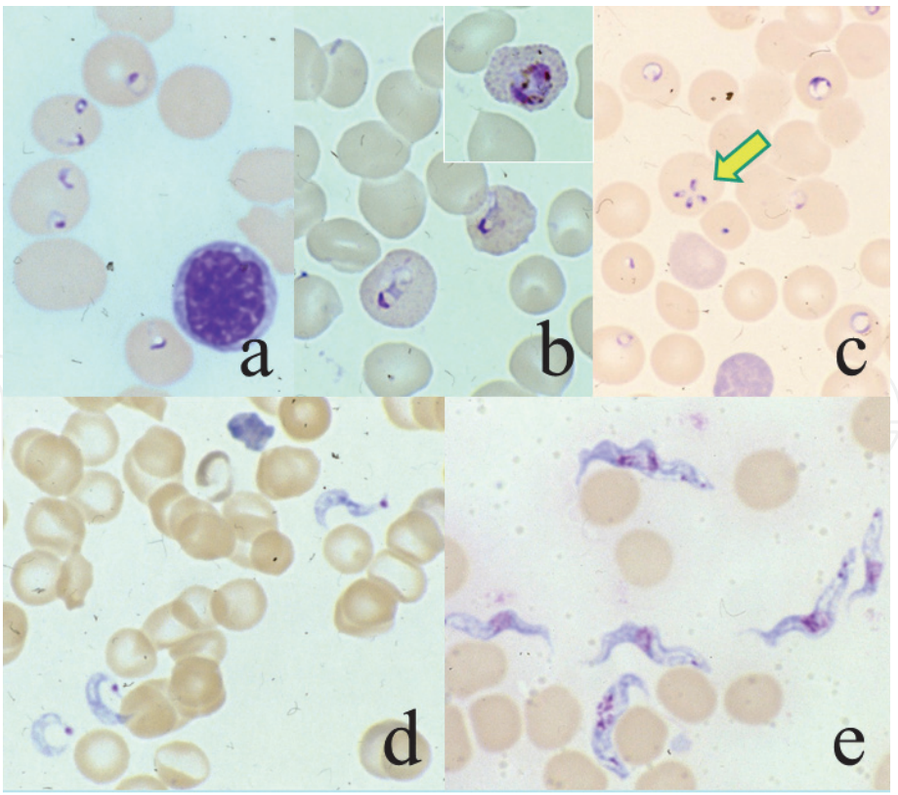

Figure 54.
Protozoa seen in the blood (Giemsa, a: Malaria falciparum*, b:* Malaria vivax*, c:* Babesia microti*, d:* Trypanocoma cruzi*, e:* Trypanosoma gambiense*). In falciparum malaria, two ring form parasites are often seen in a single red cell. More than half of red cells are infected (a). In tertian (vivax) malaria, the infected red cells are enlarged and contain Schüffner's spots (b). Inset indicates an ameboid form. In babesiosis, ring form parasites resemble those of malaria. Tetrads imitating a maltese cross (arrow) are pathognomonic of* Babesia *(c). Trypanosomiasis is featured by the appearance of flagellated trypomastigotes in the peripheral blood. Tropomastigotes of* T. cruzi*, C-shaped and having a kinetoplast at the end (d), are smaller than twisted ones of* T. gambiense *(e).*

with cytoplasmic granules (Schüffner spots) in enlarged red cells. Ameboid forms and schizonts are scattered [126].

Infection of *Babesia microti* is mediated by tick bite. Babesiosis is mainly seen in animal blood, and human cases are rarely encountered, particularly after splenectomy. Ring forms are seen in red cells, and formation of cruciform bodies (tetrads), resembling a maltese cross, is pathognomonic [127].

Trypanosoma cruzi, mediated by Triatoma bite, is identified in the peripheral blood in an acute stage of infection. C-shaped trypomastigotes with a distinct kinetoplast at the end, 20 μm in length, are seen outside the red cells. The clinical course is benign. In chronic stage, *T. cruzi* infects the cardiomyocytes causing chronic heart failure by Chagas disease. In African sleeping disease, lethal meningoencephalitis occurs. The flagellated trypomastigotes of *T. gambiense* are larger (20–30 μm in length) than those of *T. cruzi* [128].

7.3 Opportunistic protozoan infection

Opportunistic protozoan infection is commonly complicated by impaired cellular immunity (particularly in AIDS). These include amebic dysentery, giardiasis, cryptosporidiosis, toxoplasmosis and microsporidiosis. The inflammatory cellular response is poor in immunocompromised patients.

Trophozoites of *Entamoeba histolytica* are identified in cytology preparations aspirated from amebic liver abscess. The environment allowing the growth of obligate anaerobic trophozoites lacking mitochondria results in karyorrhexis of

neutrophils and loss of PAS reactivity in the background fluid due to advanced anoxia. Karyosomes (aggregated chromatins centrally located in the nucleus) are pathognomonic of protozoan cells. The plump cytoplasm of the trophozoite consists of thick perinuclear endoplasm and thin peripheral ectoplasm [129]. They often phagocytize red cells. A monoclonal antibody EHK153 detects the ameba in cell block preparations. No cyst form is discerned in the lesion. Rectal lavage from an AIDS patient complaining of severe diarrhea demonstrates opportunistic co-infection of *G. lamblia* and *E. histolytica*. **Figure 55** illustrates cytological features of amebiasis.

As reference, poorly pathogenic *Entamoeba gingivalis*, a normal and anaerobic resident in the oral cavity, may appear in the sputum (see **Figure 62c**), and neutrophils are typically phagocytized by the trophozoites [59]. *E. gingivalis* may colonize the endometrium around an intrauterine contraceptive device (IUD) in healthy women, and co-infection with *Actinomyces israelii* is needed, as illustrated in **Figure 30**.

Cysts of *Cryptosporidium parvum* in diarrheal discharge in an AIDS patient show acid-fastness, red-colored with Ziehl-Neelsen's staining. The acid-fast cysts are small-sized, measuring 3–5 μm. Cryptosporidiosis in AIDS is lethal due to the lack of effective therapeutic drugs [130].

A patient with acute myeloid leukemia post bone marrow transplantation complained myalgia the leg. Fine needle aspiration was performed from the painful muscle. Clustered tachyzoites (pseudocysts) are seen in the cytoplasm of striated muscle cells. The diagnosis of *Toxoplasma gondii*-induced myositis was made [131].

Microsporidiosis caused by *Encephalitozoon cuniculi* is seen in ascites fluid of an immunosuppressed mouse. Giemsa staining clarifies the nuclei of small cysts clustered in the cytoplasm of macrophages. Microsporidiosis may be encountered in the

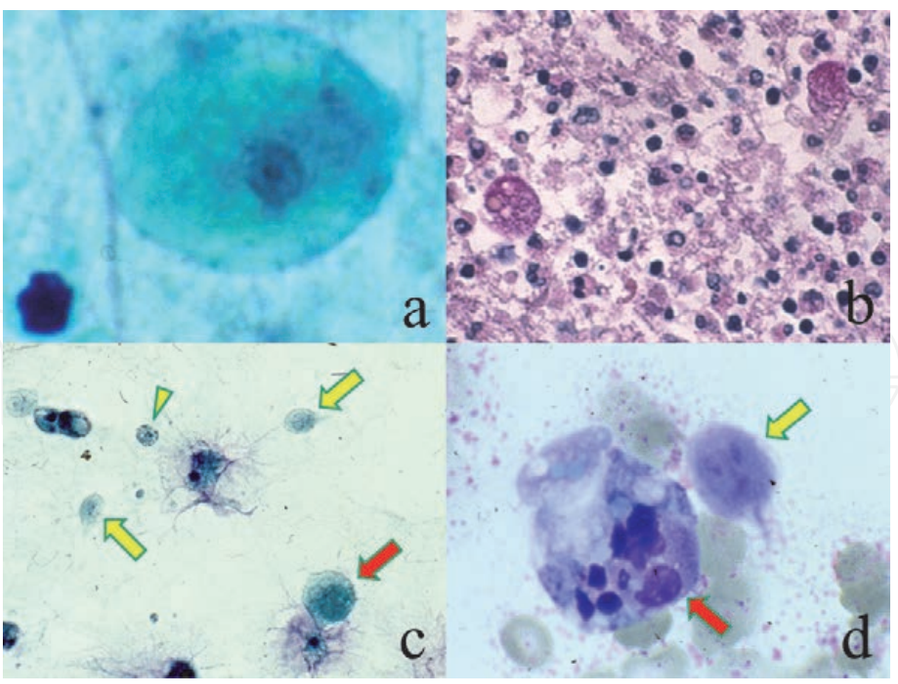

Figure 55.
Entamoeba histolytica *infection (Papanicolaou [a&c], Giemsa [d], PAS for cell block preparation [b]). The aspirate from liver abscess contains trophozoites of* E. histolytica*. They are characterized by a karyosome, (a centrally located chromatin aggregate) unique in protozoan nuclei, and plump cytoplasm consisting of thick perinuclear endoplasm and thin peripheral ectoplasm (a). Trophozoites in the cell block preparation reveal PAS reactivity. Neutrophils are devoid of glycogen because of anaerobic environment (b). Rectal lavage from an AIDS patient complaining of severe diarrhea demonstrates opportunistic co-infection of* E. histolytica *and* Giardia lamblia *(c&d). Yellow arrows indicate trophozoites of* G. lamblia*, and its cyst form is shown by the yellow arrowhead. The large-sized trophozoite of* E. histolytica *(red arrows) phagocytizes neutrophils.*

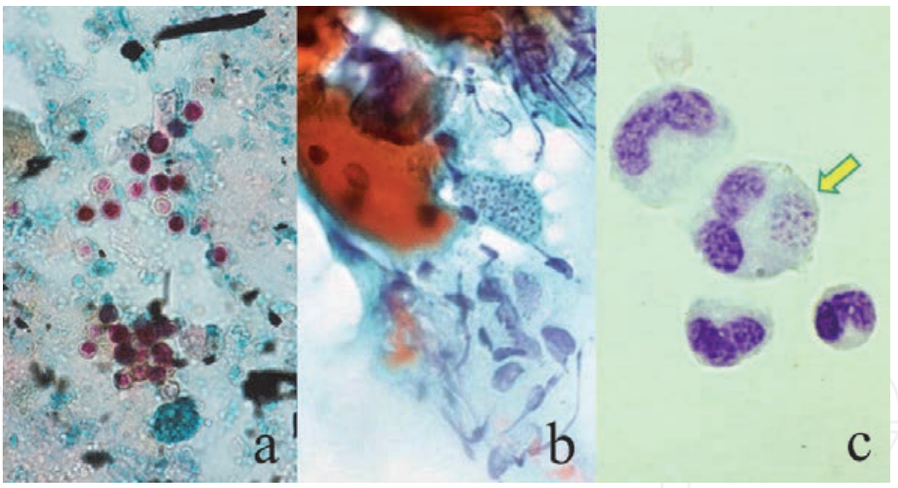

Figure 56.
Opportunistic protozoan infections (a: Ziehl-Neelsen, diarrheal feces in cryptosporidiosis, b: Papanicolaou, needle aspirate from toxoplasma myositis, c: Giemsa, microsporidiosis in ascites fluid of immunosuppressed mouse). Cryptosporidiosis provokes lethal watery diarrhea in AIDS patients. Small-sized (3–6 μm in siameter) cysts of Cryptosporidium parvum *in the fecal excretion are acid-fast (a). A patient with acute myeloid leukemia post bone marrow transplantation complained of myalgia in his leg, and the painful muscle was fine needle-aspirated. Tachyzoites of* Toxoplasma gondii *are clustered in the cytoplasm of the striated muscle cell (b).* Encephalitozoon cuniculi *infects a macrophage in ascites fluid of an immunosuppressed mouse (c). Tiny microsporidium bodies are clustered in a cytoplasmic inclusion (arrow).*

intestine, striated muscle and brain as an opportunistic complication in AIDS patients [132]. Recent studies indicate that the genus microsporidium belongs to the specialized fungus, instead of the protozoan.

Representative microscopic appearance of the latter three infections is demonstrated in **Figure 56**.

8. Cytodiagnosis of helminthic infection

Larval parasites (nematodes) and parasitic ova are occasionally experienced in cytology specimens. It should be noted that manifesting helminthic parasitosis is mostly caused by visceral larva migrans in the human body.

8.1 Larval nematodes in cytology specimens

Typical example includes disseminated strongyloidiasis, opportunistically happening in immunocompromised patients suffering from AIDS or adult T-cell leukemia/lymphoma [133, 134]. *Strongyloides stercoralis* shows percutaneous infestation of the larva via normal skin in tropical and subtropical areas. In Japan, the disease is endemic in southern Okinawa and Amami districts. Adult worms (nematodes), 2–3 mm in length, infest the small bowel mucosa, and persistent autoinfestation occurs through direct intraluminal hatching to infective larva, up to 600 μm in length. In disseminated strongyloidiasis, larval nematodes migrate to a variety of organs and tissues, and they may be seen in cytology specimens of the sputum, urine and body fluids (**Figure 57**). The cellular response against the worm is poor.

8.2 Larval nematodes in blood preparations

In human filariasis encompassing several types [135], microfilariae, 200–400 μm in length, are observed in the peripheral blood smears (**Figure 58**). Bancroftian (lymphatic) filariasis caused by *Wuchereria bancrofti* is seen worldwide, and scrotal

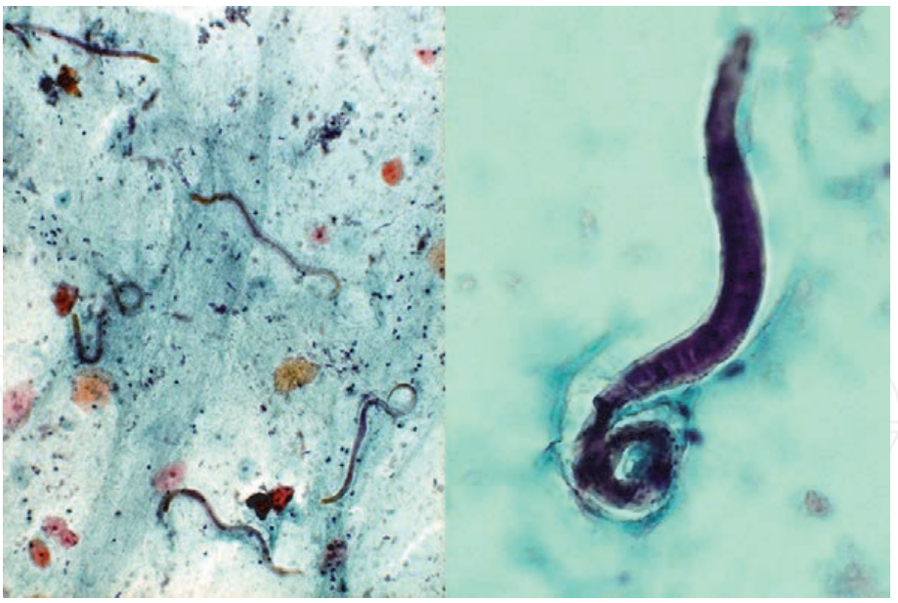

Figure 57.
Disseminated strongyloidiasis (Papanicolaou, sputum cytology, left: Low-power, right: High-power). In disseminated strongyloidiasis, larval nematodes of Strongyloides stercoralis *migrate to a variety of organs and tissues, and plural numbers of larvae are seen in sputum cytology specimen. Infective larva measures up to 600 μm in length.*

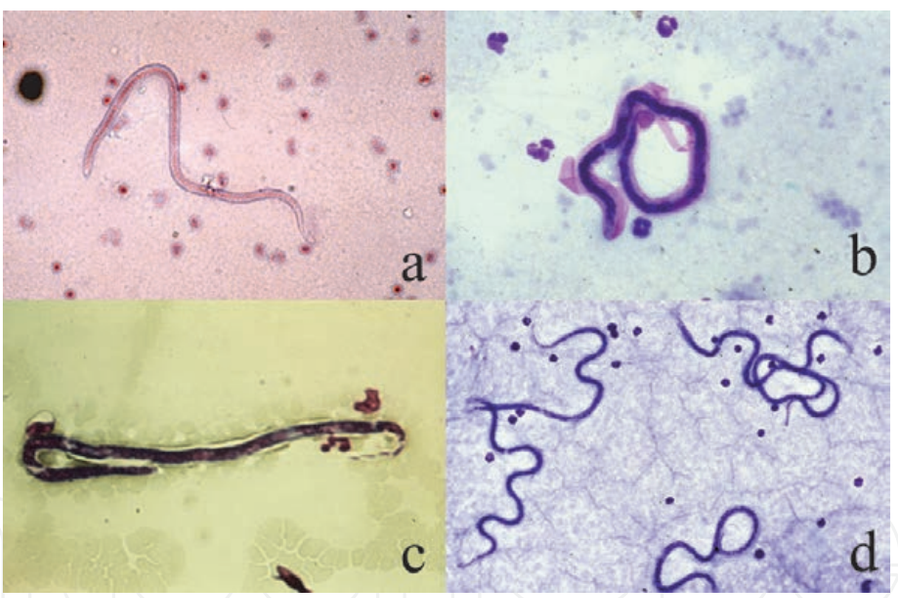

Figure 58.
Larval nematodes seen in the blood (Giemsa, a: Wuchereria bancrofti*, b:* Brugia malayi*, c:* Loa loa*, d:* Dirofilaria immitis *in dog). In human filariasis, microfilariae, 200–400 μm in length, are observed in the peripheral blood smears. The microfilariae are sheathed in bancroftian (lymphatic) filariasis (a) and in brugian filariasis endemic in subtropical Asia (b). Conjunctival African eye worm disease, Loa Loa filariasis, also accompanies sheathed microfilariae in the blood. In canine dirofilariasis, numerous unsheathed microfilariae appear in the peripheral blood.*

swelling and elephantiasis of the lower extremities are clinically featured. Brugian filariasis caused by *Brugia malayi* is endemic in subtropical Asia. The microfilariae are sheathed in both forms. Conjunctival infestation of *Loa loa*, an African eye worm, provokes sheathed microfilariae in the peripheral blood. A transparent, 2–7 mm-long adult worm is seen beneath the conjunctival mucosa. In onchocerciasis causing river blindness in the highland of central America and tropical Africa and mediated by blackfly bite, unsheathed microfilariae of *Onchocerca volvulus* appear in the peripheral blood and preferably invade the eye ball. In canine filariasis,

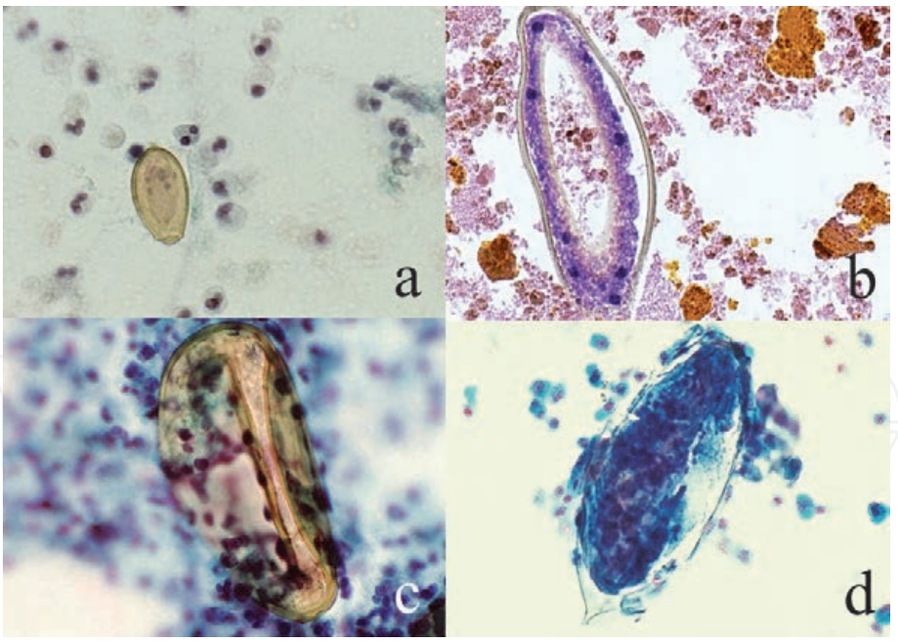

Figure 59.
Parasitic ova seen in cytology specimens (Papanicolaou [a,c&d], Giemsa [b], a: Clonorchis sinensis *Ovum in the bile, b:* Fasciola hepatica *Ovum in the bile, c:* Paragonimus westermani *ovum in the sputum, d:* Schistosoma haematobium *ovum in the urine). The ovum of* C. sinensis *is smallest, while the ovum of* F. hepatica *is largest. Large-sized asymmetric ovum of* P. westermani *is yellow/golden-colored. The large-sized ovum of* S. haematobium *is spiked at one end. The ova of* C. sinensis *and* S. haematobium *contain multinucleated and ciliated miracidium. The ova of* F. hepatica *and* P. westermani *contain unembryonated yolk cells without miracidium formation. Eosinophilic background is observed in a, c and d.*

unsheathed microfilariae of *Dirofilaria immitis* appear in the peripheral blood. See the review articles [123, 124].

8.3 Parasitic ova in cytology specimens

Parasitic ova may appear in cytology specimens. Based on their unique morphology, parasitosis of adult helminthic worms can be indicated (**Figure 59**). Small ova (30 μm in length) of *Clonorchis sinensis* [136] and large ova (130 μm in length) of *Fasciola hepatica* [137] may be seen in the bile. Large ova (around 100 μm in length) of *Paragonimus westermani* [138] and *Schistosoma haematobium* [139] may appear in the hemosputum and hemorrhagic urine, respectively. Regarding ova of *C. sinensis* in the bile, refer also to **Figure 18a**. Eosinophilic background is often associated. Foreign body granulomatous reaction (so-called egg tubercle) is provoked against ova of *S. haematobium* as illustrated in **Figure 19a**.

The ova of *C. sinensis* is the smallest one, while the ova of *F. hepatica* is the largest. Large-sized asymmetric ova of *P. westermani* are yellow/golden-colored. The large-sized ova of *S. haematobium* are spiked at one end. The ova of *C. sinensis* and *S. haematobium* contain multinucleated and ciliated miracidium. The ova of *F. hepatica* and *P. westermani* contain unembryonated yolk cells without miracidium formation.

9. Structures confusing with infectious agents

Certain microscopic structures seen in cytology specimens are occasionally confusing with infectious agents [140]. Representative examples are shown below.

9.1 Incidental airborne contamination during specimen sampling

Incidental contaminants during the process of specimen preparation should be noticeable (**Figure 60**). A variety of living bodies floating in the air may attach onto cytology specimens rich in sticky mucinous material. These include pollen [141], non-pathogenic fungi (conidia of *Alternaria alternata* [142] and hyphae of *Helicosporium* [143]) and mites [144] in house dust. Hairs of carpet beetle larvae may be contaminated from cotton swabs or wooden spatulas [145]. Star-shaped algae commonly found in fresh water marsh may be contaminated in cytology specimens via laboratory water supply [146]. They are positive with PAS and Grocott stains. Ointment matrix may be contaminated in gynecologic cytology sampled from patients suffering from vaginal candidosis. The important notice is the absence of cellular response against the substances.

9.2 Larval nematodes incidentally contaminated in cytology specimens

Sputum cytology preparations may contain a larval nematode [147]. The larva is microscopically indistinguishable from pathogenic *S. stercoralis*, but the patient is asymptomatic with negativity of human immunodeficiency virus antibody. Only one larva is observed in the specimen, and repeated examination fails to show the nematode any longer. In such a case, the patient inhaled an egg of the free-living nematode in the soil, and the ovum hatched to larva in the airway. Nematode larvae may be directly contaminated from the soil in pediatric urine preparations and scraping cytology specimens sampled from severe-degree eroded athlete foot. Representative pictures are displayed in **Figure 61**.

9.3 Structures confusing with pathogenic microbes

Certain microscopic structures may resemble pathogenic microbes [140], as shown in **Figure 62**. Sharp-margined vacuoles formed in the cytoplasm of uterine

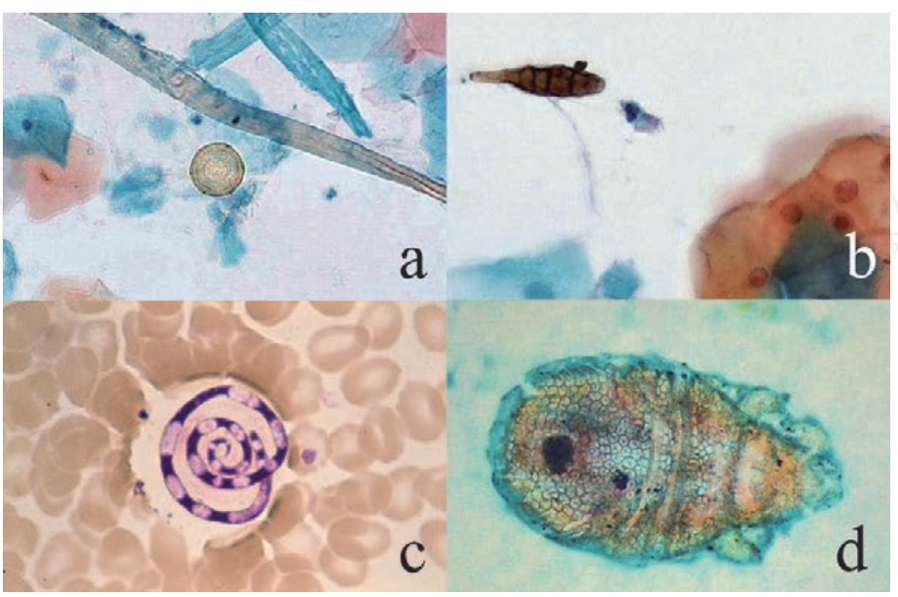

Figure 60.
Incidental airborne contamination during specimen sampling (Papanicolaou [a,b&d], Giemsa [c], a: Pollen, b: Alternaria alternata*, c:* Helicosporium*, d: Mite). A variety of living bodies floating in the air may attach onto cytology specimens rich in sticky mucinous material. A pollen is seen in the cervical smear (a). The shape, color and size of pollen depend upon the kind of flowers and blossoms. The brown-colored conidia of* A. alternata *in the cervical smear show short breaks (b). Hyphae of* Helicosporium *in the blood sample should not be confused with microfilaria (c). Mites living in house dust have four pairs of short legs (d).*

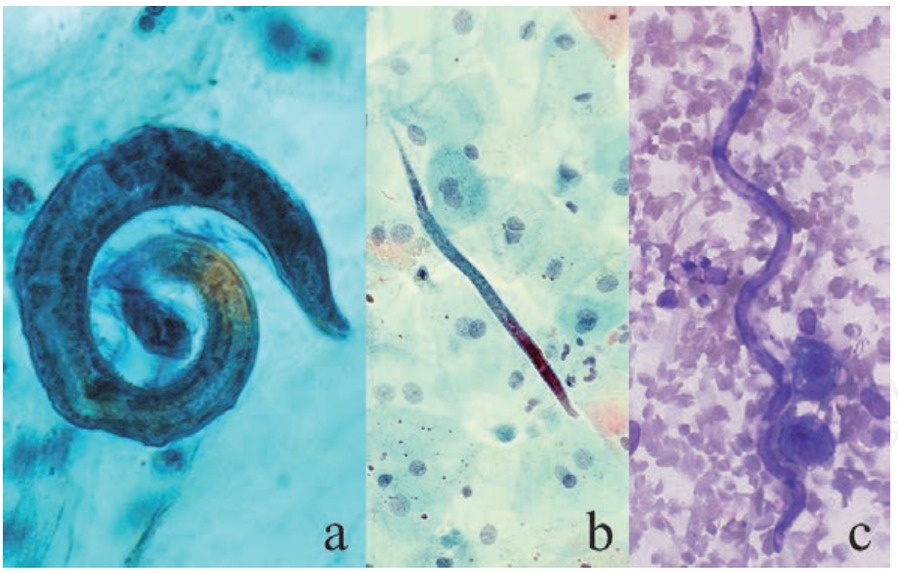

Figure 61.
Incidental contamination of nematode larvae (Papanicolaou [a&b], Giemsa [c], a: Sputum, b: Urine, c: Scraping cytology from severe-degree athlete foot). Cytology specimens may contain a single larval nematode. The larva is indistinguishable from pathogenic S. stercoralis *in disseminated strongyloidiasis. The patient remains asymptomatic. The larva of non-pathogenic free-living nematodes in the soil appears in the cytology specimen from children. The larva in the sputum (a) may have hatched from the inhaled egg in the dust, while larval nematodes are directly contaminated from the soil to the urine (b) and eroded and hemorrhagic skin lesion of the toe (c).*

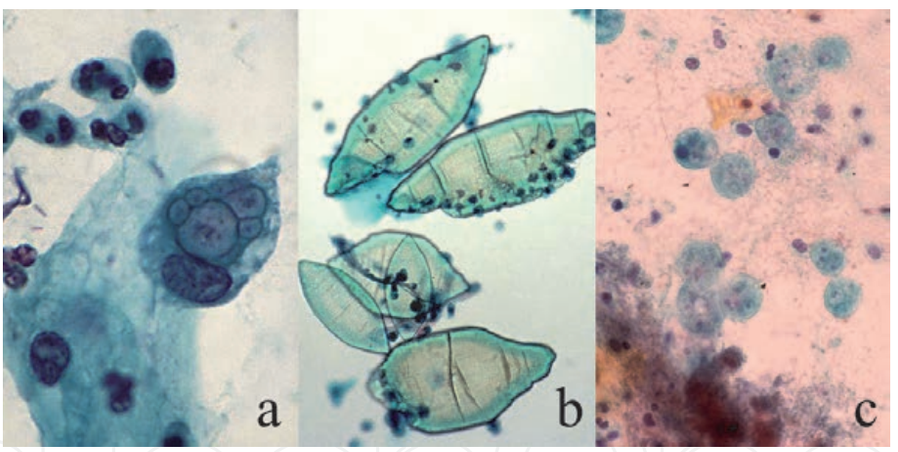

Figure 62.
Structures confusing with pathogenic microbes (Papanicolaou, a: Cervical smear, b: Urine sediment, c: Sputum). Certain microscopic structures may be confused with pathogenic microbes. Sharp-margined vacuoles formed in the cytoplasm of uterine cervical columnar/metaplastic cells resemble chlamydial cytoplasmic inclusions (a). Calcium urate crystals in the sediment of acidic urine resemble S. haematobium *ova (b). Note the size variation, thinness and the lack of miracidium in order for avoiding confusion.* Entamoeba gingivalis *aspirated into the airway must not be confused with pathogenic protozoa (c). The patient commonly suffers from severe periodontitis with bad breath.*

cervical columnar/metaplastic cells should be distinguished from chlamydial inclusions. Calcium urate crystals in the sediment of acidic urine may be confusing with *S. haematobium* ova. Note the size variation, thinness and the lack of miracidium to avoid confusion. Starch granules in sputum cytology may resemble *Paragonimus* eggs [148].

Aspirated *Entamoeba gingivalis* may be observed in sputum cytology specimens [149]. The non-pathogenic protozoa are especially plentiful in the mouth of patients with periodontitis and bad breath. Characteristically, they phagocytize neutrophils, as shown in **Figure 30**.

Airway aspiration of food residue may contain pieces of mushroom. Mushrooms in sputum cytology microscopically consist of parallel-arranged lamified hyphae similar to pathogenic *Aspergillus*. The presence of clamp connection at the site of septum is characteristic of mushroom cells [150]. Co-aspirated food-derived plant cells are often seen in the background (**Figure 63**).

9.4 Non-pathogenic fungi in sputum

Aspiration of air-floating non-pathogenic fungal conidia (spores) may induce growth of hypha-forming fungi in the sputum. Little cellular response is seen. Four different kinds of such fungi are presented in **Figure 64**: *Penicillium* spp., *Ductylaria (Ochroconis) gallopava*, *Petriellidium (Allescheria) boydii* and unknown fungus with a beaded appearance. From a clinical point of view, the appropriate recognition of non-pathogenic microorganisms in cytology specimens is requested. In other words, pathogenic hypha-forming fungi belong to either Aspergillus, Mucor or Candida. It should be noted, however, that these fungi may cause pneumonia in immunocompromised patients [151–153].

9.5 Myospherulosis

In myospherulosis (or spherulocytosis), macrophages contain clustered small globular material (endobody) in the cytoplasm, suggesting infection of yeast-form fungi such as cryptococcosis and coccidioidomycosis. They accumulate in aspirated fluid of cystic lesions in the paranasal cavity or in the breast [154, 155]. PAS and Grocott stains are negative, and they may represent hemolytic red cells or fat droplets phagocytized by the macrophages (**Figure 65**). The term myospherulosis comes from small globular structures seen in a cystic lesion formed in the striated muscle of the neck [156].

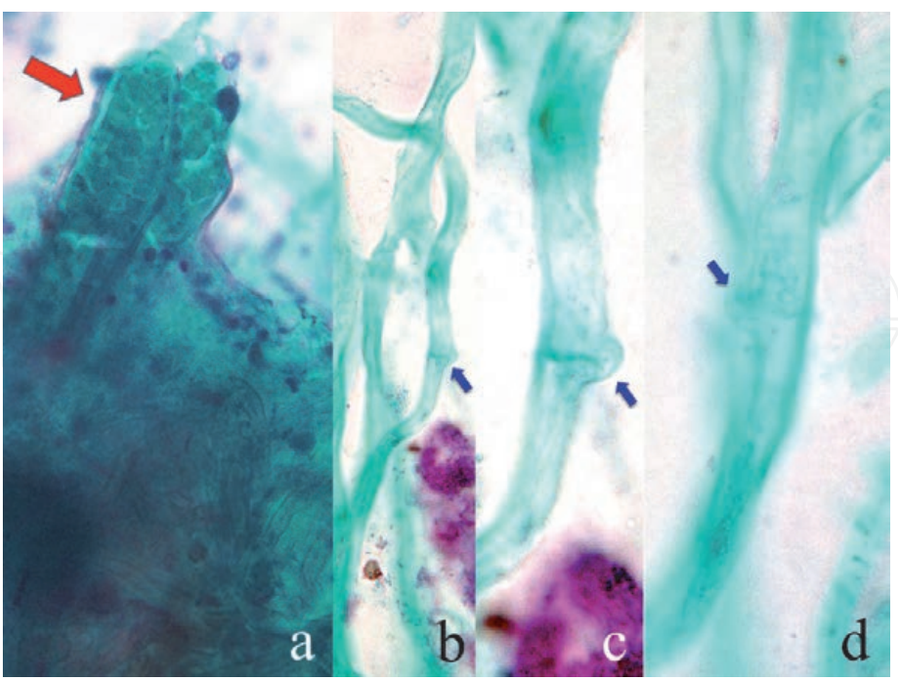

Figure 63.
Aspirated mushroom in the sputum (Papanicolaou, a: Aspirated food debris, b-d: Clamp connection). Airway aspiration of food residues may contain pieces of mushroom. Co-aspirated food-derived plant cells (red arrow) are often seen in the background (a). Mushroom cells in sputum cytology microscopically consist of parallel-arranged, lamified hyphae similar to pathogenic Aspergillus*. The presence of clamp connection (blue arrows) at the site of septum is characteristic of the mushroom cells (b-d). By courtesy of Mr. Tomohiro Watanabe, Chuken Kumamoto, Japan.*

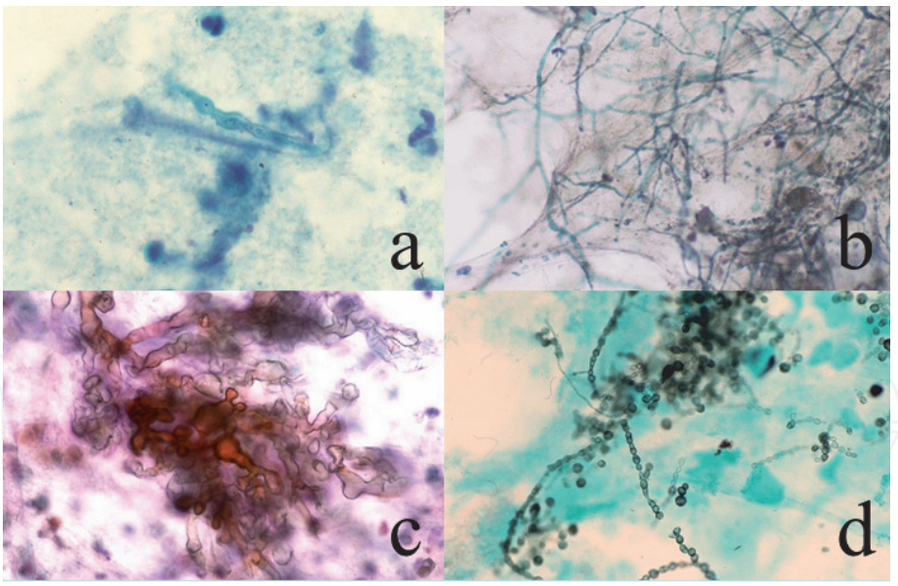

Figure 64.
Non-pathogenic fungi in sputum (Papanicolaou [a-c], Grocott [d], a: Penicillium *spp., b:* Ductylaria (Ochroconis) gallopava*, c:* Petriellidium (Allescheria) boydii*, d: Unknown fungus with a beaded appearance. Aspiration of air-floating non-pathogenic fungal conidia (spores) have induced growth of hypha-forming fungi in the sputum. Four different kinds of fungi are presented. Neutrophilic reaction is scarcely seen. Cytopathologists are requested to appropriately recognize non-pathogenic microorganisms in the sputum.*

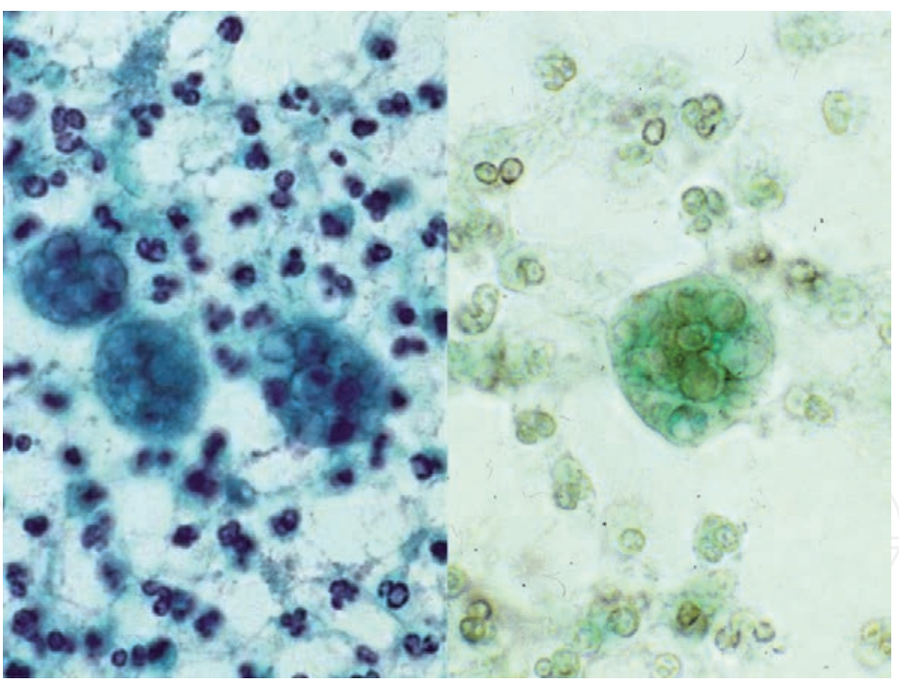

Figure 65.
Myospherulosis (aspirate from paranasal cavity, left: Papanicolaou, right: Grocott). In the aspirated cystic fluid, macrophages contain clustered small globular material (endobody) in the cytoplasm (left). Myospherulosis may resemble infection of yeast-form fungi such as cryptococcosis and coccidioidomycosis. Grocott stain is negative (right). The macrophages have phagocytized hemolytic red cells or fat droplets.

9.6 Grocott stain-positive structures confusing with cryptococcal yeasts or *Pneumocystis jirovecii*

It should be noted that Grocott methenamine silver staining stains not only fungi but also some microorganisms. Grocott may stain *Strongyloides stercoralis*, CMV and *Mycobacterium tuberculosis* [157]. Neutrophils and mucin granules are also

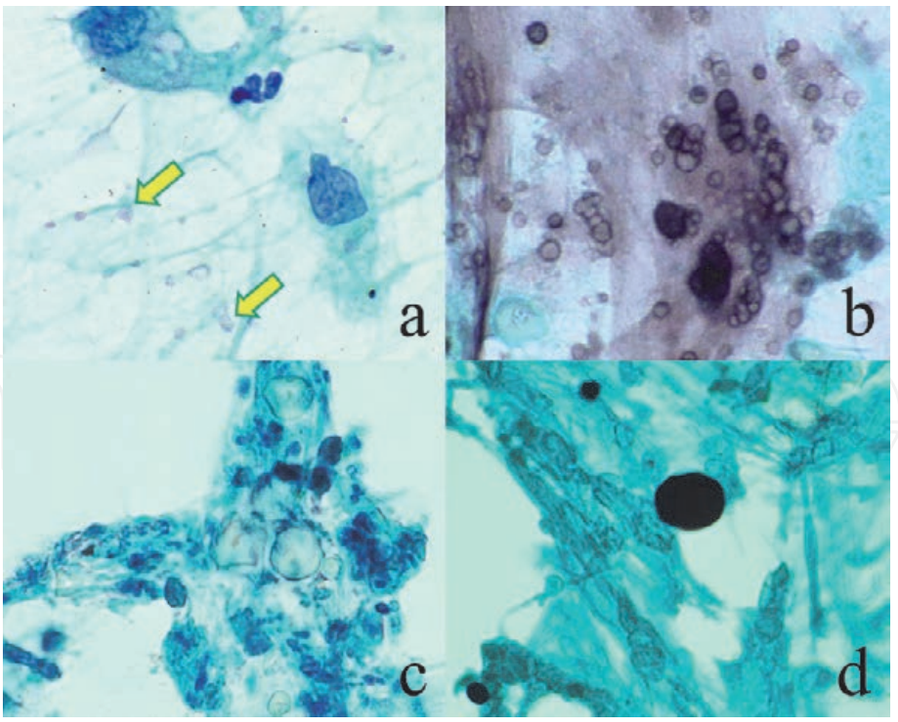

Figure 66.
Grocott stain-positive structures confusing with cryptococcal yeasts or Pneumocystis jirovecii *(Papanicolaou [a&c], Grocott [b&d], destroyed goblet cell mucin [a&b] and starch grains contaminated from rubber gloves [c&d]). In bronchial brushing (scraping) cytology specimens, mucin granules released from destroyed goblet cells (a: Arrows) show black granularity with Grocott stain (b). The Grocott-positive granules resemble cryptococcal yeasts or cysts of* P. jirovecii*. Rubber glove-derived starch grains, contaminated in cytology specimens, are also Grocott-positive (d). Size variation and Papanicolaou-stained appearance (navel-forming figure and birefringence) are helpful for the distinction from pathogens (c).*

Grocott-reactive [158]. When bronchial brushing (scraping) cytology specimens are stained with Grocott method, mucin granules released from destroyed goblet cells show black granularity. The black-stained mucin granules resemble cryptococcal yeasts or cysts of *P. jirovecii* (**Figure 66**). For the diagnosis of pneumocystosis, bronchial/alveolar lavage solution should be evaluated, instead of the bronchial brushing cytology specimen.

Starch grains powdered on the surface of rubber gloves may be contaminated in the sputum/bronchial cytology specimens [159]. Starch grains are also Grocott-reactive, and may be confused with yeast-type fungi. It is requested to use gloves without starch powders for preparing cytology specimens. Size variation and Papanicolaou-stained appearance (navel-forming figure and birefringence) make hints for distinction.

10. Conclusive remarks

The present review described varied cytomorphologic features of infection. Inflammatory cellular responses against pathogens are emphasized. Changes of sexual behavior, globalization-based increase of imported infection and the growing application of immunosuppressive therapy accelerate the chance to encounter unexpected or little-known infection. A wide variety of pathogens may cause infectious diseases. It is not easy for cytopathologists to prove the causative pathogen in cytology specimens. We must realize that the exact and prompt pathogenic diagnosis, with the aid of clinical and epidemiological information, may lead the patient to appropriate treatment. Avoidance of avoidable microbial transmission

eventually contributes to the safety of the human society. The recognition of the type of background cellular responses helps us make an appropriate cytodiagnosis.

Acknowledgements

The author cordially thanks numbers of cytotechnologists and cytopathologists who contributed to staining and supplying specimens. In particular, Mr. Tomohiro Watanabe, a veteran cytotechnologist, Chuken Kumamoto, Japan, provided the author with precious materials.

Disclosure

The author do not have any conflict of interest or funding sources in reporting the present review.

Author details

Yutaka Tsutsumi
Diagnostic Pathology Clinic, Pathos Tsutsumi, Nagoya, Aichi, Japan

*Address all correspondence to: pathos223@kind.ocn.ne.jp

References

[1] Tsutsumi Y. Application of the immunoperoxidase method for histopathological diagnosis of infectious diseases. *Acta Histochem Cytochem.* 1994; **27**: 547–560.

[2] Tsutsumi Y. Atlas of Infectious Disease Pathology. Bunkodo, Tokyo, 2000 (349 pages). https://pathos223.com/atlas/index.htm (*in Japanese*).

[3] Tsutsumi Y. Microorganisms found in cytology preparations. *Byori-to-Rinsho.* 2002; **20**(Special Issue: Cytology): 56–68 (*in Japanese*).

[4] Tsutsumi Y. Pathology of Infectious Diseases. 2003; https://pathos223.com/en/

[5] Tsutsumi Y. Infectious diseases. *Byori-to-Rinsho.* 2013; **31**(Special Issue: Topics in Cytology): 390–404 (*in Japanese*).

[6] Tsutsumi Y. Cytological diagnosis of infectious diseases. *Iyaku J.* 2018; **54**(5): 1135–1154 (*in Japanese*).

[7] Tsutsumi Y. Low-specificity and high-sensitivity immunostaining for demonstrating pathogens in formalin-fixed, paraffin-embedded sections. *Intechopen* 2019; doi: 10.5772/intechopen.85055

[8] Reynolds HY. Defense mechanisms against infections. *Curr Opin Pulm Med.* 1999; **5**(3): 136–42. doi: 10.1097/00063198-199905000-00003

[9] Accolla RS. Host defense mechanisms against pathogens. *Surg Infect.* 2006; **7**(Suppl 2): S57. doi: 10.1089/sur.2006.7.s2-5

[10] Chen L, Deng H, Cui H, et al. Inflammatory responses and inflammation-associated diseases in organs. *Oncotarget.* 2018; **9**: 7204–7218.

[11] Altan-Bonnet G, Mukherjee R. Cytokine-mediated communication: a quantitative appraisal of immune complexity. *Nature Rev Immunol.* 2019; **19**: 205–217.

[12] Lehrer RI, Bevins CL, Ganz T. Defensins and Other Antimicrobial peptides and proteins. *Mucosal Immunol.* 2005; 95–110. doi: 10.1016/B978-012491543-5/50010-3

[13] Bruni N, Capucchio MT, Biasibetti E, et al. Antimicrobial activity of lactoferrin-related peptides and applications in human and veterinary medicine. *Molecules* (Basel, Switzerland), 2016; **21**(6): 752. doi: 10.3390/molecules21060752

[14] Ellison III RT, Giehl TJ. Killing of gram-negative bacteria by lactoferrin and lysozyme. *J Clin Invest.* 1991; **88**:1080–91.

[15] van Kessel KPM, Bestebroer J, van Strijp JAG. Neutrophil-mediated phagocytosis of *Staphylococcus aureus*. *Front. Immunol.* 2014; doi. 10.3389/fimmu.2014.00467

[16] Borregaard N, Cowland JB. Granules of the human neutrophilic polymorphonuclear leukocyte. *Blood.* 1997; **89**; 3503–3521.

[17] Sinkovics JG, Horvath JC. Human natural killer cells: a comprehensive review. *Int J Oncol.* 2005; **27**(1): 5–47.

[18] Brinkmann V, Reichard U, Goosmann C, et al. Neutrophil extracellular traps kill bacteria. *Science.* 2004; **303**; 1532–1535.

[19] Shiogama K, Onouchi T, Mizutani Y, et al. Visualization of neutrophil extracellular traps and fibrin meshwork in human fibrinopurulent inflammatory lesions: I. Light microscopic study. *Acta Histochem Cytochem.* 2016; **49**: 109–116. doi. 10.1267/ahc.16015

[20] Medzhitov R. Toll-like receptors and innate immunity. *Nat Rev Immunol.* 2001; **1**: 135–145. doi.org/10.1038/35100529

[21] Medzhitov R. TLR-mediated innate immune recognition. *Semin Immunol.* 2007; **19**(1): 1–2. doi: 10.1016/j.smim.2007.02.001

[22] Perez-Lopez, A., Behnsen, J., Nuccio, SP. Raffatellu M. Mucosal immunity to pathogenic intestinal bacteria. *Nat Rev Immunol.* 2016; **16**: 135–148. doi: 10.1038/nri.2015.17

[23] Harada N, Iijima S, Kobayashi K, et al. Human IgGFc binding protein (FcgammaBP) in colonic epithelial cells exhibits mucin-like structure. J Biol Chem. 1997; 272(24): 15232–15241. doi: 10.1074/jbc.272.24.15232

[24] Kobayashi K, Ogata H, Morikawa M, et al. Distribution and partial characterization of IgG Fc binding protein in various mucin producing cells and body fluids. Gut. 2002; 51(2): 169–176. doi: 10.1136/gut.51.2.169

[25] Heinonen KM, Perreault C. Development and functional properties of thymic and extrathymic T lymphocytes. *Crit Rev Immunol.* 2008; **28**(5):441–66. doi: 10.1615/CritRevImmunol.v28.i5.40

[26] Neutra MR, Frey A, Kraehenbuhl J-P. Epithelial M cells: Gateways for mucosal infection and immunization. *Cell.* 1996; **86**: 345–348.

[27] Gatfield J, Ferrari G, Pieters J. Immunity against extracellular pathogens. *Protoplasma.* 2000; **210**, 99–107. doi: 10.1007/BF01276849

[28] Thakur A, Mikkelsen H, Jungersen G. Intracellular pathogens: Host immunity and microbial persistence strategies. *J Immunol Res.* 2019; **2019**:1356540. doi:10.1155/2019/1356540

[29] Rohra P, Yan L, Mir, F, et al. Follicular cystitis in urine cytology: a clinical and cytopathologic study. *J Pathol.* 2019; **47**(11): 1223–1228.

[30] Halford JA. Cytological features of chronic follicular cervicitis in liquid-based specimens: a potential diagnostic pitfall. *Cytopathology.* 2002; **13**(6): 364–370. doi: 10.1046/j.1365-2303.2002.00434.x.

[31] Konttinen YT, Bergroth V, Nordström D, et al. Cellular immunopathology of acute, subacute, and chronic synovitis in rheumatoid arthritis. *Ann Rhem Dis.* 1985; **44**: 549–555.

[32] Clem AS. Fundamentals of vaccine immunology. *J Glob Infect Dis.* 2011; **3**(1):73–78. doi:10.4103/0974-777X.77299

[33] Ross SC, Densen P. Complement deficiency states and infection: epidemiology, pathogenesis and consequences of neisserial and other infections in an immune deficiency. *Medicine (Baltimore)*. 1984; **63**(5): 243–273.

[34] Stebegg M, Kumar SD, Silva-Cayetano1 A, et al. Regulation of the germinal center response. *Front. Immunol.* 2018. doi: 10.3389/fimmu.2018.02469

[35] Kojima M, Nakamura S, Itoh H, et al. Clinical implication of florid reactive follicular hyperplasia in Japanese patients 60 years or older: a study of 46 cases. *Int J Surg Pathol.* 2005; **13**(2):175–180. doi:10.1177/106689690501300208

[36] Le Hir M, Bluethmann H, Kosco-Vilbois MH, et al. Differentiation of follicular dendritic cells and full antibody responses require tumor necrosis factor receptor-1 signaling. *J*

Exp Med. 1996; 183(5): 2367–72. doi: 10.1084/jem.183.5.2367.

[37] Jandl C, King C. Cytokines in the germinal center niche. *Antibodies* (Basel). 2016; **5**(1):5. doi: 10.3390/antib5010005

[38] Mary T, Raghavendra R, Nanda KG. An overview of suppurative granuloma. *Ind J Dermatopathol Diagnost Dermatol.* 2018; **5**(1): 19–26.

[39] Lou TY, Teplitz C. Malakoplakia: pathogenesis and ultrastructural morphogenesis. A problem of altered macrophage (phagolysosomal) response. *Hum Pathol.* 1974; **5**: 191–207.

[40] Ramirez GA, Yacoub MR, Ripa M, et al. Eosinophils from physiology to disease: a comprehensive review. *Biomed Res Int.* 2018; **2018**: 9095275. doi: 10.1155/2018/9095275

[41] Greenberger PA. Allergic bronchopulmonary aspergillosis. *J Allergy Clin Immunol.* 2002; **110**(5): 685–92. doi: 10.1067/mai.2002.130179

[42] Halim WGY. Schistosomiasis: progress and problems. *World J Gastroenterol.* 2000; **6**(1): 12–19. doi: 10.3748/wjg.v6.i1.12

[43] Tsutsumi Y, Fujimoto Y. Early gastric cancer superimposed on infestation of an Anisakis-like larva. A case report. *Tokai J Clin Exp Med.* 1987; **8**(3): 265–273.

[44] Tsutsumi Y. Pathology of gangrene. https://www.intechopen.com/books/pathogenic-bacteria/pathology-of-gangrene. 2020. doi: 10.5772/intechopen.93505

[45] Tsutsumi Y, Shiogama K, Sakurai K, et al. p16 immunostaining can avoid overdiagnosis in postmenopausal cervical cytology. Int Res J Med Med Sci. 2021; **9**(1): 1–8

[46] Khan S, Omar T, Michelow P. Effectiveness of the cell block technique in diagnostic cytopathology. *J Cytol.* 2012; **29**(3): 177–182.

[47] Jain D, Mathur SR, Iyer VK. Cell blocks in cytopathology: a review of preparative methods, utility in diagnosis and role in ancillary studies. *Cytopathology.* 2014; **25**(6): 356–371.

[48] Tsutsumi Y. Large granular lymphocytes in ascitic fluid. *Byori-to-Rinsho.* 2002; **19**(1): 80–81 (*in Japanese*).

[49] Churukian CJ. List of miscellaneous methods and information. Histochemical Stains Methods. 2009. https://www.urmc.rochester.edu/urmc-labs/pathology/stainsmanual/index.html?RESTAININGSLIDES

[50] Tasho T, Mitsui Y, Ishikura M, el al. Study on restaining of discolored cytological slides. *Igaku Kensa.* 2014; **63**(6): 394–699 (*in Japanese*).

[51] Marshall AE, Cramer HM, Wu HH. The usefulness of the cell transfer technique for immunocytochemistry of fine-needle aspirates. *Cancer Cytopathol.* 2014; **122**(12): 898–902.

[52] Itoh H, Miyajima Y, Osamura RY, Tsutsumi Y. A study of quick "cell transfer" technique. *J Jpn Soc Clin Cytol.* 2002; **41**(4): 302–303 (*in Japanese with English abstract*).

[53] Harada E, Miura K, Tsutsumi Y. How to peel off cover slips quickly. *Byori-to-Rinsho.* 2003; **21**(11): 1306–1307 (*in Japanese*).

[54] Capobianco G, Marras V, Wenger JM, et al. P16 immunostaining and HPV testing in histological specimens from the uterine cervix. *Eur J Gynaecol Oncol.* 2013; **34**(3): 227–230.

[55] Kawai K, Tsutsumi Y. How to recover sections on broken glass slides. *Kensa-to-Gijutsu* 1999; **27**(11): 1315–1316 (*in Japanese*).

[56] Hori S, Itoh H, Tsutsumi Y, Osamura RY. Immunoelectron microscopic detection of chlamydial antigens in Papanicolaou-stained vaginal smears. *Acta Cytol.* 1995; **39**(4): 835–837.

[57] Hori S, Kawai K, Tsutsumi Y, Osamura RY. Ultrastructural demonstration of *Chlamydia trachomatis* DNA by *in situ* hybridization using a biotinylated DNA probe, in comparison with immunoelectron microscopy. *Med Sci Res.* 1991; **19**: 429–430.

[58] Clark CG, Diamond LS. Colonization of the uterus by the oral protozoan *Entamoeba gingivalis*. *Am J Trop Med Hyg.* 1992; **46**(2): 158–160. doi: 10.4269/ajtmh.1992.46.158

[59] Okada H, Matsumoto T, Morikawa M, et al. Clinicopathological and cytological study of *Entamoeba gingivalis*. *J Jpn Soc Clin Cytol.* **41**(5): 321–326 (*in Japanese with English abstract*).

[60] Powers CN. Diagnosis of infectious diseases: a cytopathologist's perspective. *Clin Microbiol Rev.* 1998; **11**(2): 341–365.

[61] Lepargneur JP. Protective role of Doderlein flora. *J Gynecol Obstet Biol Reprod.* 2002; **31**(5): 485–494.

[62] Ventolini G. Progresses in vaginal microflora physiology and implications for bacterial vaginosis and candidiasis. *Womens Health (Lond).* 2016; **12**(3): 283–291.

[63] Demirezen S. Review of cytological criteria of bacterial vaginosis: examination of 2,841 Papanicolaou-stained vaginal smears. *Diagn Cytopathol.* 2003; **29**(3): 156–159.

[64] Onderdonk AB, Delaney ML, Fichorova RN. The human microbiome during bacterial vaginosis. *Clin Microbiol Rev.* 2016; **29**(2): 223–238.

[65] Mendling W, Palmeira-de-Oliveira A, Biber S, Prasauskas V. An update on the role of *Atopobium vaginae* in bacterial vaginosis: what to consider when choosing a treatment? A mini review. *Arch Gynecol Obstet.* 2019; **300**(1): 1–6.

[66] Vinette-Leduc D, Yazdi HM, Jessamine P, Peeling RW. Reliability of cytology to detect chlamydial infection in asymptomatic women. *Diagn Cytopathol.* 1997; **17**(4): 258–261.

[67] Hare MJ, Toone E, Taylor-Robinson D, et al. Follicular cervicitis: colposcopic appearances and association with Chlamydia trachomatis. *Br J Obstet Gynaecol.* 1981; **88**(2): 174–80. doi: 10.1111/j.1471-0528.1981.tb00964.x.

[68] Chan PA, Robinette A, Montgomery M, et al. Extragenital infections caused by *Chlamydia trachomatis* and *Neisseria gonorrhoeae*: a review of the literature. *Infect Dis Obstet Gynecol.* 2016; Article ID 5758387, 17 pages.

[69] Harvey HA, Ketterer MR, Preston A, Lubaroff D, Williams R, Apicella MA. Ultrastructural analysis of primary human urethral epithelial cell cultures infected with *Neisseria gonorrhoeae*. *Infect Immun.* 1997;**65**(6): 2420–2427.

[70] Michael CW, Davidson B. Pre-analytical issues in effusion cytology. *Pleura Peritoneum.* 2016; **1**(1): 45–56.

[71] Prins JM. Endotoxin, antibiotics and inflammation in Gram-negative infections. *Endotoxin in Health and Disease* (eds. Brade H, Opal S, Vogel S, Morrison D), Dekker, New York, 1999; 887–897.

[72] O'Driscoll NH, Lamb AJ. Morphological and ultrastructural changes in bacterial cells as an indicator of antibacterial mechanism of action.

Cell Mol Life Sci. 2016; **73**(23): 4471–4492.

[73] Bjarnsholt T. The role of bacterial biofilms in chronic infections. APMIS 2013; 136(Suppl): 1–51.

[74] Flemming HC, Wingender J, Szewzyk U, et al. Biofilms: an emergent form of bacterial life. *Nat Rev Microbiol.* 2016; **14**(9): 563–575.

[75] Sattar SBA, Sharma S. Bacterial pneumonia. In: StatPearls. Treasure Island (FL): StatPearls Publishing; March 6, 2020. PMID: 30020693

[76] Ishiguro T, Yoshii Y, Kanauchi T, et al. Re-evaluation of the etiology and clinical and radiological features of community-acquired lobar pneumonia in adults. *J Infect Chemother.* 2018; **24** (6): 463–469.

[77] Kandi V. Human Nocardia infections: a review of pulmonary nocardiosis. *Cureus.* 2015; **7**(8): e304. doi:10.7759/cureus.304

[78] Shariff M, Gunasekaran J. Pulmonary nocardiosis: review of cases and an update. *Can Respir J.* 2016; **2016**: 7494202. doi:10.1155/2016/7494202

[79] Mabeza GF, Macfarlane J. Pulmonary actinomycosis. *Eur Respir J.* 2003; **21**: 545–551.

[80] Wong VK, Turmezei TD, Weston VC. Actinomycosis. *BMJ* 2011; **343**: d6099. doi: 10.1136/bmj.d6099

[81] Tani EM, Schmitt FC, Oliveira ML, et al. Pulmonary cytology in tuberculosis. *Acta Cytol.* 1987; **31**(4): 460–463.

[82] Jain D, Ghosh S, Teixeira L, Mukhopadhyay S. Pathology of pulmonary tuberculosis and non-tuberculous mycobacterial lung disease: facts, misconceptions, and practical tips for pathologists. *Semin Diagn Pathol.* 2017; **34**(6): 518–529.

[83] Tsutsumi Y. Occupational risk of tuberculosis in pathology. 2003; https://pathos223.com/en/review.htm#Occupational

[84] Prasad CSBR, Narasimha A, Kumar MLH. Negative staining of mycobacteria. A clue to the diagnosis in cytological aspirates: two case reports. *Ann Trop Med Public Health.* 2011; **4**(2): 110–112.

[85] Alderwick LJ, Harrison J, Lloyd GS, Birch HL. The mycobacterial cell wall. Peptidoglycan and arabinogalactan. *Cold Spring Harb Perspect Med.* 2015; **5** (8): a021113. doi: 10.1101/cshperspect.a021113

[86] Moon HW, Hur M. Interferone-gamma release assays for the diagnosis of latent tuberculosis infection: an updated review. *Ann Clin Lab Sci.* 2013; **43**(2): 221–229.

[87] Mazur-Melewska K, Mania A, Kemnitz P, et al. Cat-scratch disease: a wide spectrum of clinical pictures. *Postepy Dermatol Alergol.* 2015; **32**(3): 216–220.

[88] Cutler SJ. Relapsing fever: a forgotten disease revealed. *J Appl Microbiol.* 2010; **108**: 1115–1122.

[89] Lion C, Escande F, Burdin JC. *Capnocytophaga canimorsus* infections in human: review of the literature and cases report. *Eur J Epidemiol.* 1996; **12** (5): 521–533.

[90] Hughes JM, Wilson ME, Wertheim HFL, et al, *Streptococcus suis*: an emerging human pathogen. *Clin Infect Dis.* 2009; **48**(5): 617–625.

[91] Shimada J, Hayashi I, Inamatsu T, et al. Clinical trial of in-situ hybridization method for the rapid

diagnosis of sepsis. *J Infect Chemother.* 1999; **5**(1): 21–31.

[92] Fukuyama, H., Yamashiro, S., Kinjo, K. et al. Validation of sputum Gram stain for treatment of community-acquired pneumonia and healthcare-associated pneumonia: a prospective observational study. *BMC Infect Dis.* 2014; **14**, 534. Doi: 10.1186/1471-2334-14-534

[93] Ogawa H, Kitsios GD, Iwata M, Terasawa T. Sputum Gram stain for bacterial pathogen diagnosis in community-acquired pneumonia: a systematic review and Bayesian meta-analysis of diagnostic accuracy and yield. *Clin Infect Dis.* 2020; **71**(3): 499–513.

[94] Ramana KV, Kandi S, Bharatkumar PV, et al. Invasive fungal infections: a comprehensive review. *Am J Infect Dis Microbiol.* 2013; **1**(4): 64–69.

[95] Guarner J, Brandt ME. Histopathologic diagnosis of fungal infections in the 21st century. *Clin Microbiol Rev.* 2011; **24**(2): 247–280.

[96] Achkar JM, Fries BC. Candida infections of the genitourinary tract. *Clin Microbiol Rev.* 2010; **23**: 253–273.

[97] Rodrigues CF, Silva S, Henriques *M. candida glabrata*: a review of its features and resistance. *Eur J Clin Microbiol Infect Dis.* 2014; **33**(5): 673–688.

[98] Guého E, Improvisi L, de Hoog GS, Dupont B. *Trichosporon* on humans: a practical account. *Mycoses.* 1994; **37**(1–2): 3–10.

[99] Setianingrum F, Rautemaa-Richardson R, Denning DW. Pulmonary cryptococcosis: A review of pathobiology and clinical aspects. *Med Mycol.* 2019; **57**(2): 133–150.

[100] McHugh KE, Gersey M, Rhoads, DD, et al. Sensitivity of cerebrospinal fluid cytology for the diagnosis of cryptococcal infections: a 21-year single-institution retrospective review. *Am J Clin Pathol.* 2019; **151**(2): 198–204.

[101] Dahiya S, Mathur SR, Iyer VK, et al. Diagnosis of Pneumocystis pneumonia by bronchoalveolar lavage cytology: experience at a tertiary care centre in India. *Indian J Chest Dis Allied Sci.* 2005; **47**(4): 259–265.

[102] Gilroy SA, Bennett NJ. Pneumocystis pneumonia. *Semin Resp Crit Care Med.* 2011; **32**(6): 775–782.

[103] Fischler DF, Hall GS, Gordon S, et al. Aspergillus in cytology specimens: a review of 45 specimens from 36 patients. *Diagnost Cytol.* 1997; **16**(1): 26–30.

[104] Assante G, Camarda L, Locci R, et al. Isolation and structure of red pigments from *Aspergillus flavus* and related species, grown on a differential medium. *J Agric Food Chem.* 1981, **29**(4): 785–787.

[105] Oda M, Saraya T, Wakayama M, et al. Calcium oxalate crystal deposition in a patient with Aspergilloma due to *Aspergillus niger*. *J Thorac Dis.* 2013; **5** (4): E174-E178.

[106] Naran S, Lallu S, Kenwright D. Pulmonary mucormycosis diagnosed by brushing cytology. A case report. *NZ J Med Lab Sci.* 2008; **62**(2): 32–34.

[107] Raveenthiran V. Gastrointestinal mucormycosis mimicking necrotizing enterocolitis of newborn. *J Neonatal Surg.* 2013; **2**(4):41.

[108] Tsutsumi Y. The shapes of pathogens. *Kagakuryoho-no-Ryoiki* 2017; **33**(10): 1928–1946 (*in Japanese*).

[109] Tsutsumi Y, Kawai K, Hori S, Osamura RY. Ultrastructural visualization of human papillomavirus DNA in verrucous and precancerous

squamous lesions. *Acta Pathol Jpn.* 1991; **41**(10): 757–762.

[110] Thiel MA, Bossart W, Bernauer W. Improved impression cytology techniques for the immunopathological diagnosis of superficial viral infections. *Br J Ophthalmol.* 1997; **81**(11): 984–988.

[111] Naib ZM. Cytological diagnosis of herpes simplex virus infection. *Clin Dermatol.* 1984; **2**(2): 83–89.

[112] Fugl A, Andersen CL. Epstein-Barr virus and its association with disease: a review of relevance to general practice. *BMC Fam Pract.* 2019; **20**(1): 62. doi: 10.1186/s12875-019-0954-3.

[113] Weiss RL, Snow GW, Schumann GB, Hammond ME. Diagnosis of cytomegalovirus pneumonitis on bronchoalveolar lavage fluid: comparison of cytology, immunofluorescence, and in situ hybridization with viral isolation. *Diagn Cytopathol.* 1991; **7**(3): 243–247.

[114] Suwabe H, Yabe H, Tsutsumi Y. Relapsing hemorrhagic varicella. *Pathol Int.* 1996; **46**(8): 605–609.

[115] Singh HK, Bubendorf L, Mihatsch MJ, et al. Urine cytology findings of polyomavirus infections. In: Ahsan N (eds) *Polyomaviruses and Human Diseases. Advances in Experimental Medicine and Biology*, vol 577, 2006; pp. 201–212, Springer, New York, USA.

[116] Imam T. The complexities in the classification of protozoa: a challenge to parasitologists. *Bayero J Pure Appl Sci.* 2011; **2**(2). DOI: 10.4314/bajopas.v2i2.63805

[117] Muller M. Energy metabolism of protozoa without mitochondria. *Ann Rev Microbiol.* 1988; **42**: 465–488.

[118] Leanza V, Carlo Pafumi, Leanza G, D'Agati A. Cytology of *Trichomonas vaginalis*. *EC Microbiol.* 2016; **3**(3): 451–454.

[119] Ortega YR, Adam RD. Giardia: overview and update. *Clin Infect Dis.* 1997; **25**(3): 545–550.

[120] Buret AG. Immunopathology of giardiasis: the role of lymphocytes in intestinal epithelial injury and malfunction. *Mem Inst Oswaldo Cruz.* 2005; **100**(Suppl.1). doi: 10.1590/S0074-02762005000900032

[121] Patel SP, Schaefer JL, Jaber R, et al. The value of cytology smears for Acanthamoeba keratitis. *Case Rep Ophthalmol Med.* 2016; **2016**: 4148968. doi:10.1155/2016/4148968

[122] Kassi M, Tareen I, Qazi A, Kasi PM. Fine-needle aspiration cytology in the diagnosis of cutaneous leishmaniasis. *Ann Saudi Med.* 2004; **24**(2): 93–97.

[123] Moody AH, Chiodini PL. Methods for the detection of blood parasites. *Clin Lab Haematol.* 2000; **22**: 189–201.

[124] Rosenblatt JE, Reller LB, Weinstein MP. Laboratory diagnosis of infections due to blood and tissue parasites, *Clin Infect Dis.* 2009; **49**(7): 1103–1108.

[125] Armah H, Wired EK, Dodoo AK, et al. Cytokines and adhesion molecules expression in the brain in human cerebral malaria. *Int J Environ Res Public Health.* 2005; **2**(1): 123–131. doi: 10.3390/ijerph2005010123

[126] Adeoye GO, Nga IC. Comparison of quantitative buffy coat technique (QBC) with Giemsa-stained thick film (GTF) for diagnosis of malaria. *Parasitol Int.* 2007; **56**(4): 308–312.

[127] Hunfeld KP, Hildebrandt A, Gray JS. Babesiosis: recent insights into an ancient disease. *Int J Parasitol.* 2008; **38**(11): 1219–1237.

[128] Garcia L. Trypanosomiasis, In *Diagnostic Medical Parasitology*, 5th Ed. ASM Press, Washington, DC, 2007, pp. 218–248. doi: 10.1128/9781555816018.ch9

[129] Skappak C, Akierman S, Belga S, et al. Invasive amoebiasis: a review of Entamoeba infections highlighted with case reports. *Can J Gastroenterol Hepatol.* 2014; **28**(7): 355–359.

[130] Checkley W, White AC, Jaganath D, et al. A review of the global burden, novel diagnostics, therapeutics, and vaccine targets for *Cryptosporidium*. *Lancet Infect Dis.* 2015; **15**(1): 85–94.

[131] Swierzy IJ, Muhammad M, Kroll J, et al. Toxoplasma gondii within skeletal muscle cells: a critical interplay for food-borne parasite transmission. *Int J Parasitol.* 2014; **44**(2): 91–98.

[132] Franzen C. Microsporidia: a review of 150 years of research. *Open Parasitol J.* 2008; **2**(1): 1–34.

[133] Keiser PB, Nutman TB. *Strongyloides stercoralis* in the immunocompromised population. *Clin Microbiol Rev.* 2004, **17**(1): 208–217.

[134] Mukaigawara M, Narita M, Shiiki S, et al. Clinical characteristics of disseminated strongyloidiasis, Japan, 1975–2017. *Emerg Infect Dis.* 2020; **26**(3): 401–408.

[135] Taylor MJ, Hoerauf A, Bockarie M. Lymphatic filariasis and onchocerciasis. *Lancet.* 2010; **376**(9747): 1175–1185.

[136] Fujiya K, Ganno H, Ando M, Chong J-M. *Clonorchis sinensis* ova in bile juice cytology from a patient with severe hyperbilirubinemia and portal vein thrombosis. *Diagn. Cytopathol.* 2016; **44**: 223–225.

[137] Gulsen MT, Savas MC, Koruk M, et al. Fascioliasis: a report of five cases presenting with common bile duct obstruction. *Neth J Med.* 2006; **64**(1): 17–19.

[138] Doanh PN, Horii Y, Nawa Y. Paragonimus and paragonimiasis in Vietnam: an update. *Korean J Parasitol.* 2013; **51**: 621–627.

[139] Nmorsi OP, Ukwandu NC, Ogoinja S, et al. Urinary tract pathology in *Schistosoma haematobium* infected rural Nigerians. *Southeast Asian J Trop Med Public Health.* 2007; **38**(1): 32–37.

[140] Tsutsumi Y. Contamination of non-pathogenic microbes. 2003. https://pathos223.com/en/case/case237.htm

[141] Accorsi CA, Mazzanti MB, Forlani L, Rivasi F. Pollen grains in human cytology, *Grana.* 1991; **30**(1): 102–108.

[142] Radio SJ, Rennard SI, Ghafouri MA, Linder J. Cytomorphology of Alternaria in bronchoalveolar lavage specimens. *Acta Cytol.* 1987; **31**(3): 243–248.

[143] Yoon K-H. Peripheral blood smear contamination with *Helicosporium* fungi resembling microfilaria. *Ann Lab Med.* 2015; **35**(1): 169–171.

[144] Farley ML, Mabry LC, Hieger LR. Mites in pulmonary cytology specimens. *Diagn Cytopathol.* 1989; **5**(4): 416–426.

[145] Bechtold E, Staunton CE, Katz SS. Carpet beetle larval parts in cervical cytology specimens. *Acta Cytol.* 1985; **29** (3): 345–352.

[146] Agarwal A, Helliwell TR. Marsh stars in Liverpool. *J Clin Pathol.* 2005; **58** (10): 1104–1106.

[147] Tsutsumi Y. Nematode larva in urine. https://pathos223.com/en/case/case151.htm

[148] Martínez-Girón R, Martínez-Torre C. False Paragonimus eggs in sputum

cytology. *J Cytol.* 2019; **36**(4): 209–210. Starch granules

[149] Dao AH. *Entamoeba gingivalis* in sputum smears. *Acta Cytol.* 1985; **29**(4): 632–633.

[150] Niederpruem DJ, Jersild RA, Lane PL. Direct microscopic studies of clamp connection formation in growing hyphae of *Schizophyllum commune*. I. The dikaryon. *Arch Mikrobiol.* 1971; **78**, 268–280.

[151] Gill MV, Schoch PE, Rinaldi MG, et al. *Penicillium janthinellum* in sputum and bronchoalveolar lavage in an AIDS patient with pneumonia. *Clin Microbiol Infect.* 1997; **3**: 261–264.

[152] Meriden Z, Marr KA, Lederman HM, et al. *Ochroconis gallopava* infection in a patient with chronic granulomatous disease: case report and review of the literature, Med Mycol. 2012; 50(8): 883–889.

[153] Mader JT, Ream RS, Heath PW. Petriellidium boydii (Allescheria boydii) sphenoidal sinusitis. *JAMA.* 1978; **239** (22): 2368–2369.

[154] Hata S, Kanomata N, Kozuka Y, et al. Cytologic appearance of myospherulosis of the breast diagnosed by fine-needle aspirates: a clinical, cytological and immunocytochemical study of 23 cases. *Diagn Cytopathol.* 2011; **39**(3): 177–180.

[155] Phillip V, Becker K, Bajbouj M, Schmid RM. Myospherulosis. *Ann Diagn Pathol.* 2013; **17**(4): 383–389.

[156] McClatchie S, Warambo MW, Bremner AD. Myospherulosis: a previously unreported disease? *Am J Clin Pathol.* 1969; **51**: 699–704.

[157] Wright AM, Mody, DR, Anton, RC, Schwartz, MR. Aberrant staining with Grocott's methenamine silver: utility beyond fungal organisms. *J Am Soc Cytopathol.* 2017; **6**: 223–227.

[158] Agarwal A, Helliwell TR. Marsh stars in Liverpool. *J Clin Pathol.* 2005; **58** (10): 1104–1106.

[159] Sahay K, Mehendiratta M, Rehani S, et al. Cytological artifacts masquerading interpretation. *J Cytol.* 2013; **30**(4): 241–246.